Diesel Exhaust Particles Alter Endothelial Tube Permeability

by

MING-WEI CHAO

A Dissertation submitted to the

Graduate School-New Brunswick

Rutgers, The State University of New Jersey and

The Graduate School of Biomedical Sciences

University of Medicine and Dentistry of New Jersey

In partial fulfillment of the requirements

For the degree of

Doctor of Philosophy

Graduate Program in Toxicology

Written under the direction of

Dr. Marion Gordon

And approved by

_____

_____

_____

_____

_____

New Brunswick, New Jersey

[October, 2009]

ABSTRACT OF THE DISSERTATION

Diesel Exhaust Particles Alter Endothelial Tube Permeability

By MING-WEI CHAO

Dissertation Director:

Marion K. Gordon

Epidemiological studies suggest that an increase of diesel exhaust particles (DEP) in ambient air corresponds to in an increase in hospital recorded myocardial infarctions within 48 hr after exposure. Among the many theories to explain this data are endothelial dysfunction and translocation of DEP into the vasculature. We hypothesized that translocation of DEP occurs because endothelial cells become permeable after exposure. To support this hypothesis, *in vitro*-assembled endothelial tubes were used to evaluate how DEP affected parameters influencing permeability, i.e., cell-cell junction integrity, and proinflammatory and oxidative stress-induced upregulation of Vascular Endothelial Growth Factor (VEGF, also known as Vascular Permeability Factor). Our first experiments demonstrated that the adherens junction molecule, VE-Cadherin, becomes redistributed from the membrane at cell-cell borders to the cytoplasm in response to DEP,

separating the plasma membranes of adjacent cells. DEP were occasionally found in the endothelial cell cytoplasm and in the tube lumen. A second set of experiments demonstrated that DEP induced the generation of ROS, such as H_2O_2 in the HUVEC tube cells. Transcription factor Nrf2 was translocated to the cell nucleus and activated transcription of the antioxidative enzyme HO-1. ELISA assays determined that DEP increased secretion of pro-inflammatory cytokines IL-6 and TNF-α. The oxidative and pro-inflammatory responses both induced secretion of VEGF, a factor known to enhance permeability. Usually, vascular permeability is associated with activation of the Akt pathway leading to increased cell survival. A third set of experiments found that DEP-induced permeability was instead associated with increased apoptosis. This was the associated with deactivation of the Akt pathway. These results suggest mechanisms for how DEP may affect *in vivo* capillaries.

Dedication

To my mother, Der-li Liu and my father, Hsien-Pong Chao, whose love and support helped make the completion of this thesis a reality. It is impossible to thank you enough for a lifetime of support.

To my fiancé, Chia-Yi Tseng, for her warmth and encouragement. You gave me hope and strength beyond any words. I will always appreciate how you believe in me.

Acknowledgement

I am truly grateful to the faculty, students, and staff of the Joint Graduate Program in Toxicology at Rutgers University. The completion of my thesis would not have been possible without their help and generosity. I would like to specifically express my appreciation to the following individuals:

Dr. Marion Gordon, for her extraordinary patience, perseverance, guidance and encouragement. I benefited tremendously from her scientific expertise and mentorship and am indebted to her for the opportunity to complete this degree. She is also responsible for the purple that now exists in my wardrobe;

The members of my dissertation committee, Drs. Donald Gerecke, Robert Laumbach, Kathy Svoboda, and Lori White, for their support, excellent advice and valuable guidance;

Drs. Carol Gardner, Jeffery Laskin, Kathryn Uhrich, Chung S. Yang, Renping Zhou, for their help and for generously allowing me to use their laboratory facilities and equipment;

Drs. Michael Gallo, Kenneth Reuhl, and Gisela Witz, for their support, guidance and their selfless availability at the moment's notice;

The Pharmacology and Toxicology administrators Bernadine Chmielowicz and Sandi Selby. You made my time here have fewer problems;

The members of my lab, Rita Hahn, Dr. Yoke-Chen Chang, Iris Po, Andrea Desantis, John Beloni, Dr. Jeibo Lu, Lakshmi Raman, Melannie Soriano, James Wnag,

Hongmei Zhang, and Dr. Peihong Zhou, who provided comradery, as well as help and advice in many of the experiments that I have performed;

And last, but not least, my cousin, Joanna Chiu, for her excellent help and valuable advice in my graduate career.

Table of Contents

Lists of tables

List of figures

List of abbreviations

ARE   antioxidant response elements

BAD   Bcl-xL/Bcl-2 associated death

CNS   central nervous system

COPD   Chronic bronchitis, chronic obstructive pulmonary disease

CYP450   cytochrom P-450

DCFH-DA   2', 7'-dichlorohihydrofluorescein diacetate

DEP   diesel exhaust particles

DNP   dinitro-pyrene

EGF   epidermal growth factor

FGF   fibroblast growth factors

FKHR   Forkhead factors

GM-CSF   granulocyte macrophage colony stimulating factor

GSK3   glycogen synthase kinase 3

GST   glutathione S-transferase

HO-1   heme oxygenase-1

HUVEC   human umbilical vein endothelial cells

IKKα IκB kinase α

IL-1β interleukin-1β

IL-6   interlukin-6

IL-8   interleukin-8

JAMA   junctional adhesion molecule-A

LDH	lactate dehydrogenase
Mdm2	murine double minute-2
MTS	
	[3-(4,5-dimethylthiazol-2-yl)-5-(3-carboxymethoxyphenyl)-2-(4-sulfophenyl)-2H-tetrazolium]
NAC	N-acetyl cysteine
Nrf2	nuclear factor erythroid 2-related factor 2
NQO-1	NADPH-quinone oxidoreductase-1
PAH	polycyclic aromatic hydrocarbon
PIGF	placenta growth factor
PKB	protein kinase B
PM	particulate matter
PT	prothrombin time
ROS	reactive oxygen species
SnPP	tin protoporphyrin IX
SOD	superoxide dismutase
STAT	signal transducer and activator of transcription
TNF-α	tumor necrosis factor-α
TUNEL	fluorometric TdT-mediated dUTP nick end labeling
VE-cadherin	vascular endothelial cell cadherin
VEGFR-2	vascular endothelial growth factor receptor-2
VPF/VEGF	vascular permeability factor/vascular endothelial growth factor
YAP	Yes-associated protein

Introduction

1. Air Pollution in General and Adverse Health Effects

Air pollution is a complex mixture containing gaseous chemicals, liquids, and solid phase particles of various sizes, shapes, surface area, and chemical composition. In urban areas, the main source of air pollution is the combustion of fossil fuels from automobiles, diesel trucks, ships, and construction equipment. However, the specific composition of the pollutants is variable, and depends on geography, climate, and emission source (Brook *et al.* 2003). Air pollution levels parallel the incidence of allergies, asthma, and rhinitis, as well as cardiovascular disorders (Sydbom *et al.* 2001). Diesel exhaust is a common pollutant in the air of cities in industrialized countries.

1.1. Chronic Effects of Diesel Exhaust

Epidemiology indicates that long term exposure to ambient PM (particulate matter), a major component of diesel exhaust, adversely affects the health of those exposed. Chronic bronchitis, chronic obstructive pulmonary disease (COPD), asthma, heart failure, and even lung cancer can result, due to the carcinogenic or mutagenic components in the inhaled air (Wichmann 2007). Furthermore, for people living in areas where air pollution levels are high, the long-term exposure correlates with higher levels of atherosclerosis (Suwa et al. 2002). Chronic exposure to air pollution indirectly places a tremendous burden on the health care system, and is a significant cause of morbidity and mortality.

1.2. Acute Effects of Diesel Exhaust

Short term effects, observed within 48 hr after exposure, include acute eye and nose irritation, neurophysiological symptoms, respiratory symptoms, headache and fatigue. Ambient particulates have also been correlated with serious cardiovascular events, such as myocardial infarctions or strokes (Brook 2008; Pope 2007). Short-term elevations of particulate matter with diameters 2.5 μm and smaller (PM$_{2.5}$), in the air at a concentration as little as 10 μg/m^3, increase mortality by 1% (Pope and Dockery 2006). An acute exposure to a concentration of 50 μg/m^3 of PM$_{2.5}$ causes an average of 1.2 deaths per day in a population of 1 million (Pope and Dockery 2006).

1.3. Tissue Targets of Particles

Several organ systems are adversely affected by exposure. These include the lungs, the brain, the blood, the vasculature, and the heart (Brook 2008; Pope and Dockery 2006). Lungs are affected by many substances in diesel exhaust, such as nitric oxides that can lead to ozone production, which injures lung tissue (Krivoshto et al. 2008). Traffic pollution triggers asthma symptoms (Mamessier et al. 2006). Several diesel-related hydrocarbons, such as PAH and quinone, are potentially carcinogenic. Long-term DE exposure increases the risk of lung cancer (Ishinishi et al. 1986; McClellan 1987) and non-neoplastic lung lesions including fibrosis, edema, bronchitis, chronic alveolitis and asthma (Heinrich et al. 1986; Iwai et al. 1986; McClellan 1987).

Air pollution affects the brain. A possible connection between pollutants and Parkinson's disease has been investigated, and has shown decreases in the number of dopaminergic neurons in the brain tissue of exposed mice (Block et al. 2004). Residents in Mexico City who were chronically exposed to a complex mixture of air pollutants had

histopathologic changes in their brains similar to those seen in patients with Alzheimer's disease (Calderon-Garciduenas et al. 2002). Also, dogs exposed to severe air pollution exhibited chronic inflammation and acceleration of Alzheimer's-like pathology (Calderon-Garciduenas et al. 2004). The results suggested that chronic exposure of ambient air exposure may affect learning ability, coordination, memory, and judgment in both children and adults.

Blood is not immune from the effects of air pollution. Two components in air pollution, CO and NO_2, reduced the prothrombin time (PT) for clotting blood for 1218 healthy people from the Lombardia Region of Italy (Baccarelli et al. 2007). In addition, air pollutants may significantly increase fibrinogen, factor VIII, and platelet hyperactivity.

The reproductive system is affected by air pollution as well. Chronic exposure to ambient air pollution is linked to low birth weight in infants, as well as to premature births, congenital abnormalities, and elevated infant mortality rate (Dolk and Vrijheid 2003). Diesel emissions have also been shown to correlate with a decrease in sperm count (Watanabe 2005), and sperm motility (Fredricsson *et al.* 1993). Exposure to nitrophenols in diesel exhaust diminished the number of Sertoli cells in an animal model (Taneda *et al.* 2004). Other studies have also shown aberrant sex hormone production in female rats chronically exposed to diesel exhaust, resulting in increased levels of testosterone and masculinization (Taneda *et al.* 2004).

Heart and vascular consequences are also observed after exposure to pollution. There is a higher incidence of ischemic heart disease in smokers who are chronically exposed to diesel emissions (Finkelstein *et al.* 2004). Men who had a previous myocardial infarction, and who were exposed to diesel exhaust during moderate exercise, showed an

increase in coronary vasoconstriction and altered myocardial energetics (Mills *et al.* 2007). Air pollutants reduce heart rate variability, cause ventricular arrhythmia, and increase left-ventricular end-diastolic pressure in animal models (Anselme *et al.* 2007; Wold *et al.* 2006). At levels encountered in an urban environment, inhalation of diesel exhaust impaired two important and complementary aspects of vascular function in humans: the regulation of vascular tone and endogenous fibrinolysis by increasing fibrinogen and plasminogen activator inhibitor-1 (Mills *et al.* 2007; Mills *et al.* 2005). A key fact that led to the hypothesis of this thesis is that with exposure to high levels of diesel exhaust for times as short as 1 hr, there is an increased risk of myocardial infarction (Peters *et al.* 2004).

2. Diesel Exhaust Particles (DEP)

2.1. Composition

DEP arise from diesel-powered engines, and are a mixture of chemicals: gases, water soluble and insoluble components, and particles. Combustion products (nitrogen, water, and CO_2 CO, NO_X, aldehydes, ketones, phenols, and sulphur compounds) are present. Several components have mutagenic and carcinogenic properties. DEP components also include sulfur compounds, heavy metals and hydrocarbons, such as aldehydes, quinones, benzo[*a*]pyrenes, polycyclic aromatic hydrocarbons (PAHs) (Kumagai *et al.* 1997; Wichmann 2007). A schematic of DEP is shown in Fig 1-1, reproduced from Wichmann et al. (Wichmann 2007), as taken from EPA/600/8-90/057F, May 2002.

Fig 1-1. Schematic diagram of DEP. Reproduced from U.S. EPA (2002) Health effects assessment document for diesel engine exhaust. EPA/600/8-90/057F, May 2002.
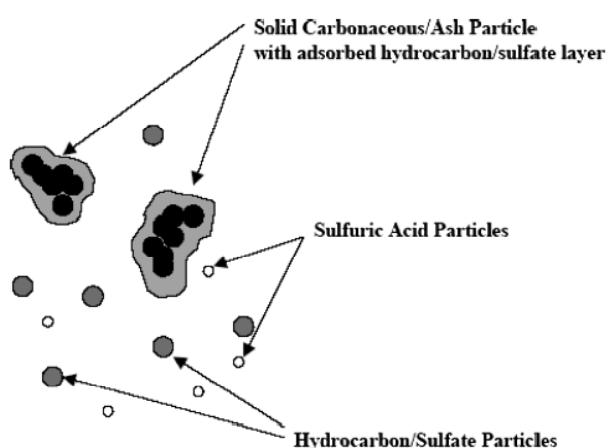
2.2. Particle Size

The aerodynamic diameter of inhalable coarse particles is around 10 μm (i.e., PM_{10}). Combustion typically generates particle sizes smaller than or equal to 2.5 μm in diameter (i.e., $PM_{2.5}$). Within $PM_{2.5}$ are ultrafine PM, or nanoparticles, with diameters smaller than 100 nm (i.e., $PM_{0.1}$). As seen in Fig 1-2 below (Cormier *et al.* 2006), the smaller the particle, the deeper it can be deposited in the respiratory tract. PM_{10} deposits mainly in the upper respiratory tract and may be cleared by mucociliary actions. $PM_{2.5}$ and $PM_{0.1}$ penetrate the alveolar regions of the lung, whereas the ultrafine PM can also penetrate the epithelium (Oberdorster 2001). Clearance of fine and ultrafine PM is mediated mainly by phagocytic activity and particle dissolution (Wagner and Foster 1996).

Fig 1-2. Distribution of PM in the airways. PM ≥10 µm in diameter enter the nose and mouth. The thoracic fraction, PM$_{10}$, passes the larynx and penetrates the trachea and bronchial regions of the lung, distributing mainly at pulmonary bifurcations. The respirable fraction, PM$_{2.5}$, and ultrafine PM, PM$_{0.1}$, enter the nonciliated alveolar regions and deposit deep within the lungs. Figure adapted from Environ Health Perspect, 2006, 114:6,810–817.
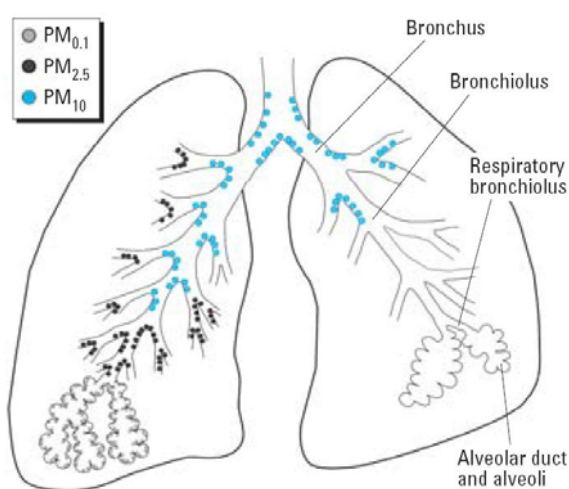
2.3. Mechanisms for how Particles cause cardiovascular diseases

Many factors are likely to influence how short or long term exposure to diesel particles cause adverse cardiovascular effects. Autonomic control could be altered (Peretz *et al.* 2008); proinflammatory (Tornqvist *et al.* 2007), and pro-thrombitic responses could be initiated (Brook *et al.* 2004; Pope and Dockery 2006); or the endothelium could fail to function properly (Tornqvist *et al.* 2007). Such activities could lead to myocardial ischemia (Mills *et al.* 2007) and platelet aggregation, resulting in thrombosis (Brook *et al.* 2003; Nemmar *et al.* 2003), and potentially an acute coronary infarct. These are discussed in more detail below.

Fig 1-3. Putative biological pathways show how PM may cause cardiovascular events. AT2, angiotensin II; CVA, cerbrovascular accident; CHF, congestive heart failure; ET, endothelins; MI, myocardial infarction; PSNS, parasympathetic nervous system; ROS, reactive oxygen species; SNS, sympathetic nervous system; UFP, untra-fine particles; WBC, white blood cells. Adapted from Brook, Clinical Science, 115, 175-187, 2008.
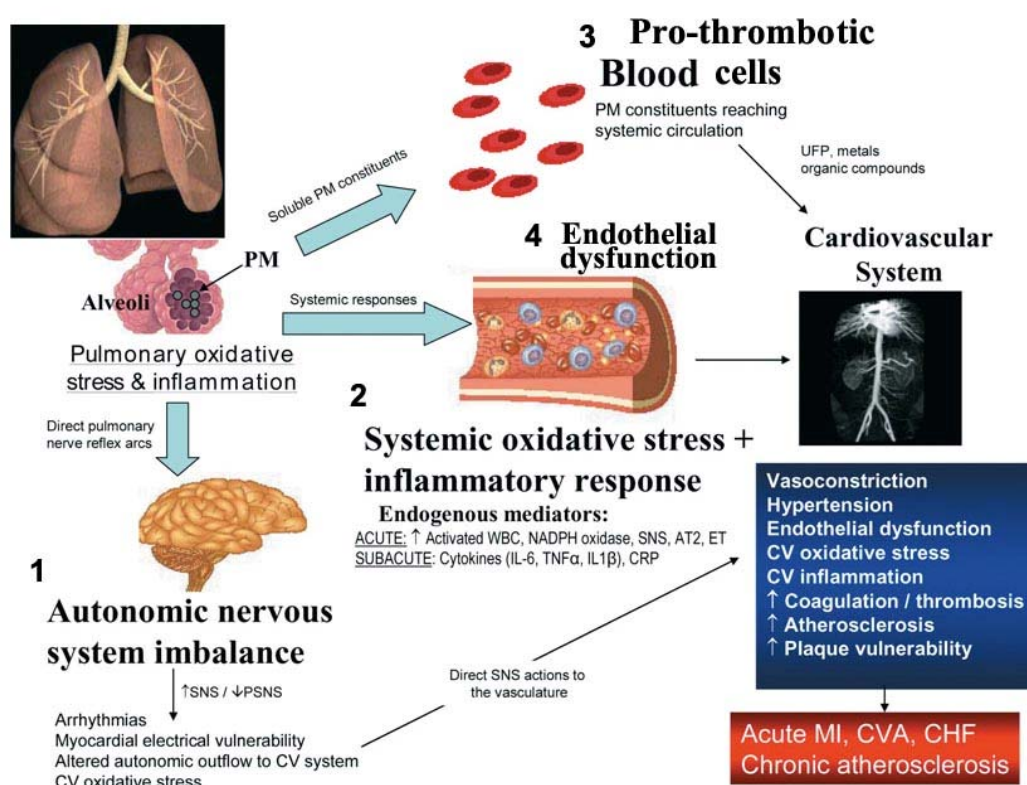
2.3.1. Autonomic Dysfunction

The autonomic nervous system plays a huge role in cardiac rhythm, and has been

hypothesized to be a critical mechanism for how DEP cause cardiovascular events. In general, reduction of heart rate variability reflects a disturbance of cardiac autonomic function and predicts an increased risk for sudden death or mortality. Pope et al. (1999) reported that higher levels of ambient air pollution significantly reduced the overall heart rate in elderly humans (Pope *et al.* 1999). Impaired and increased cardiac vagal autonomic tone has been correlated with the frequency domain in heart rate variability (Pope *et al.* 1999). Inhalation of $PM_{2.5}$ can cause a systemic sympathetic stress response affecting heart rate variability and causing tachyarrhythmias (Brook *et al.* 2003). Long-term exposure to $PM_{2.5}$ can trigger inflammatatory responses that can damage cardiac myocytes and electrophysiological function (Stone and Godleski 1999).

2.3.2. Pro-inflammatory and Oxidative Damage

Many reports have suggested that DEP initiate an inflammatory response that ultimately causes injury. *In vitro* studies have demonstrated that $PM_{2.5}$ up-regulate the secretion of pro-inflammatory cytokines such as interleukin-1β (IL-1β), interleukin-6 (IL-6), and tumor necrosis factor-α (TNF-α) in macrophages, as well as epithelial, and endothelial cells (Auger *et al.* 2006; Jalava *et al.* 2005; Rusznak *et al.* 2000; Veranth *et al.* 2008). Additionally, cultured bronchial epithelial cells exposed to DEP also released interleukin-8 (IL-8) and granulocyte macrophage colony stimulating factor (GM-CSF) in a time and dose dependent manner. Both of these are known to be involved in allergic diseases (Bonvallot *et al.* 2001; Takizawa *et al.* 2000).

Exposure to DEP also induces generation of free radicals that lead to a state of cellular oxidative stress. This has been shown to causes significant damage in both cell

cultures and animal models (Hiura *et al.* 1999; Hiura *et al.* 2000; Li *et al.* 2002; Sagai *et al.* 1993). *In vitro* studies demonstrate that DEP upregulate antioxidant enzymes in various types of cells, including bronchial and pulmonary epithelial cells (Sugimoto *et al.* 2005; Takizawa *et al.* 2000), macrophages, lymphocytes (Al-Humadi *et al.* 2002) and endothelial cells (Bai *et al.* 2001). DEP induce the generation of H_2O_2 (Park *et al.* 2006), a powerful oxidizer which can be converted into hydroxyl radicals (.OH). In organisms, hydrogen peroxide is naturally produced as a byproduct of oxygen metabolism, therefore enzymes such as catalase catalyze conversion of hydrogen peroxide to water and oxygen. In fact, catalase is the most abundant enzyme in the human body.

DEP have a carbonaceous core onto which the toxic components of exhaust are absorbed. These chemicals contain two main families of organic compounds: polycyclic aromatic hydrocarbons (PAHs) and quinines, which can be oxygenated to quinone derivatives that produce ROS in the cells via redox cycling. PAHs desorbed from DEP bind the cytosolic aryl hydrocarbon receptor and induce phase I metabolization enzymes cytochrome P450 1A1 (CYP1A1) and cytochrome P450 1A2 (CYP1A2) in the lung (Bonvallot *et al.* 2001; Rengasamy *et al.* 2003). This mechanism produces electrophilic and reactive metabolites such as 1-nitropyrene (1-NP), 1,3-dinitropyrene (1,3-DNP), and 1,8-dinitropyrene (1,8-DNP). Such oxidative stress can induce DNA damage (Landvik *et al.* 2007). Furthermore, in the lung, DEP-induced chemical derivatization of quinones cause free radicals and diminish the antioxidant capacity of redox cycling via the enzymes CYP reductase and NADPH oxidase. Quinones are suspected to be responsible for the production of superoxide anion (O_2^-) and hydroxyl radicals (Kumagai *et al.* 1997; Risom *et al.* 2005). This can occur as follows: Redox cycling quinones undergo a one electron

reduction to form semi-quinones (Monks and Lau 1992), then semi-quinones are recycled to the original quinones with the formation of O_2^-. The detoxification of quinones occurs by a two electron reduction initiated by the phase II reaction with NADPH-quinone oxidoreductase-1 (NQO-1). Quinones are electrophilies that are able to participate in ROS damage by inducing covalent modification of proteins and DNA strands. Thus, the modification of DEP organics results in DNA adducts, DNA strand breakages, and can result in cell death.

DEP exposure has been shown to generate an ROS response that can overwhelm the antioxidative proteins (Bai *et al.* 2001). To maintain redox cycling equilibrium for cell survival, the cells release antioxidants such as glutathione S-transferase (GST), superoxide dismutase (SOD), NADPH-quinone oxidoreductase-1 (NQO-1), and hemeoxygenase-1 (HO-1). These help neutralize the potent injuries ROS can cause. For example, in response to a 24 hr free radical stimulation, endothelial cells upregulate heme-oxygenase-1 (HO-1) (Fredenburgh *et al.* 2007). This is accomplished by cytoplasmic nuclear factor erythroid 2-related factor 2 (Nrf2) translocating from the cytoplasm to the nucleus where it binds to the antioxidant response element (ARE) that resides in the promoter regions of anitoxidant genes. This upregulates HO-1 mRNA levels via Nrf2/ARE-enhancement of transcription (Chen *et al.* 2003; Hsieh *et al.* 2009).

It is important to realize that ROS and proinflammatory responses go hand in hand. For example, in the bloodstream, TNF-α has pro-oxidative properties, and stimulates generation of ROS in the cardiac muscle of patients with heart failure (Eleuteri *et al.* 2009). In patients with heart failure TNF-α enhances platelet superoxide anion (O_2^-) production (De Biase *et al.* 2003). Also, in airway epithelial cells, the components of DEP adsorbed on

particles elicit inflammation through CYP reductase and NADPH oxidase (Baulig *et al.* 2003). These activate cytokine secretion as well as an oxidative stress response.

2.3.3. Pro-thrombotic Effects

DEP exposure contributes to activation of leukocytes and platelets, and these may ultimately play a role in promoting the progression of atherosclerosis, of which a sequela is life-threatening thrombosis (Pope and Dockery 2006). Pro-thrombotic effects of DEP have been shown by the direct addition of DEP to hamster blood causing platelet aggregation (Nemmar *et al.* 2002). In addition, thrombus formation was increased in evaluations of hamster femoral veins after intratracheal installation of DEP (Nemmar *et al.* 2002; Nemmar *et al.* 2004b).

2.3.4. Endothelial Dysfunction

Endothelial dysfunction is a reduction or loss of normal physiological processes carried out by the endothelium, the cells that line the inner surface of blood vessels. Normal functions of endothelial cells include mediation of coagulation, platelet adhesion, immune function, blood volume control and electrolyte balance of the intravascular and extravascular spaces. Endothelial dysfunction can result from disease processes, such as septic shock and diabetes, or from environmental insults, such as air pollution and tobacco smoke (Pope and Dockery 2006). Importantly, particulate air pollution has been associated with increased blood pressure in cardiac rehabilitation patients (Zanobetti *et al.* 2004) and in those with chronic obstructive pulmonary disease (Ko and Hui 2009). PM-related endothelial dysfunction could be a key event in the development of atherosclerosis, having

effects long before clinically obvious vascular pathology is found.

The aspect of endothelial dysfunction that caught our attention is endothelial permeability. There is evidence that $PM_{2.5}$ is more toxic because of the larger surface area of small particles (Ferin and Oberdorster 1992; Oberdorster *et al.* 1994; Peters *et al.* 1997). To investigate how $PM_{2.5}$ might cause pro-thrombotic effects leading to myocardial infarctions, particles were followed for whether or not they crossed the pulmonary epithelium and entered the systemic circulation, putting them in a position to cause direct toxic effects on vascular endothelium and the heart (Brook *et al.* 2003). Ultrafine ^{13}C labeled carbon particles, in whole body inhalation chambers showed that particles could deposit in the lung, reach the blood compartment, and travel to the liver (Oberdorster 2002). However, intratracheal installation of [192]Iridium particles showed that the amount of material reaching the systemic circulation was very low, although translocation did occur (Kreyling *et al.* 2002). In a multi-particle study, ^{99m}Tc labeled carbon particles were inhaled by humans and radiolabel was found in blood within minutes, while intratracheal installation of DEP in animals enhanced venous thrombus formation (Nemmar *et al.* 2002; Nemmar *et al.* 2004b). Inhaled ultrafine titanium dioxide showed particles within and beyond the alveolar epithelial barrier, on the luminal side of airways and alveoli, and even some within capillaries (Geiser *et al.* 2005). Rats who were ventilated with aerosols of 20 nm or 80 nm iridium, or with 25 nm [192]iridium-labeled carbon particles demonstrated that, 24 hr later, most of the particles were in the peripheral lung, although small percentages (typically less than 1%) reached other organs. Slightly more than 1% of the 20 nm-sized particles ended up in the blood compartment (Kreyling *et al.* 2009). Overall, these observations suggest that translocation into the systemic circulation is a real, if infrequent,

phenomenon. It is possible that the infrequency of translocation of inhaled particles to the circulation is overshadowed by the toxicity of the interaction of particles with platelets in the blood. This idea has led us to design experiments to investigate what mechanisms might be involved in DEP reaching the circulation.

Vascular Endothelial Cell Growth Factor-A (VEGF-A), initially discovered functionally and termed vascular permeability factor (VPF) (Connolly *et al.* 1989; Dvorak 2002; Ferrara and Henzel 1989; Keck *et al.* 1989; Senger *et al.* 1983) is a likely candidate for making endothelial cells permeable enough to allow translocation of DEP into the vasculature. HO-1 induces VEGF-A expression (Dulak *et al.* 2008), thereby modulating vasculature permeability (Deramaudt *et al.* 1998; Freitas *et al.* 2006). Oxidative stress in endothelial cells after DEP exposure should increase VEGF-A secretion, and contribute to endothelial dysfunction by making capillaries permeable.

3. Model systems used to study DEP-induced health effects

Studies have been performed in humans, animals and in culture to attempt to understand how DEP cause injury. Below are just a few examples of these model systems, highlighting some of the types of results one can obtain.

3.1. Human studies

Human exposure studies have been carried out by using inhalation chambers with controlled DEP emission. The exposure chamber is a critical system that is designed to maintain the same size of experimental particle, and obtain consistent chemical properties

of DEP components. In other studies, volunteers in areas of pollution have been recruited to wear personal monitors. Monitors have also been placed in public areas to collect measurements on pollutants to correlate with a local population. The goal is to correlate the level of pollution with as many kinds of physical measurements as possible. These can include lung function, heart function, with blood pressure and other assessments, as well as cognitive function.

BAL fluid collected from exposed patients has shown that 18 hr after diesel exhaust exposure there is a significant decrease in the number of mast cells in the bronchi and an increase in neutrophils in the bronchoalveolar region (Rudell *et al.* 1999). Exposure to diesel exhaust caused increases in airway resistance as well as airway inflammation with BAL neutrophilia, and macrophage phagocytosis was reduced (Rudell *et al.* 1996).

Nasal lavage and nasal scraping have been useful to study the inflammatory response to DEP and the relation of DEP to allergies. The effect of DEP exposures (1, 0.3 or 0.15 µg DEP in 200ul saline) has been examined by nasal lavage (Diaz-Sanchez *et al.* 1994). After 0.3 mg DEP treatment for 4 days, IgE was increased significantly in the nasal lavage, but other Ig-classes were not detected. When combined with an allegen, DEP acted as an adjuvant. A combination of 0.3 mg DEP and the ragweed allergen *Amb a I* increased not only IgE production, but also expression of immunoglobulin-G4 (IgG_4) in the lavage fluid. Cells in the lavage mRNA for Th2-type cytokines, IL-4, IL-5, IL-6, IL-10, and IL-13 (Diaz-Sanchez 1997). The limitation of the studies is that it only accounts for components that are collected into the lavage fluid.

3.2. Animal studies

Rodents can be used for chronic and acute diesel exposure studies. In one chronic study, mice were exposed 6 hr/day to diesel exhaust for 6 months in whole body exposure chambers. Results showed that exhaust suppressed T-cells proliferation, but increased B-cells proliferation at 30 $\mu g/m^3$ exposures (Burchiel *et al.* 2004).

Many acute studies in animals involve intratracheal installation to study the *in vivo* toxicity of DEP. DEP were found to cause severe lung injury and high mortality in mice when 400-1,000 μg DEP/mouse was instilled intratracheally (Sagai *et al.* 1993). Death was caused by endothelial cell damage and pulmonary edema. Furthermore, Inoue et al. (2006) demonstrated that inhalation of DE on lung inflammation related to lipopolysaccharide. They treated mice for 12 hr with DEP and lipopolysaccharide. Lung inflammation and lung expression of pro-inflammatory chemokines including macrophage chemoattractant protein-1 and keratinocyte chemoattractant were evaluated 24 hr after intratracheal administration. DEP inhalation decreased lipopolysaccharide-elicited inflammatory cell recruitment into the bronchoalveolar lavage fluid as compared with clean air inhalation (Inoue *et al.* 2006). On the other hand, one experiment was carried out to clarify the roles of chronic DEP exposure on rat lung tumorigenesis. The male rats were intratracheally administered DEP for 10 months. After the treatment, lung tumorigenesis and DNA adduct formation were observed in the animals administered DEP with exposure to NO_2 and/or SO_2, but not in the administered DEP alone. These findings demonstrated that DEP cause DNA damage in alveolar epithelial cells, and that long term exposure to components like NO_2 and/or SO_2 in air pollution promotes induction of lung tumors (Ohyama *et al.* 1999).

Pertinent to our studies are the animal studies showing ultrafine particles may pass from the lung into the systemic circulation (Kreyling *et al.* 2002; Kreyling *et al.* 2009; Nemmar *et al.* 2006; Nemmar *et al.* 2002; Nemmar *et al.* 2004b; Nemmar *et al.* 2003; Nemmar *et al.* 2001; Oberdorster 2002).

3.3. *In vitro* Studies

To look more closely at cell-type specific responses of DEP-induced cytotoxicity, and mechanisms for how DEP exposure causes injury, *in vitro* studies have been performed on human and animal cells, using lung and nasal epithelial cells, macrophages, endothelial cells (monolayer), and platelets. While not as biologically relevant as using animals, cell culture systems avoid the compounded results from multiple cell types, and assess the contribution of DEP to the transformation, signal generation, or apoptosis, etc, of a single cell type. The examples below illustrate this point.

Airway epithelial cells play a prominent role in the pathogenesis of respiratory disease. DEP exposure increased the release of pro-inflammatory cytokines IL-6, IL-8, and GM-CSF in nasal and bronchial epithelial cell (Devalia *et al.* 1997). After exposure to DEP with diameters ranging from 25-35 nm, a human bronchial epithelial cell line, BEAS-2B, phagocytized the particles and secreted IL-6 and IL-8 (Steerenberg *et al.* 1998). Nasal epithelia, cultured in an air-liquid interface to maintain the cells' differentiation state, were exposed to DEP for 24 hr and demonstrated a local inflammatory response with IL-8 and amphiregulin. However, evidence for initiating a systemic inflammatory response was not observed. No IL-1β secretion was seen, and only weak non-reproducible secretion of TNF-α. Small nanoparticles (< or =40 nm) were internalized, but not larger ones (Auger *et*

al. 2006). DEP induced cell death in normal human bronchial epithelial (NHBE) cells, mainly by generation of hydrogen peroxide and nitrogen monoxide. Moreover, exposure of NHBE cells to high concentrations of DEP decreased the cellular levels of glutathione (GSH) (Matsuo *et al.* 2003). In another human airway epithelial cell study, DEP induced a dose-dependent stimulatory effect on eotaxin production by activating NF-κB, but did not induce signal transducer and activator of transcription (STAT) (Takizawa *et al.* 2003).

Alveolar macrophage studies on DEP exposure demonstrated that more IL-1β was secreted after exposure high doses of DEP, but that TNF-α levels were unaffected by varying DEP concentrations. Furthermore, the organic extracts of DEP inhibited LPS-stimulated production of IL-1β and TNF-α (Yang *et al.* 1997).

Monolayer cultures have been the only endothelial cell model used to study the effects of DEP (until our work). Human pulmonary artery endothelial and human umbilical vein endothelial cells (HUVECs) have been shown to respond to DEP by generating ROS. Antioxidant enzymes, such as SOD and catalase, as well as the compounds N-(2-mercaptopropionyl)-glycine (MPG) and ebselen (a selenium-containing compound with glutathione peroxidase-like activity) reduced the cytotoxicity of DEP. Also, inhibiting NO synthase with L-NAME and L-NMA also attenuated DEP-induced cytotoxicity (Bai *et al.* 2001).

3.4. *In vitro* Capillary-like Tubes

Hundreds of studies have followed angiogenesis by observing the ability of compounds to induce *in vitro* endothelial tube formation. We have used these capillary-like structures after they are fully assembled to evaluate how DEP might affect the vasculature.

In contrast to endothelial cells plated on plastic as monolayers, endothelial cells applied to Matrigel for tube formation do not proliferate. *In vivo*, endothelial cell proliferation is strictly prohibited and requires specific signals (the "angiogenic switch") to overcome the proliferation blockade (Clement *et al.* 1999; Hanahan and Folkman 1996). Endothelial tubes replicate this *in vivo* property of prohibited proliferation. Angiogenesis studies have demonstrated that endothelial capillary tubes formed *in vitro* have many similarities with capillaries *in vivo* (Donovan *et al.* 2001; Grant *et al.* 1991; Zimrin *et al.* 1995). Lubarsky and Krasnow (2003) have demonstrated that endothelial cells form lumens and tubular structures during morphogenetic processes (Lubarsky and Krasnow 2003). To illustrate these events, Iruela-Arispe and Davis (2009) prepared a movie of *in vitro* endothelial cell morphogenesis in which initial endothelial cell invasion was followed by the appearance of endothelial luminal structure (Iruela-Arispe and Davis 2009). The movie not only showed that vessel morphogenesis is a highly dynamic process involving invasion, motility, and lumenogenesis, but also provided direct evidence that *in vitro* endothelial tubes are more similar to *in vivo* capillaries than endothelial monolayers are.

4. Properties of Endothelial Cells

4.1 Endothelial Junctions

Intercellular endothelial cell junctions mediate adhesion and communication between neighboring endothelial cells or epithelial cells. In the endothelium, junctional complexes are gap junctions, tight junctions, and adherens junctions. Gap junctions are communication structures, which allow the passage of small molecule weight (smaller than

1,000 Daltons) solutes between adjoining cells. The connexins allows for chemical communication between cells, through the transmission of small second messengers, such as IP_3 and Ca^{2+} (Olk *et al.* 2009).

In epithelial cells tight junctions mediate some permeability function and maintain cell polarity by subdividing the plasma membrane into apical and basolateral domains. However, tight junctions in endothelial cells have not been as extensively studied. This is likely because: (1) tight junctions are not clearly localized in endothelia, and they are mixed in with other junctions; and (2) The organization of tight junctions in the vessels varies—they are well developed in arteries, but less distinct in veins, venules, and capillaries. However, in the brain they are well organized and contribute to the blood brain barrier (Bazzoni and Dejana 2004).

Like other junctional organelles, tight junctions are composed of both integral membrane proteins and intracellular proteins, each capable of multiple functions (Stevenson and Keon 1998). The transmembrane proteins include occludin, claudins, and junctional adhesion molecule-A (JAM-A). The intracellular proteins include ZO proteins (ZO-1, ZO-2, and ZO-3), and AF-6/Afadin, PAR-3/ASIP, and MUPP-1 (Bazzoni and Dejana 2004).

Adherens junctions are important structural determinants of endothelial cells that play a role in permeability. These organelles are also formed by a complex network of transmembrane proteins linked to the cytoskeleton and to signaling proteins. A major important characteristic of endothelial adherens junctions is that they are dynamic. Endothelial cells can quickly change the structure of the adherens junctions to allow the passage of plasma or circulating blood cells (Dejana *et al.* 2008). Endothelial junctions

reorganize in response to whatever is required at a particular time for the tissue they are found in (Simionescu and Simionescu 1991).

The adherens junctions contains VE-Cadherin, aka cadherin 5 (Lampugnani *et al.* 1992), desmoplakin, plakoglobin, β-catenin, α-catenin, p120, and VEGFR-2, with minor amounts of vinculin and alpha-actinin. They do not contain any of the usual desmosomal cadherins (desmogleins and desmocollins), nor E- and M-cadherin. The arrangement of adherens junctions from *in vivo* vessels has been reconstructed from electron micrographs, and micrographs of capillary tubes formed *in vitro* demonstrate that the *in vivo* and *in vitro* structures are similar (Schmelz and Franke 1993; Zhou *et al.* 2004).

4.2. Vascular permeability

Vascular permeability is of medical interest because it is involved in pathological conditions such as diabetic retinopathy and tumor growth (Folkman and Hanahan 1991; Folkman and Klagsbrun 1987). Angiogenesis, the spouting of new capillaries from preexisting blood vessels, has been found to be an important component in the pathogenesis of these disorders (Folkman and Klagsbrun 1987). During the angiogenesis process, endothelial cells become permeable, bud from the existing vessel, then are stimulated to proliferate and extend new capillary tubules in response to soluble endothelial growth factors (Folkman and Klagsbrun 1987). Vascular endothelial cell growth factor-A (VEGF-A) is a major mediator in both physiological and pathophysiological angiogenesis (Ferrara *et al.* 1993). Initially identified in the media of tumor cell lines as vascular permeability factor (VPF), VEGF-A is synthesized and released from normal cells such as endothelial cells, vascular smooth cells, lung epithelial

cells, and pituitary folliculo-stellate cells. Although VEGF-A and other growth factors including fibroblast growth factors (FGF) and epidermal growth factor (EGF) are able to stimulate endothelial cell growth and migration (Unemori *et al.* 1992), only VEGF-A is capable of enhancing vascular permeability (Connolly *et al.* 1989).

VEGF-A is the prototype member of a gene family that also includes placenta growth factor (PlGF), VEGF-B, VEGF-C, VEGF-D, and orf-virus-encoded VEGF-E (Ferrara *et al.* 2007). Because VEGF-A is the only one capable of enhancing vascular permeability, we will limit our discussion to this molecule. As mentioned, VEGF-A was initially discovered functionally and was called vascular permeability factor (VPF) (Connolly *et al.* 1989; Dvorak 2002; Ferrara and Henzel 1989; Keck *et al.* 1989; Senger *et al.* 1990; Senger *et al.* 1983). It can be alternatively spliced into 5 different isoforms including VEGF-A$_{121}$, VEGF-A$_{145}$, VEGF-A$_{165}$, VEGF-A$_{189}$, and VEGF-A$_{206}$ (Breen 2007). Permeability does not easily correlate with any particular isoform, and it has been suggested that persistent VEGF-A expression may be the crucial permeability factor to consider (Esser *et al.* 1998). The role of VEGF-A in cancer-related angiogenesis has been reported in thousands of papers, along with VEGF-A inhibitors for therapy. Because VEGF-A increases vascular permeability to plasma and plasma proteins, cancer-related edema is often also treated with inhibitors of VEGF-A (Gerstner *et al.* 2009).

VEGF-A binds to two highly related receptors, VEGFR-1 (aka Flt-1) and VEGFR-2 (aka KDR or Flk-1). VEGFR-2 is the major mediator of the mitogenic and angiogenic effects, while VEGFR-1 appears to modulate VEGFR-2 function. Both, however, contribute to permeability in reponse to VEGF-A (Holmes *et al.* 2008; Olsson *et al.* 2006). Binding of VEGF-A to VEGFR-2 makes the complex undergo dimerization and

ligand-dependent tyrosine phosphorylation to transmit pro-permeability and pro-survival (or anti-apoptotic) signals through the phosphatidylinositol 3-kinase (PI3K)/Akt pathway in endothelial cells (Gerber *et al.* 1998).

Another big contributor to permeability is the adherens junctions. Intact adherens junctions are required to prevent capillary leakiness (i.e., permeability) (Gallicano *et al.* 2001). However, endothelial permeability must be quickly adjustable to be able to respond to local conditions. This is regulated in part by the dynamic opening and closure of endothelial adherens junction. Dynamic redistribution of VE-cadherin from the capillary endothelial cell membrane to patches near the cell-cell junctions occurs in response to external stimuli such as inflammation (Gabrys *et al.* 2007; Lim *et al.* 2001). Dissolution of these junctions results in relocation of components to cytoplasm, where they do NOT undergo degradation, but instead they transmit signals or are reused (Guo *et al.* 2007; Lim *et al.* 2001). Agents that increase permeability by affecting the adherens junctions are inflammatory cytokine IL-6 and H_2O_2 (Dudek and Garcia 2001; Kevil *et al.* 1998; Maruo *et al.* 1992; Mehta and Malik 2006). A depiction of how adherens junctions open to allow permeability is shown in Fig 1-4.

Fig 1-4. Factors affecting endothelial junctions and permeability. (A) Under normal conditions, VE-cadherin, plakoglobin (plako), β-catenin (βcat), p120, and α-catenin (αcat) cluster at junctions in a zipper-like structure. (B) Phosporylation (P) of tyrosine residues on VE-cadherin and the other junctional proteins can disrupt cell to cell interactions. Such disruption would disorganize the VE-cadherin complex and increase endothelial permeability. (C) Permeabilizing agents may act by causing

endothelial cell retraction, causing intercellular gaps that break the adherens junctions. (D) Antibodies against VE-cadherin are known to disrupt cell to cell adhesion and open intercellular gaps that increases vascular permeability. Adapted from Dejana et al. Journal of Cell Science, 121:2115-2122, 2008.
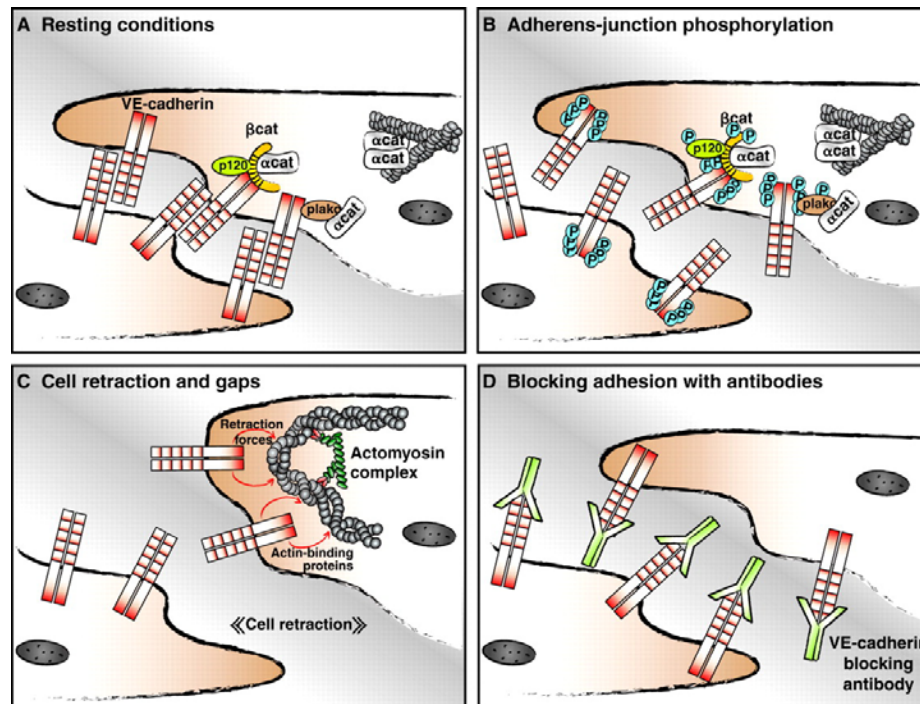
Activation of the Akt pathway has been implicated in blood vessel permeability (Chen *et al.* 2005). However, this pathway plays a large number of roles in the regulation of many essential cellular functions, including glycogen metabolism (Skurk *et al.* 2005), cellular transformation (Bellacosa *et al.* 2005), and cell survival (Franke *et al.* 1997; Somanath *et al.* 2006). In normal vasculature, survival is maintained through an association of VE-cadherin with VEGFR-2. The complex activates PI3-kinase and leads to the phosphorylation of Akt (Carmeliet *et al.* 1999; Dejana 2004). A simplified schematic of elements involved in the cell survival pathway are shown in Fig 1-5.

Fig 1-5. The association of VEGFR-2 and VE-cadherin facilitates endothelial cell survival.
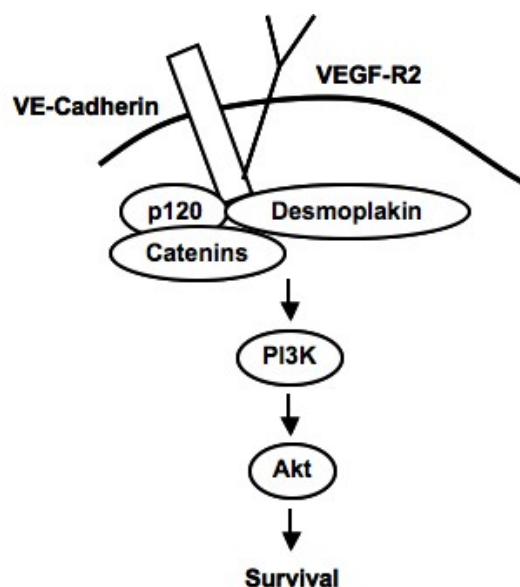
The downstream substrates that facilitate cell survival include Bcl-xL/Bcl-2 associated death (BAD), Forkhead factors receptor (FKHR), IκB kinase-α (IKKα), murine double minute-2 (Mdm2), Yes-associated protein (YAP), caspase-9, and glycogen synthase kinase 3 (GSK3). Although a variety of pathways can mediate apoptosis, the p53 pathway has a common element with the PI3-kinase/Akt survival pathway: Mdm2 protein. Mdm2 is a negative regulator of p53-mediated transcription (Alarcon-Vargas and Ronai 2002; Honda *et al.* 1997; Oliner *et al.* 1993). PI3-kinase/Akt serves as an important anti-apoptotic signal by phosphorylating Mdm2 at Ser-166 and Ser-186. This phosphorylated Mdm2 binds p53, preventing apoptosis (Ogawara *et al.* 2002). DEP exposure down-regulates Mdm2, increasing p53 phosphorylation in macrophages (Yun *et al.* 2009).

Akt-mediated permeability is shown as part of Figure 1-6 (taken from Kowanet and Ferrara, 2006). VEGFR-2 and VE-Cadherin are in close proximity in the membrane. A Src (Src or Shb) kinase is associated with VE-cadherin, but does not phosphorylate it until VEGFR-2 is bound by VEGF and is phosphorylated. By bridging the two transmembrane molecules, Src allows the phosphorylation of VE-cadherin. This series of events facilitates VEGF-A-dependent PI3K activation, which facilitates cell survival. In addition, the VEGF-A-VEGFR-2-VE-caderin interactions may initiate a pathway leading to increased production of NO, which results in an increase of vascular permeability.

Fig 1-6. Akt-mediated permeability.
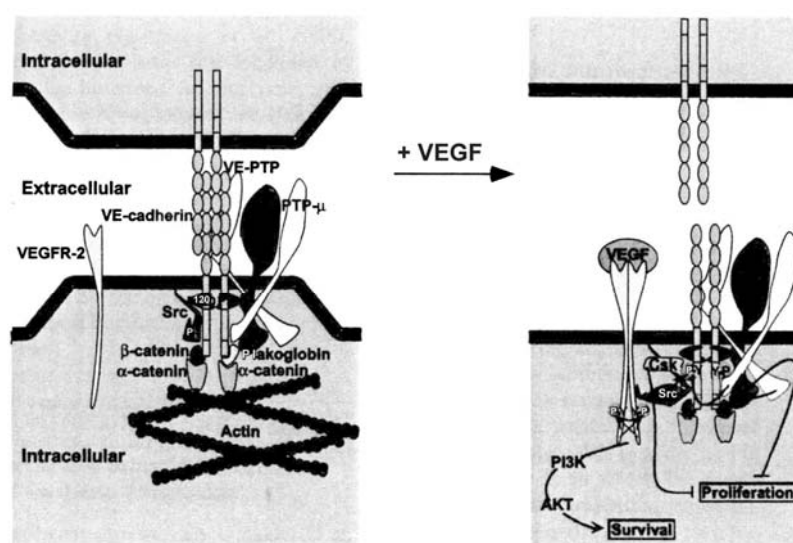
Adapted fromWallez et al., Trends in Cardiovasc Med 16:55-59, 2006

Statement of Hypothesis

My hypothesis is that some of the acute effects caused by inhaling DEP may result from translocation of particles from the alveolar space to the capillary lumen. Translocation could occur if DEP were found to cause cell-cell junctional damage, an event that could allow particles to pass into the vessel lumen. Translocation could also result if vessels were made more permeable by DEP. If vessels become more permeable, a likely cause would be induction of Vascular Endothelial Growth Factor-A (VEGF-A, aka Vascular Permeability Factor) secretion in response to DEP. In addition, DEP may initiate signaling through the Akt pathway, which has been shown to increase vascular permeability. Once in the capillaries, DEP would be in a position to directly affect leukocytes and platelets, cells known to play a role in the acute effects of DEP.

To test the hypothesis, Human Umbilical Vein Endothelial Cells (HUVECs) assembled into capillary-like tubes were used to address the following three specific aims:

Specific aims

Aim 1: To evaluate whether diesel exhaust particles cause the redistribution of the permeability-modulating junctional molecule, VE-cadherin, away from the plasma membrane; also, to assess whether particles gain access to the lumen of preformed endothelial tubes after 24 hr exposures to DEP. The cytotoxicity of various concentrations of DEP was assessed and the redistribution of the cell-cell attachment molecule VE-cadherin was evaluated in human umbilical vein endothelial cell (HUVEC) tubes. Epifluoresence and confocal microscopic imaging of the cell membrane using a VE-cadherin antibody verified that the adherens junction molecule is redistributed away from the cell membrane to an internal location in response to DEP. The data from these

experiments also demonstrated that particles are found within the endothelial cell cytoplasm and with the lumen of endothelial tubes. The results suggest that the three dimensional character of HUVEC tubes is useful for providing information on the mechanisms of DEP toxicity.

Aim 2: **To evaluate whether diesel exhaust particles exposure alters vasculature permeability by generating ROS and by inducing the secretions of pro-inflammatory cytokines**. *In vitro* endothelial tubes were evaluated for mechanisms likely to increase vascular permeability. Examined were the induction of endothelial proinflammatory cytokines, reactive oxygen species, such as H_2O_2, and HO-1 dependent VEGF-A secretion in response to DEP. The oxidative stress induced by DEP caused generation of H_2O_2, which is known to cause VE-Cadherin redistribution and to make vessels leaky. As a result of oxidative stress, hemeoxygenase-1 was induced, as were pro-inflammatory cytokines TNF-α and IL-6. In addition, induction of HO-1, TNF-α and IL-6 was found to be linked to an increase in VEGF-A levels. These data suggest that DEP exposure results in vascular permeability by inducing pathways that generate anti-oxidant and pro-inflammatory responses.

Aim 3: **To identify whether the Akt pathway contributes to endothelial permeability.** Permeability can be increased by the activation of the Akt pathway, as can cell survival. Because DEP cause apoptosis and permeability, the Akt pathway can contribute to only one, or neither, of these phenotypes. We hypothesized that DEP activated Akt to favor permeability. Our results suggest that the hypothesis was incorrect. Increasing levels of

DEP reduced phosphorylation of Akt, thus inhibiting the survival pathway. However, low levels of DEP caused lower levels of death, and correlated with upregulation of the anti-apoptotic protein Mdm2. Binding of Mdm2 with p53 would attenuate the p53 pro-apoptotic activity. At the high dose of DEP, Mdm2 expression was not maintained, freeing p53 to induce apoptosis.

Chapter I

Vascular Endothelial Cell-Cadherin is Redistributed Away From the Plasma Membranes of Endothelial Tubes in Response to Diesel Exhaust Particles

ABSTRACT

The integrity of the adherens junctions in response to diesel exhaust particles (DEP) was evaluated *in vitro* using human umbilical vein endothelial cell (HUVEC) tubes. There was no net proliferation or net cell death of untreated endothelial tubes in 48 hour cultures. Increasing concentrations of DEP added to tubes induced increased cytotoxicity. DEP also increased the redistribution of Vascular Endothelial Cell-Cadherin (VE-Cad) away from the cell-cell junctions to an intracellular location. Since tubes are three dimensional, particles could be identified as being on cells, being within cells or being within the tubular lumen. Endothelial tubes offer a simulated biological-like setting to study the effect of DEP on the permeability and leakiness of vessels in the absence of inflammatory cells, and may contribute to the understanding of the acute and chronic cardiovascular effects of inhaled diesel exhaust.

Key Words: VE-cadherin; endothelial cells; endothelial tubes; diesel exhaust particles; toxicity

Abbreviations: DEP, diesel exhaust particles; HUVEC, human umbilical vein endothelial cells; $PM_{2.5}$, particulate matter with diameters equal or less than 2.5 μm; VE-Cad, vascular endothelial cadherin.

INTRODUCTION

Epidemiological and experimental studies demonstrate an association between short term exposure to ambient air fine particulate matter and adverse cardiovascular events (Peters *et al.* 2001; Pope and Dockery 2006). Well characterized diesel exhaust particles (DEP) derived from a Japanese automobile engine (Bai *et al.* 2001; Sagai *et al.* 1993; Singh *et al.* 2004) may provide a partial explanation for the epidemiology, since involuntary aspiration delivery of these particles to mouse lungs caused injury characterized by vascular leakage. Organic extracts from these particles showed little effect (Singh *et al.* 2004), suggesting that injury from these specific DEP reflect a particle-dependent vascular response. The fraction of particulate matter with diameters equal to or less than 2.5 μm ($PM_{2.5}$) has been associated with adverse cardiovascular effects (Brook *et al.* 2004; Fan *et al.* 2008; Pope *et al.* 2004; Pope and Dockery 2006; Samet *et al.* 2000). In general, smaller particle sizes appear to be more toxic (Ferin and Oberdorster 1992; Oberdorster *et al.* 1994; Peters *et al.* 1997). The particulate content of diesel exhaust is a significant contributor to $PM_{2.5}$ in urban areas (Franck and Herbarth 2002; Kinney *et al.* 2000; Yue *et al.* 2006).

The mechanisms underlying the cardiovascular effects of $PM_{2.5}$ have not been fully elucidated. In one hypothesized pathway, ultrafine particles (those with 0.1 μm, which are a component of $PM_{2.5}$) cross the pulmonary epithelium and enter the systemic circulation. This could lead to direct toxic effects on vascular endothelium and the heart (for review, see Brook *et al.* 2003). In support of this, inhaled ultrafine ^{99m}Tc labeled carbon particles were shown to reach the lungs (Brown *et al.* 2002; Nemmar *et al.* 2002). Particles likely gained access to the circulation, since within one hour, one group showed they accumulate

in the liver (Nemmar *et al.* 2002). Other evidence for translocation of particles to the circulation was present in Oberdorster et al., 2002; Kreyling et al., 2002; Nemmar et al., 2004; Geiser et al., 2005; and Kreyling et al., 2009.

As an *in vitro* model system to dissect the impact of DEP and other particulate matter on *in vivo* capillary endothelia, investigators have exclusively used monolayer cultures of endothelial cells. However, many lines of evidence suggest that a more *in vivo*-like differentiated state is achieved when cells in culture are plated on an extracellular matrix that is similar to their *in vivo* matrix (Barcellos-Hoff *et al.* 1989; Hadley *et al.* 1985). It has long been known that endothelial cells in culture on a basement membrane matrix make endothelial tubes, therefore, cultured tubes were used to model the three dimensional character of *in vivo* capillaries. Studies of angiogenesis over the last 30 years have demonstrated that endothelial capillary tubes formed *in vitro* have many similarities with capillaries *in vivo* (Donovan *et al.* 2001; Grant *et al.* 1991; Zimrin *et al.* 1995). Therefore, endothelial tubes were formed *in vitro* and were used for the purpose of testing the integrity of their adherens junctions after exposure to DEP.

Here it is reported that DEP exposure causes cytotoxicity and redistribution of vascular endothelial cell cadherin (VE-Cad) in human umbilical vein endothelial cell (HUVEC) tubes. Epifluoresence and confocal microscopic imaging of the cell membrane using VE-Cad antibody showed the junctional molecule is redistributed away from the cell membrane to an internal location in response to DEP. Overall, the data demonstrate that endothelial tube networks offer an additional *in vitro* tool for evaluating the mechanisms of DEP toxicity.

MATERIALS AND METHODS

Cell culture

Normal human umbilical vein endothelial cells (HUVECs) from Clonetics (Lonza Walkersville, Inc.) at passages 5-15 were cultured in EBM-2 Bulletkit medium (Lonza), an endothelial cell growth medium containing 2% FBS. In addition, medium was supplemented with phosphate buffered saline and Tween-80 to make the final concentration 1x PBS, 0.05% Tween-80 (1x PBS is 137 mM NaCl, 2.7 mM KCl, 10 mM Sodium Phosphate dibasic, 2 mM Potassium Phosphate monobasic, pH 7.4.). This was done to minimize differences between non-DEP exposed controls and DEP treated samples, since the DEP were dissolved in 1x PBS, 0.05% Tween-80. In all cases below, the term "medium" refers to medium/PBS-Tween-80. Cells were grown in a 5% CO_2 atmosphere at 37°C in tissue culture flasks. Medium was changed every day. For cell propagation, monolayers were subcultured to about 85% confluency. Note that the experiments reported involve endothelial tubes. However, monolayer cultures were tested in several experiments for comparison and understanding. Such tests are mentioned in the Materials and Methods section, but data are not shown in the results.

Endothelial capillary tube cultures

For endothelial capillary tube cell cultures, a basement membrane matrix substratum, 10 mg/ml LDEV-free Matrigel (BD Biosciences), was used to coat 12-well and 6-well dishes on ice for tube formation. 120 μl Matrigel per well was used for the 12 well plates, and 150 μl/well for the 6 well plates. The Matrigel was allowed to solidify at 37°C for 30 minutes before adding cells. HUVECs were plated onto 12-well (using 6×10^4 cells per well) and 6-well (using 1.5×10^5 cells per well) in EBM-2 Bulletkit medium

(Lonza) with the supplemented PBS and Tween as described above. In both cases, this represented a cell density of 156 cells/mm^2. When monolayer cultures were plated for comparison, HUVECs were plated at the same density on plastic dishes.

Timing of endothelial capillary tube formation

HUVECs were seeded onto Matrigel-coated 6 well plates at 1.5 X 10^5 cells/well, and were allowed to form tubes at 37°C. Medium was changed everyday. At 1, 2, 4, 6, 12, and 24 hours after plating, cells were fixed with 4% paraformaldehyde for 10 minutes at room temperature. DAPI (1 ml/well of 300 nM final concentration in PBS) was used to stain nuclei after fixing. Capillary tube formation was observed by phase contrast microscopy (Zeiss-Axiovert 40 Inverted Microscope), and photos were taken at 100X magnification. By 12 hours after plating capillary endothelial tube formation was complete.

Diesel exhaust particles (DEP)

DEP were collected from a Japanese automobile diesel engine by Dr. Masaru Sagai, Aomori University of Health and Welfare, Aomori, Japan (Sagai *et al.* 1993) and characterized in other studies (Bai *et al.* 2001; Singh *et al.* 2004). These particles were dispersed in three different ways to find the best method of achieving a particle size of PM$_{2.5}$ and smaller. The first sample was suspended in sterile phosphate buffered saline (PBS) and vortexed for 3 minutes. The second sample was vortexed for 3 minutes in PBS containing 0.05% Tween 80, and the third sample was vortexed for 3 minutes and sonicated at 60 Hz for 5 minutes in PBS containing 0.05% Tween 80. Particles were fixed with 4% paraformaldehyde, applied to a slide and examined at 630X magnification by confocal microscopy (Leica TCS SP2 Spectral Confocal Microcope) 24 hours after adding

them to the culture medium to evaluate sizes. This showed a particle range from around 2.5 µm to 100 nm, the limit of light microscopy. Since smaller particles were likely present, particle size was also measured using dynamic light scattering on a Zetasizer Nano ZS90 with Malvern DTS software version 5.10 (Malvern Instruments, Malvern, MA), an instrument in the laboratory of Dr. Kathryn Uhrich, Department of Chemistry, Rutgers University. Measurements were made with the assistance of Sarah Sparks and Sarah Hehir. The following conditions were employed: temperature, 25°C; material RI, 1.59; material absorption, 0.01; dispersant RI, 1.33; viscosity, 0.8881 (cP); measurement position, 4.65 (mm). The mean of 6 runs (120 sec/run) revealed an average diameter of 254.7 nm ± 138.72 SD. Since there is a ten fold difference between the mean and the largest sizes, it is likely there is a ten fold difference between the mean and the smallest sizes. If true, this suggests particles range from 2.5 µm to 25 nm.

Proliferation assay (MTS)

Cell proliferation was measured using a colorimetric proliferation assay kit that measures mitochondrial enzyme activity via conversion of MTS (3-(4,5-dimethylthiazol-2-yl)-5-(3-carboxymethoxyphenyl)-2-(4-sulfophenyl)-2H-tetrazo lium) and phenazine methosulfate to formazan (MTS kit, Promega). HUVECs (6 X 10^4 cells/well) were seeded onto Matrigel pre-coated 12-well plates to form *in vitro* capillary tubes. Once plated, cells were incubated for 12 hours at 37°C prior to starting the experiment (i.e., defined as the "zero" time point). This timing allowed for complete formation of tubes, and did nothing adverse to the cultures. One set of cultures were assayed at the zero time point, another set at 24 hours post zero time point, and a third set at

48 hours post zero time point. At these times, cells were rinsed 3 times with cold PBS. A mixture of 60 µl water-soluble kit reagent plus 300 µl fresh medium was added to each well for a 1 hour incubation at 37°C in the dark. Supernatants (100 µl/well) were collected and the absorbance of the produced formazan was measured at 490 nm. This absorbance reflects the total number of live cells in each sample. (Monolayers were used in parallel as an internal comparison. Unlike tube cells, monolayer cells proliferated every 24 hours until the dish was confluent. With the addition of DEP, the proliferative capacity of monolayers decreased after a 48 hours exposure. DEP at 1, 5, 10, 50 and 100 µg/ml showed monolayer cell proliferation levels of 95%, 71%, 40%, 0% and 0% respectively, compared to the proliferative level of untreated cells. Data not shown.)

Cytotoxicity assay

Cytotoxicity was evaluated using the CytoTox-Homogeneous Integrity Assay Kit (Promega). This assay measures lactate dehydrogenase (LDH), a stable cytosolic enzyme, that is released into medium when cells are lysed. HUVECs (6 X 10^4 cells/well) were seeded onto 12-well plastic plates or onto 12-well Matrigel pre-coated plates for the assay (156 cells/mm^2, as in all experiments). For some experiments no DEP were used. For others, capillary tube cells were treated with DEP as described in the proliferation assay. At 0, 24 and 48 hours after DEP exposure, cells were collected by centrifugation, separating them from the LDH in the supernatant/medium released by dead cells. The pellet of cells was lysed by a 1 hour incubation in 200 µl lysis solution (Promega). The relative fluorescence (described in RFUs, relative fluorescence units) of LDH at 490 nm was measured. The fluorescent value of an unexposed sample was used as the positive control, defining the maximum amount of LDH released (defined as 100%). The absorbance level

of test samples was expressed as a percentage of this maximum. These represent surviving cells. (For comparison, monolayer cultures with 1, 5, 10, 50, and 100 μg/ml DEP showed survivability of 99.3 +/- 2.26%, 91.2 +/- 4.15%, 82.0 +/- 2.33 % , 67.1 +/-4.24% 29.2 +/- 3.78 %, and 9.1 +/- 1.63%, respectively--data not shown.)

Tube Immunofluorescence Permeability assays

HUVECs (6 X 10^4 cells/well) were seeded onto Matrigel coated 2-well chamber slides for tube formation prior to DEP exposure. After a 24 hour DEP exposure, tubes were rinsed with PBS and fixed with 4% paraformaldehyde for 10 minutes at room temperature. Nonspecific reactivity of tubes was blocked by addition of 2% normal goat serum with 0.02% sodium azide (NaN_3) in PBS for 1 hour at room temperature. The capillary tube cells were then incubated with primary anti-human VE-Cadherin (BD Biosciences) monoclonal antibody at a 1:50 dilution (20 μl in 1 ml blocking buffer, i.e., 2% normal goat serum) for 1 hour at room temperature. Goat anti-mouse secondary antibody labeled with Alexa 488 (green color, Jackson Immuno Research) was used at a 1:100 dilution (10 μl in 1 ml PBS) for 1 hour at room temperature. When confocal microscopy was used, nuclei were stained by adding 1 ml 20 μM DRAQ5 (Alexis) to each well for 10 minutes at room temperature. Slides were covered with Prolong Gold (Invitrogen) anti-fade mounting media and incubated at 4^oC overnight. All images were observed at 100X and 400X magnifications on an epifluorescence microscope (Olympus IX71 Inverted Microscope) or at 630X magnification (water lens, N.A. 1.3) on a Leica TCS SP2 Spectral Confocal Microscope.

Semi-quantitation of discontinuities in VE-Cad was assessed on confocal images by counting the number of interruptions in the fluorescence pattern residing in a stretch of 20

µm or more of plasma membrane in the plane of focus. Such regions were also used to determine the number and size of VE-Cad globules, i.e., regions where VE-Cad was pulling away from the membrane toward an intracellular position. Globules were scored as equal to or under10 µm, or greater than 10 µm.

Western Analyses

After 24 hours DEP treatment, tube cells were collected with the Matrigel and sonicated for 1 minute in lysis buffer (20 mM Tris-HCl, 0.5% deoxycholate, 0.5% SDS, 1% Triton X-100, 1% Nonidet P-40, 1 mM Na_3VO_4 and 0.1% protease inhibitor). The Matrigel, which hardens at room temperature, was pelleted by centrifuging at 10,000 rpm for 10 minutes. The protein concentration of the supernatant was measured at absorbance 540 nm using the bicinchoninic acid method (BCA Protein Assay, Pierce). Samples were loaded at 20-30 µg/well onto SDS polyacrylamide gels for electrophoresis. The proteins were transferred to 0.22 µm PVDF membrane using electrophoretic transfer (Bio-Rad). Nonspecific reactivity was blocked for 1 hour at room temperature with standard 1x TBST buffer containing 3% BSA and 0.02% NaN_3. Primary antibodies against VE-Cad (BD Biosciences), β-catenin, (Abcam), actin and GAPDH (Sigma), diluted 1:1000, 1:2000, 1:1000, and 1:5000, respectively, with blocking buffer, were added to the blots and incubated overnight at 4^oC. After washing in 1x TBST, secondary antibodies conjugated with horseradish peroxidase (HRP) were diluted 1:5000 in 5% milk, 1x TBST, and applied to the blots for a 1 hour incubation at room temperature. Blots were then reacted with ECL reagent (Pierce) containing luminol, a substrate of HRP, and exposed to X-ray film.

Statistics

For statistical analysis, each experiment was performed in triplicate 3-5 times. The results were expressed as means ± SD for three independent experiments, and analyzed by using Student t-tests. A value of $p < 0.05$ was considered statistically significant.

RESULTS

Culture of human umbilical vein endothelial cell tubes

In vitro endothelial tubes were used to model how DEP might affect capillaries *in vivo*. To begin, the parameters of tube formation in culture were established. HUVECs were seeded into wells of Matrigel-coated plates at a density of 156 cells/mm^2. Phase contrast microscopy was used to determine how long it took for all cells to be incorporated into tubes, visualizing network formation at 1, 2, 4, 6, 12, and 24 hours after plating (not shown). At 1 hour, many cells had attached to the Matrigel, and by 2 hours the cells had sent out processes and had begun connecting to neighboring cells. By 4 hours, formation was extensive, and was very nearly complete by 6 hours. By 12 hours (Fig. 2-1), the tube formation process was totally complete, therefore this time point was used as the "zero" time point for all subsequent experiments adding DEP to tube cultures. Nuclear staining supported the observation that by 12 hours every cell was indeed incorporated into the *in vitro* capillary network. The phenotype of the capillary tubes remained the same for the longest time tested, which was 8 days after plating (not shown).

To evaluate whether culturing adversely affected endothelial tubes, cultures were assessed for their proliferative capacity in culture. Using an MTS assay, 6 X 10^4 HUVECs were plated as monolayers on Matrigel-coated dishes at a density of 156 cells/mm^2. Cell

proliferation was evaluated at 0, 24, and 48 hours after plating. Unlike traditional monolayer cultures, the tube endothelial cells did not show net proliferation after tubes were formed, even though large areas of the plate were unoccupied and available to the cells. The LDH cytotoxicity assay measures cell survivability. By comparing the LDH value of the cells at the end of the experiment (48 hours) with that at the beginning of the experiment (i.e., the number of cells initially added to the dish at the zero time point), one can determine the difference in cell number between the time points. The LDH assays demonstrated that the endothelial tube cell number was stable with time, i.e., the cells did not die as a response to being cultured (not shown).

Diesel Exhaust Particles (DEP)

The present study employed DEP derived from a Japanese automobile engine (Sagai *et al.* 1993), which have been characterized and used in other studies (Bai *et al.* 2001; Singh *et al.* 2004). An advantage of using these particles is that, despite being stored for years, delivery of 25 μg and 100 μg to mouse lungs by involuntary aspiration caused inflammation and injury (vascular leakage of microalbumin), while organic extracts of these particles showed little effect (Singh *et al.* 2004). This suggests that any observations that were made reflected a particle-dependent vascular response. Because particulate matter with diameters less than or equal to 2.5 μm ($PM_{2.5}$) is considered to cause adverse health effects, prior to applying DEP to cells, methods were evaluated for dispersing the particles to this size. One method suspended particles in PBS, with vortexing for 3 minutes before usage. Doing this, the resulting average particle size was estimated to be approximately 30 μm (Fig. 2-2A). A second method suspended particles in PBS containing 0.05% Tween 80, followed by vortexing for 3 minutes. This dispersed particles to an

average diameter of 10 μm (PM_{10}), as shown in Fig. 2-2B. The third method proved to be the best, vortexing particles in PBS containing 0.05% Tween 80 for 3 minutes, then sonicating them at 60 Hz for 5 minutes. As shown in Fig. 2C, particles were dispersed to microscopic sizes. While a few particles were about 5 μm (~1%), the preponderance of particles were under 2.5μm ($PM_{2.5}$). Many particles were as small as 0.1 μm (100 nm), the limit of light microscopy (see Fig. 2-2D, a higher magnification of the boxed area in panel C). Magnified views were used to count the number of 0.1 μm DEP in the total number of particles in randomly selected fields. This suggested that 0.1 μm DEP ($PM_{0.1}$) represented about 15% of the total particles visible by light microscopy. To measure particle size in a different way, dynamic light scattering was performed using a Zetasizer Nano ZS90. The mean diameter of dispersed DEP was 254.7 nm. DEP dispersed by this Tween/vortexing/sonicating method were used for all subsequent experiments comparing the impact of the particles on the behavior of tube culture cells.

LDH assays were used to evaluate how cytotoxic DEP were to tube cells. The percentage of cell survival was evaluated after 24 hours by comparing the amount of LDH at the end of the experiment with values of comparable controls representing the pre-exposure cell levels. As shown in Table 1, after 24 hours with no added DEP, essentially all of the cells were alive. Using 1 μg/ml DEP, 89% of the tube cells survived a 24 hour exposure, while at 5 μg/ml, 83% survived. At 10 μg/ml, 50 μg/ml, and 100 μg/ml DEP, the 24 hour survival rate was 79%, 59%, and 49%, respectively.

Although DEP toxicity is apparent from the LDH assays, tubes retained the skeleton of their tube structure (Fig. 2-3), even with the highest DEP concentration. A phase contrast image of a 100 μg/ml DEP treatment sample (Fig. 2-3D) shows that about

half of the tube cells are elongated, similar to cells treated with no or low concentrations of DEP, and about half of the cells are rounded up, looking like freshly plated, newly attached cells (Fig. 2-3D). All, however, remain in the pattern of the original endothelial tube.

Response of VE-cadherin to DEP

The integrity of the endothelial cell-specific adherens junction, of which vascular endothelial cell cadherin (VE-Cad, aka cadherin-5) is a component, is a measure of how leaky capillaries are (Gallicano *et al.* 2001). Therefore the cell-cell junctional integrity of tubes was examined after DEP exposure using VE-Cad antibody. Three separate experiments were performed using this antibody, to evaluate by epifluorescence the localization of the junctional molecule after DEP treatment. As seen in Fig. 2-4A-C, VE-Cad clusters at the cell borders of non-treated cultures, outlining the cells in a regular pattern. The pattern of VE-Cad after a 24 hour exposure of HUVEC tubes to 1 μg/ml of DEP is similar to the untreated control tubes (Fig. 2-4D-4F), but the 10 μg/ml DEP samples shows some changes in distribution of VE-Cad (Fig. 2-4G-4I, see arrows). These changes in VE-Cad distribution are local. While much of the VE-Cad is found sharply localized to the plasma membrane, small spherical globules of VE-Cad were sporadically observed (Fig. 2-4, arrows), and were frequently associated with a loss of sharpness at the cell-cell junction. This more amorphous appearance indicated loosening of the VE-Cad from the membrane with expansion into the intracellular space. At the 100 μg/ml concentration of DEP (Fig. 2-4J-L) the VE-Cad is internalized, with very little remaining at the cell junctions. Such phenotypes have been correlated with endothelial cell leakage (Bazzoni and Dejana 2001; Dejana *et al.* 2008).

Because wide field epifluorescence microscopy is a sum of all the planes of a 3D image, local small changes in cell-cell junctions are masked. To evaluate whether VE-Cad was redistributing after exposure with the lowest DEP concentration, 1 µg/ml, single optical planes were viewed by confocal microscopy. Untreated controls (Fig. 2-5A-C) show that VE-Cad outlines the endothelial cell membranes where they are in the plane of focus. Many cells had only a portion of the membrane in the plane of focus. With 1 µg/ml DEP, occasional globules or discontinuities were seen in the VE-Cad staining (arrows in Fig. 2-5D-F) more frequently than in the non-treated sample. Such discontinuities were not discernible in the wide field epifluorescence micrographs. At 10 µg/ml (Fig. 2-5G-I) many more punctate spots of VE-Cad are observed. These punctate patterns indicate local alterations in the adherens junctions. At 100 µg/ml (Fig. 2-5J-L) the VE-Cad is totally intracellular, indicating dissolution of the adherens junctions, just as observed with the wide field epifluorescence microscopy. A semi-quantitation of the changes in VE-Cad was compiled from the images in two ways. One method was to measure discontinuities in plasma membranes that were in the plane of focus, as indicated in Figure 2-6A. While some discontinuities represent the natural fluctuating of plasma membrane in and out of the plane of focus, the number of discontinuities increased with increasing DEP concentration (Fig. 2-6B). The second method was an assessment of the number and size range of fluorescent globules of VE-Cad being internalized, as indicated in Fig. 2-6C. Globules of 10 µm or less, as well as those greater than 10 µm were measured. Smaller globules increase with increasing exposures, and are the predominant size in 1 and 10 µg/ml DEP exposures. At 100 µg/ml, there are many smaller and larger sized globules, with the >10 µm being more abundant (Fig. 2-6D). This semiquantitative data demonstrates an

increasing trend in plasma membrane discontinuities and VE-Cad aggregation into globules after exposure to increasing concentrations of DEP.

The fact that the intensity of the VE-Cad fluorescent signal merely relocalized, but did not seem to diminish with increasing DEP concentration, was of interest. To examine this further, untreated and DEP-treated tubes were collected and lysed for protein extraction. Western analyses showed that the levels of VE-Cad, as well as β-catenin, were not significantly altered with increasing DEP concentration (Fig. 2-7). VE-Cad appeared as 2 bands, the full length 130 kDa form, and a product ~95 kDa which could be either the shed product or the degradation product after internalization. Both forms were present in the untreated control endothelial tube extracts, as well as the DEP-treated extracts, thus DEP had no net affect on the levels of each form of VE-Cad. Total β-catenin levels were also unchanged by DEP exposure.

Next, the location of DEP in HUVEC tube cultures after 24 hours was examined. Many images visualized DEP in the vicinity of, or touching, tubes. Because endothelial cells in tubes are in a three dimensional structure, confocal micrograph Z stacks were useful for localizing particles. Fig. 2-8A shows several particles in a phase contrast image from a 10 μg/ml DEP exposure. The cross lines in Fig. 2-8B show where Z stack images were captured from the confocal planes of focus. The z plane image in panel B is taken in the center of the cellular structure, and shows 2 diesel particles at the level of the nuclei (arrows). This indicates they are in the interior of the cells, and not in the lumen of the tube. In another area (Fig. 2-9), a phase contrast image is overlapped with the confocal images focused at the top of the tube (panel A), at the middle of the tube (panel B), and at the bottom of the tube, close to the Matrigel (panel C). The particle is in sharp focus when the

z-section is focused on the middle of the structure, suggesting the particle is in the tubular lumen. As seen in the bottom z plane image, the particle appears to be surrounded by the green fluorescence of the VE-Cad detected by immunoreactivity. The side y and bottom z plane images show further support that the DEP particle is contained in a tubule's lumen (Fig. 2-9B). Therefore, the confocal images in Figs. 2-8 and 2-9 suggest that added particles can be translocated to sites either within the tube cells, or possibly within a tubular lumen.

DISCUSSION

The mechanisms involved in the adverse cardiovascular responses to inhaled DEP are as yet unclear. Exposure chambers have yielded crucial animal and human data, i.e., demonstrating a diesel-induced increase in thrombus formation after exposure (Lucking *et al.* 2008) and endothelial-specific studies with monolayer cultures have unveiled important vascular-related information (Bai *et al.* 2001; Furuyama *et al.* 2006; Li *et al.* 2009; Sumanasekera *et al.* 2007). To elucidate mechanisms for how DEP can cause such effects, more laboratory research model systems are needed. In the present work an *in vitro* HUVEC tube model simulating a capillary structure, is used to study what may occur at the organizational level of the capillary. Endothelial tubes were treated with well characterized DEP derived from a Japanese automobile engine (Sagai *et al.* 1993; Bai *et al.* 2001; Singh *et al.* 2004). These same particles, delivered to mouse lungs in aspiration studies at doses of 25 μg and 100 μg, caused lung inflammation and vascular leakage. Organic extracts of these DEP showed little effect (Singh *et al.* 2004).

For this study DEP were dispersed to an average diameter of ~260 nm. As such, many particle will fit the ultrafine biologically relevant size of $PM_{0.1}$ (100 nm). Thus, the particle preparation contains sizes expected to reach deeper into the respiratory tract of the lung (Nemmar *et al.* 2006; Oberdorster *et al.* 1994). It is possible that the most biologically relevant studies reported here are those in which particles at a concentration of 1 μg/ml were used, a level of DEP that did not cause appreciable endothelial cell death, but did show evidence of VE-Cad internalization. This is because *in vivo* there is no evidence that particles cause death of capillary endothelial cells. Since VE-cadherin relocation has been shown to compromise barrier function (Kevil *et al.* 2001), it is noteworthy that the 1 μg/ml concentration induced more relocalization of VE-Cad than controls without significant cell death. A concentration of 5 μg/ml DEP, which allows about 83% of the cells to survive, may or may not be in the range of biological relevance. Unfortunately, there is no experimental data available that measures the viability of lung capillary endothelial cells *in vivo* after DEP exposure. Damage assessment of diesel-exposed animals consists mostly of vascular leakage (Singh *et al.* 2004), which cannot differentiate between endothelial cell death and separation of cell junctions.

While *in vitro* endothelial tubes are not a perfect model for *in vivo* capillaries (Donovan *et al.* 2001), they do exhibit similar behaviors. The morphology of endothelial tubes approximates that of *in vivo* capillaries, and the lack of proliferation in the tubular structure is also like that of *in vivo* capillary endothelial cells (Hadley *et al.* 1985), where proliferation is strictly prohibited. In fact, networks of capillary tubes remain healthy and vital for up to 8 days without any sign of net proliferation. (Homeostasis may be occurring in tubes, with a small level of proliferation to offset a small amount of cell death; the

experiments in this study were not designed to detect this.) Because monolayers of HUVEC cells double every 24 hours until their substratum's surface is confluent, it is likely that tubes represent a more differentiated and *in vivo*-like model for capillaries.

VE-Cad resides in the endothelial adherens junction (Carmeliet *et al.* 1999; Dejana 2004; Dejana and Del Maschio 1995; Taddei *et al.* 2008; Zhou *et al.* 2004). This cell-cell junction also contains β-catenin, plakoglobin and desmoplakin, but is practically negative for vinculin and alpha-actinin. The arrangement of adherens junctions from *in vivo* vessels has been reconstructed from electron micrographs, and it has been demonstrated that capillary tubes formed *in vitro* have the same VE-cadherin-containing structures (Schmelz and Franke 1993; Zhou *et al.* 2004). Furthermore, capillary leakiness (i.e., permeability) has been related to the adherens junctions (Gallicano *et al.* 2001; Kevil *et al.* 2001). The dissolution of the cell-cell adherens junctional molecules results in components of the junction relocating intracellularly (Guo *et al.* 2007; Lim *et al.* 2001). External stimuli such as inflammation have been demonstrated to cause the dynamic redistribution of VE-Cad (Gabrys *et al.* 2007; Lim *et al.* 2001).

Interestingly, endothelial tubes exposed to DEP in culture recapitulate these phenomena. The redistribution of VE-Cad in tubes after exposure, displaying a phenotype that is like that observed in leaky capillaries, is consistent with the observations of vessel leakiness in animals forced to inhale the same DEP employed here (Singh *et al.* 2004). In the experiments of this study, with increasing DEP concentration, increasing levels of VE-Cad moved from a membrane localization to a cytoplasmic localization. The data presented suggest that if inhaled DEP reach the alveolar capillaries, they may have some ability to impact the adherens junction, causing the capillary cell-cell junctions to become

permeable. Even though it is shown that VE-Cad moved from a membrane localization to a cytoplasmic localization with the higher DEP concentrations, the tubes still maintained their three dimensional morphology, suggesting that other types of cell-cell junctions remain functional. Whether or not DEP has any effect on other junctions has not been tested. What is clear is that the results with DEP exposure resemble what occurs with exposure to H_2O_2, where VE-Cad is internalized and is coupled with barrier dysfunction (Kevil *et al.* 2001). It is likely that increasing DEP levels do, indeed, induce increased generation of reactive oxygen species that lead to a similar internalization of VE-Cad and membrane leakiness. This will be examined in future work.

The level of VE-Cad at the cell surface is determined by several factors. One is by cytoplasmic binding partners that modulate whether the cadherin is endocytosed or degraded (Xiao *et al.* 2003a; Xiao *et al.* 2003b). VE-Cad is known to undergo intracellular degradation after internalization, producing a product of ~95 kDa. Disassociation of p120 catenin from the cytoplamic domain of VE-Cad is thought to trigger internalization of the cadherin (Xiao *et al.* 2003a), which can proceed to a pathway where the tail is cleaved, removing the β-catenin binding domain. It is suspected that this cleavage fates the molecule for lysosomal degradation (Xiao *et al.* 2003b). However, VE-Cad has also been shown to be internalized without being cleaved (Xiao *et al.* 2003b). Furthermore, VE-Cad may be shed from the cell surface (Harren *et al.* 1998). Adding another complication to the possible molecular events, it has been postulated that recycling of VE-Cad can occur (Vincent *et al.* 2004). Support for this idea comes from another cadherin family member, E-cadherin (Le *et al.* 2002; Le *et al.* 1999). It is not known whether degradation or shedding is the cause of the lower molecular weight VE-Cad band in our endothelial tubes,

but the two forms of VE-Cad have been shown to be present in Westerns derived from monolayer cultures of HUVECs (Groten *et al.* 2000). Because the two forms of VE-Cad are constant with and without DEP treatment, the favored idea is that the consistency of the level of the two bands may reflect recycling. If DEP were to induce degradation, the net levels of the smaller band, representing the degradation product of VE-Cad, would be expected to increase on the Western; alternatively, if DEP were to induce shedding, the smaller shed fragment would diffuse into the medium and not be isolated in the cell lysate preparation. This would result in decreased amounts of the smaller band on the Western blots. The results, however, show no change in levels of the two bands, and best fit the idea of recycling.

Finally, confocal microscopy provided the advantage of antibody localization in three dimensions, demonstrating that DEP can enter endothelial cells and possibly reach the endothelial tube lumen in the culture model. This was, in fact, the goal of the study. If this occurs even to a small degree in lung capillaries, it suggests that, *in vivo*, DEP may transverse the capillaries and gain access to the bloodstream. Entry into the lumen could occur in three ways: (a) particles may attach to the external side of the endothelial plasma membrane, cause damage externally, and penetrate into the capillary; (b) particles may be endocytosed by the cell where they then cause intracellular damage; and (c) particles may slip between the cells via disrupted junctional complexes. Once inside the vessel, DEP could interact with platelets or initiate an immune response. Although cell-cell junction alterations can be observed in the endothelial tubes, the data cannot definitively differentiate between translocation of particles by crossing cell membranes or by passage between interrupted cell-cell junctions.

Overall, endothelial tubes may be a useful and informative model system to study the mechanisms of action of DEP on the vasculature. The HUVEC tube data presented here lends support to the idea that ultrafine particles may cross the pulmonary epithelium, encounter the alveolar capillary endothelium, and enter the systemic circulation, where direct toxic effects on vascular endothelium and the heart may be possible (Brook *et al.* 2003). Endothelial tube studies provide a three dimension type of information different from what can be obtained using endothelial cells in monolayer culture.

Table 1. Cytotoxicity of DEP on HUVEC tubes

	LDH at 24 hour
Conc. of DEP (µg/ml)	Cell Survivability (%)
0	98.7 ± 0.36
1	89.1 ± 1.87
5	82.7 ± 0.79*
10	79.4 ± 4.31*
50	58.9 ± 0.77*
100	48.3 ± 8.25*

Cell Survivability of HUVECs in tube cultures treated with DEP for 24 hours, as assessed by LDH assays. Data are expressed as the mean ± SD of three independent experiments, each performed in triplicate (i.e., 9 plates). *$p < 0.05$ to the cell control (0 µg/ml).

FIGURES

Fig. 2-1. HUVEC tube formation, complete by 12 hours after plating, as verified by comparing the phase contrast images with the images of DAPI stained nuclei. No nuclear stain is evident in any area on the plate that is not part of a tube, indicating that every cell was incorporated into the tubular network. This is true for both the 12 hour and the 24 hour time points. (Magnification 100X).
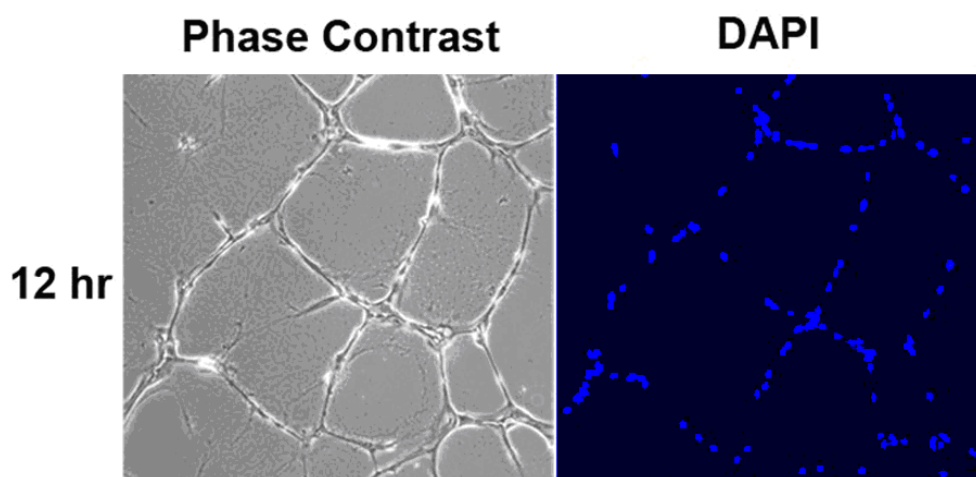
Fig. 2-2. Phase contrast images obtained on the Leica TCS SP2 Spectral Confocal Microscope to determine the distribution of particle shapes, sizes, and diameters at 630X magnification with magnification bars. Panel A, DEP diluted in PBS to 100 μg/ml and vortexed 3 minutes. 1 ml was applied to a slide. Panel B, DEP diluted in PBS containing 0.05% Tween-80, then vortexed 3 minutes prior to examination; Panel C, DEP diluted in PBS containing 0.05% Tween-80, then vortexed 3 minutes, followed by sonication for 5 minutes. The majority of particles are $PM_{2.5}$; Panel D is an enlarged image of the area enclosed by the red square in panel C. Many particles are of very small sizes. Several have diameters of 0.1 μm ($PM_{0.1}$), the limit of light microscopy. The arrow points to a particle of this size.
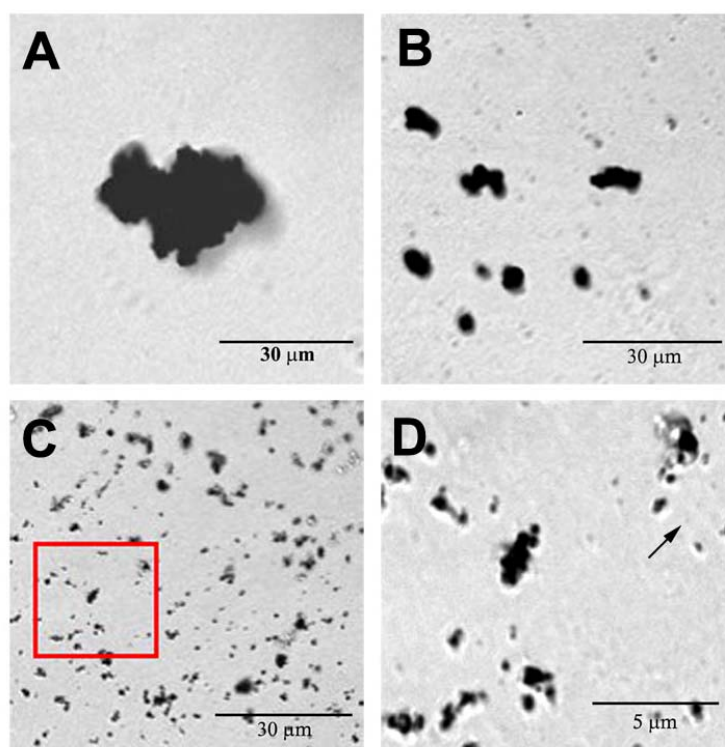
Fig. 2-3. Phase contrast micrographs of capillary tubes treated with various concentrations of DEP for 24 hours. Panel A, non-treated control; Panel B, medium containing a final concentration of 1 µg/ml DEP; Panel C, medium containing a final concentration of 10 µg/ml DEP; Panel D, medium containing a final concentration of 100 µg/ml DEP. Arrows in panel C point to individual diesel particles, magnification 100X. Dynamic light scattering of particles demonstrated the mean diameter was 254.7± 138.72 nm.
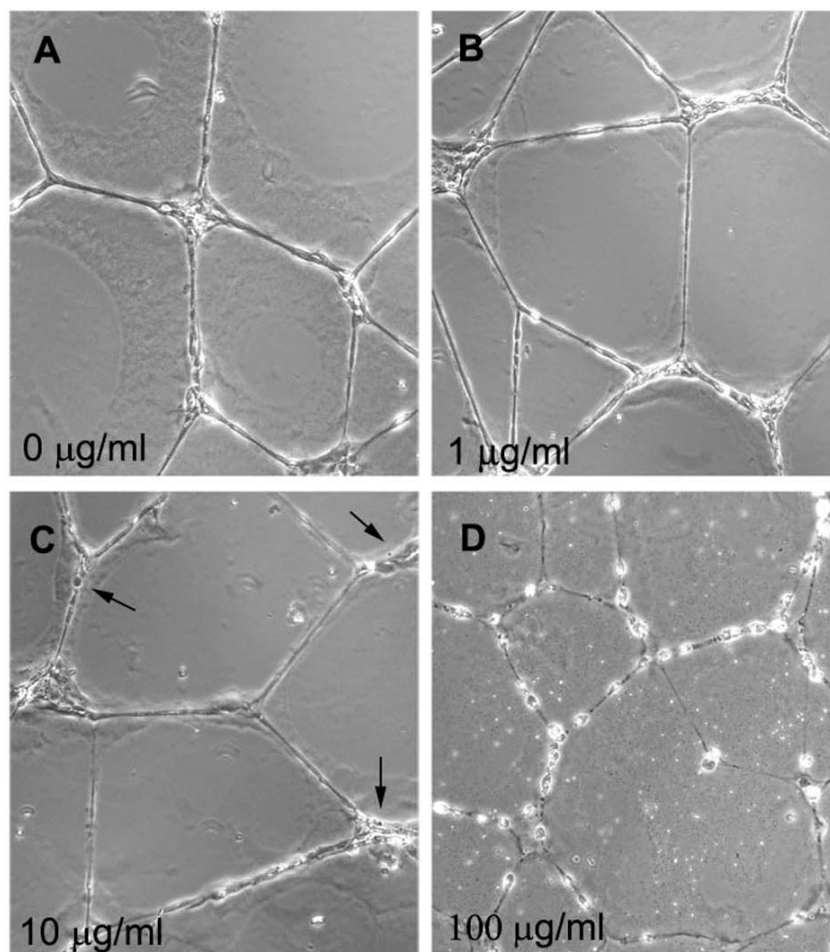
Fig. 2-4. Widefield epifluorescence immunolocalization of VE-Cad in endothelial tubes treated with DEP for 24 hours. Panels A-C, control, non-treated capillary tubes; Panels D-F, tubes treated with 1 µg/ml DEP; Panels G-I, tubes treated with 10 µg/ml DEP; Panels J-L, tubes exposed to 100 µg/ml DEP. Arrows indicate where there is a loss of sharpness to the VE-Cad antibody staining. Images were obtained on an Olympus IX71 Inverted Microscope at 400X magnification. All images were obtained with the same digital camera settings. Scale bar = 30 µm.

0 μg/ml DEP

1 μg/ml DEP

10 μg/ml DEP

100 μg/ml DEP
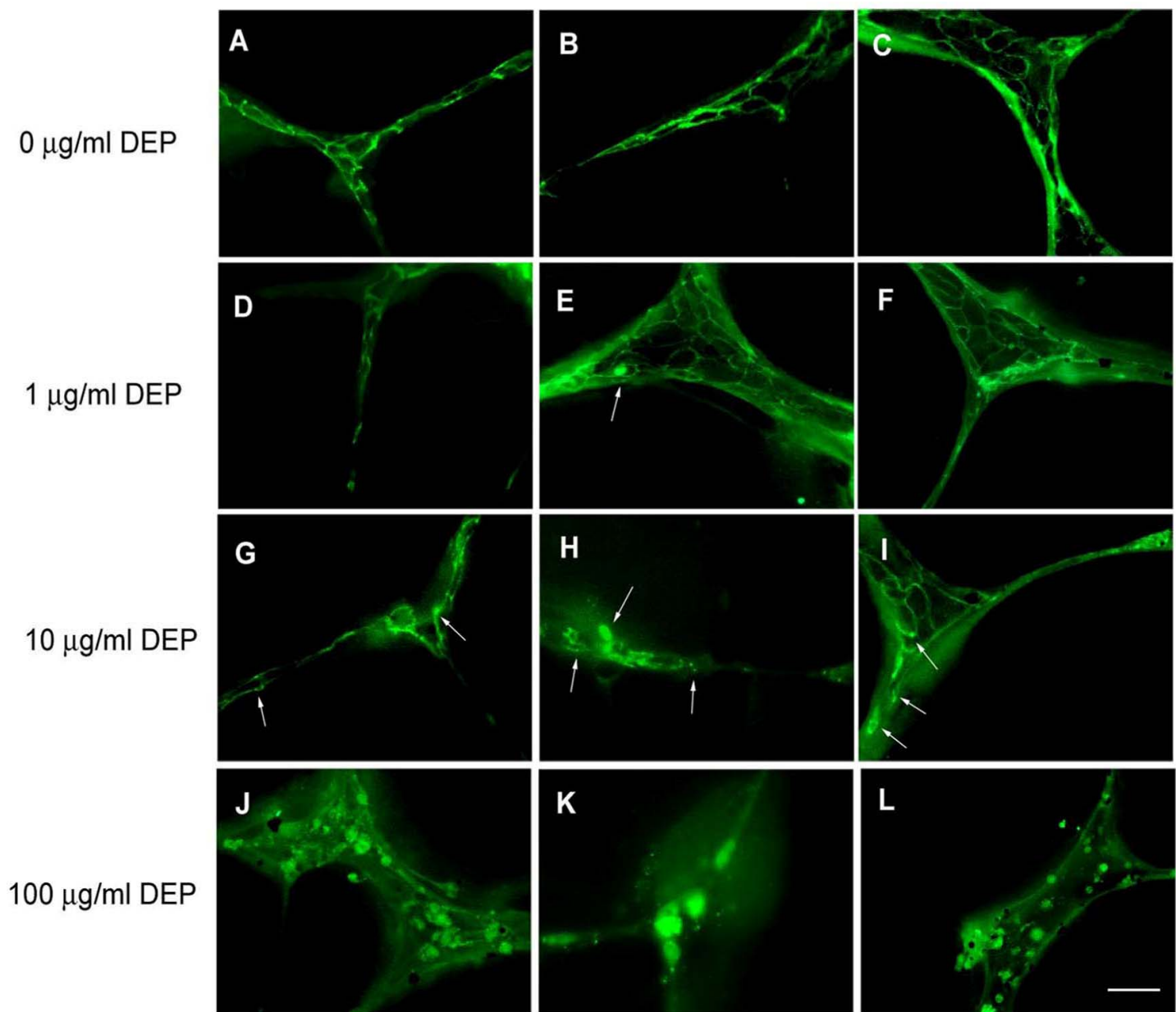
Fig. 2-5. Confocal images of single optical sections to detail the distribution of VE-Cad in response to DEP exposure for 24 hours. Panels A-C, non-treated control endothelial capillary tubes; Panels D-F, tubes treated with 1 µg/ml DEP; Panels G-H, 10 µg/ml DEP; Panels I-J, 100 µg/ml of DEP. Arrows show discontinuities and punctate fluorescent globules. In J-L, VE-Cad staining was diffuse throughout the cells. Almost none was discernible as being localized to the plasma membrane. Images were obtained using a Leica TCS SP2 Spectral Confocal Microscope at 630X magnification using identical settings for all photos. Scale bar = 30 µm.
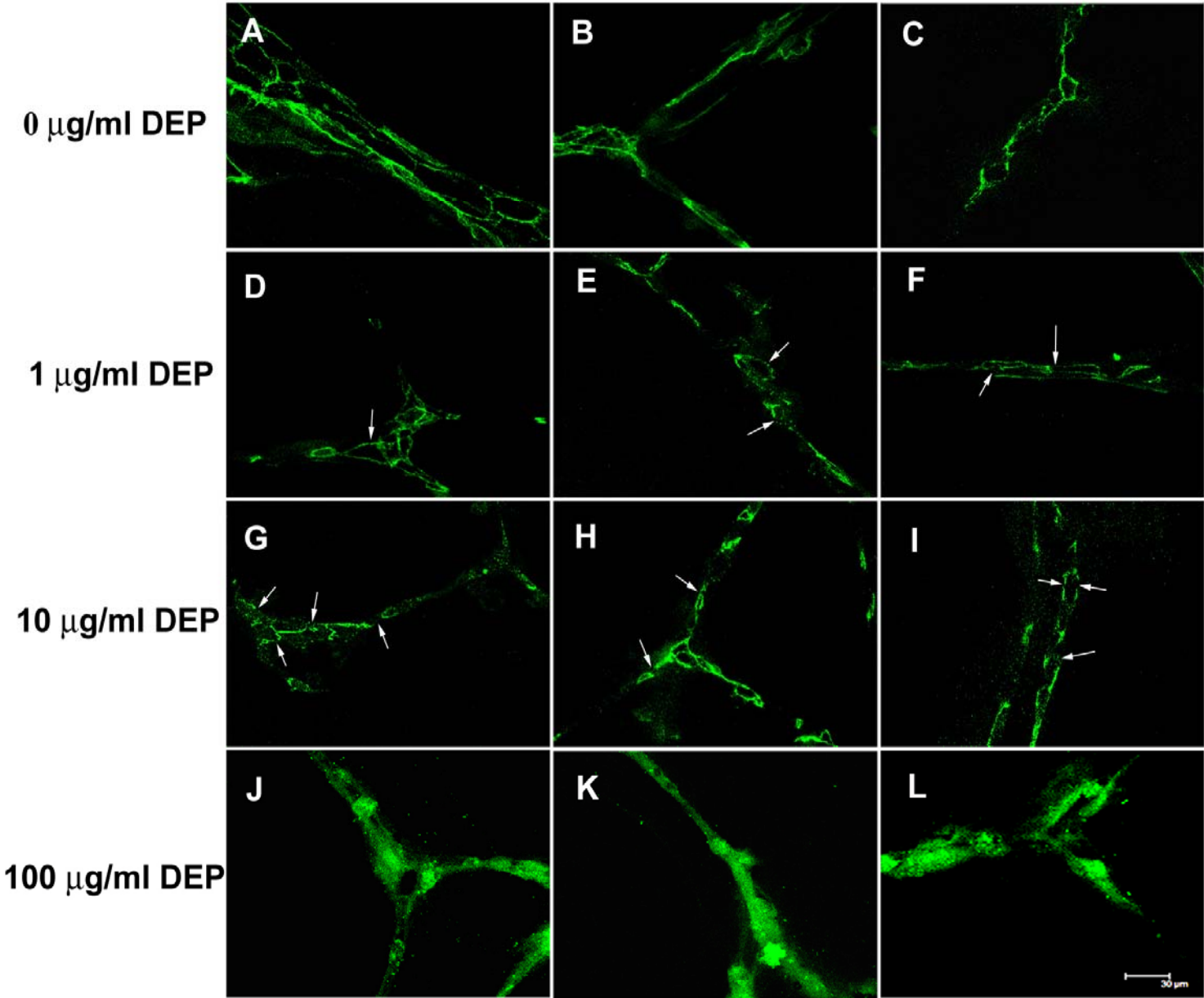
Fig. 2-6. Semi-quantitation VE-Cad discontinuities and globule formation. In panel A, the left side shows an example of ~25 µm of plasma membrane in the plane of focus that was magnified (right side of panel) to count the number of interruptions in the fluorescence pattern. Arrows indicate discontinuities of VE-Cad in the plane of focus. Panel B is a compilation of such determinations from more than 12 different samples of each DEP concentration (0, 1, and 10 µg/ml) The VE-Cad pattern of the 100 µg/ml DEP exposed samples was so disrupted that it was nearly impossible to find ~25 µm of fluorescence localized to the plasma membrane. *$p < 0.05$ to the cell control (0 µg/ml) analyzed by using Student t-tests. Panel C, left, contains an example of an area where VE-Cad was in the plane of focus and was magnified in the right panel. Panel D, VE-Cad globules of fluorescence (arrows) from panel C were counted and and scored as either equal to or under 10 µm, or as greater than 10 µm sized. The globules represent VE-Cad pulling away from the membrane toward an intracellular position.

A

30 μm

B

VE-Cad Discontinuities per 100 cells

Concentration of DEP (μg/ml)

C

30 μm

D

VE-Cad Globules per 100 cells

□ = 10 μm
■ > 10 μm

Concentration of DEP (μg/ml)
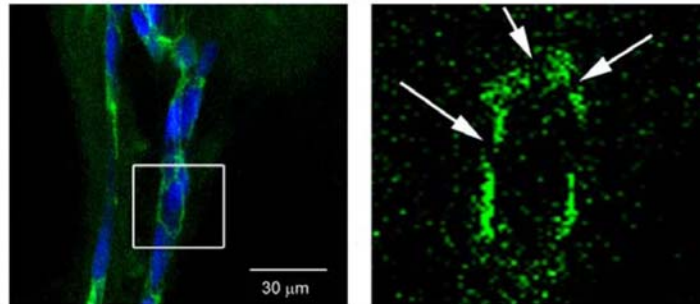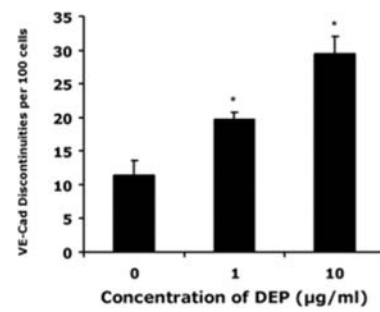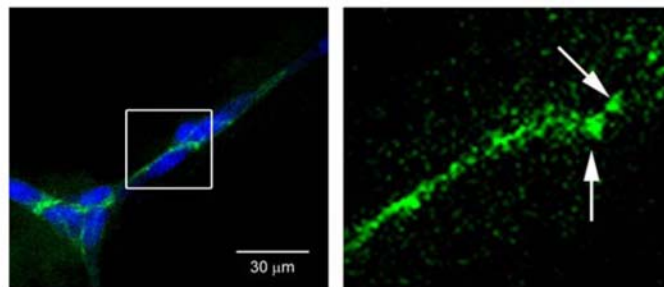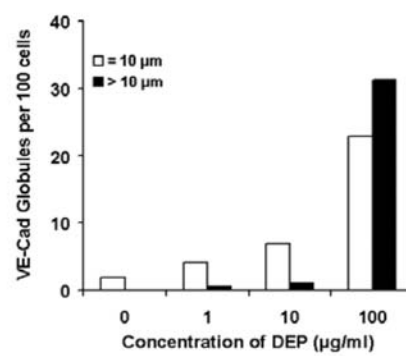
Fig. 2-7. Endothelial tubes reacted with 0, 1, 10 or 100 µg DEP for 24 hr were used to extract protein for Western analysis. (A) Antibodies against the adherens junction proteins VE-cadherin and β-catenin were probes. Blots were stripped to reprobe with antibodies against actin and glyceraldehyde-3-phosphate dehydrogenase. The latter assured that equal amounts of protein were loaded in the wells. (B) Histograms show a quantification of junction proteins levels after 24 hr exposure to DEP. Bars are the relative fold change compared to the control with no added DEP.

(A)
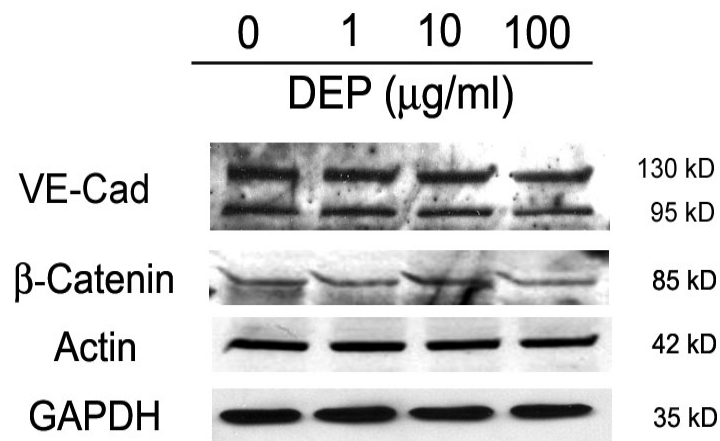
(B)
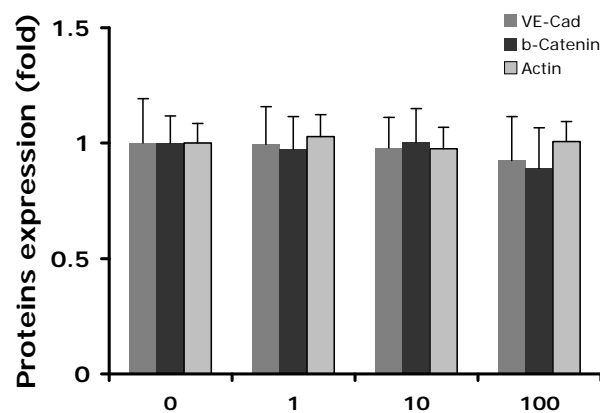
Fig. 2-8. Phase contrast image (Panel A) and a z-plane confocal image taken midway through a tube, focused at the point where lines of the x- and y-planes cross. Green color indicates VE-cadherin antibody staining, and blue is nuclear staining with DRAQ5. The diesel particles (arrows) are at the same depth in the tube structure as blue stained nuclei (Panel B). Scale bars = 30 μm.
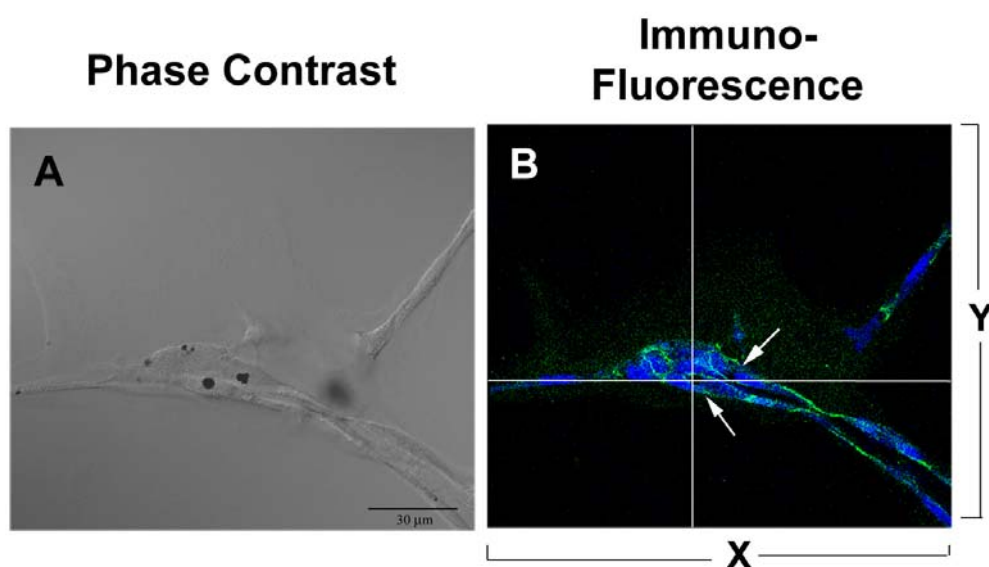
Fig. 2-9. Overlaid phase contrast (gray colored transmitted image) and confocal images of an unbranched tube containing a diesel particle (VE-Cad detected with green labeled secondary antibody, and nuclei stained blue with DRAQ5). The x- and y-axis lines cross at the point where the microscope was focused for the Z stack analysis. In the fluorescent images, the z-plane was focused at the top of the tube (Panel A), at the middle of the tube (Panel B), and at the bottom of the tube (Panel C), demonstrating that the particle is not on the exterior of the tube, nor is it at the base near the Matrigel, but is internal in the tube. Scale bar = 30 μm.
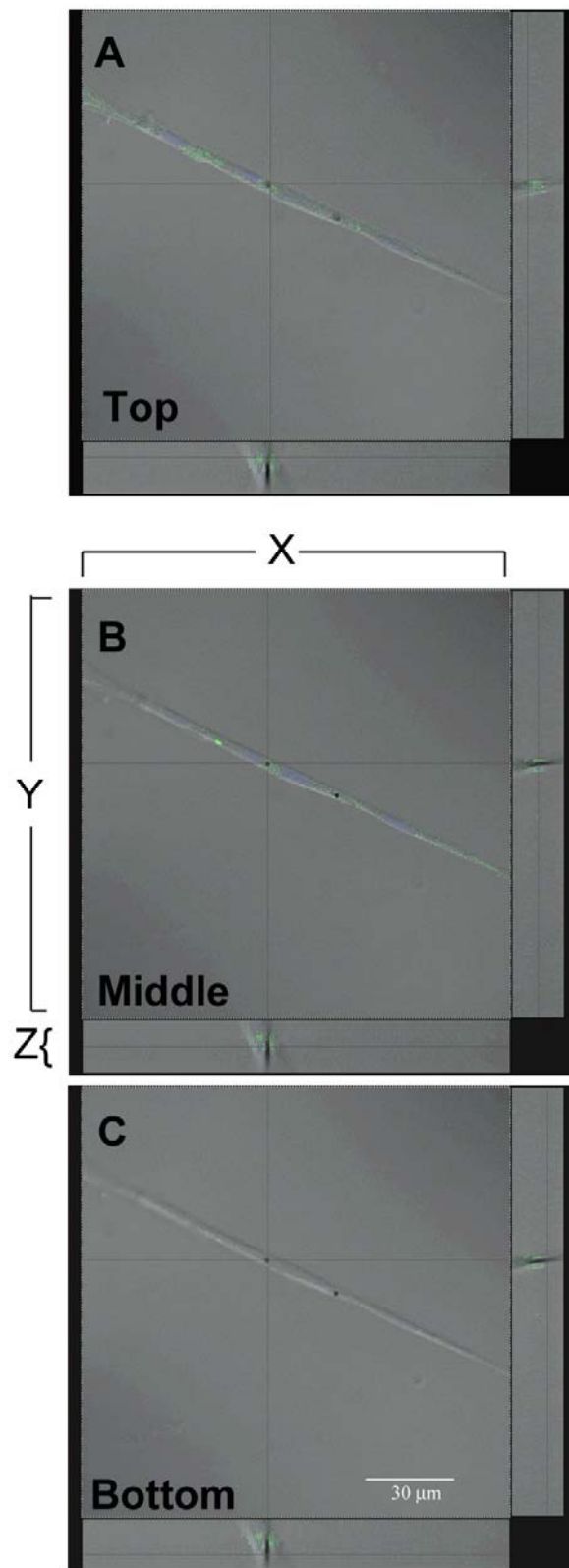
Chapter II

ROS and Pro-inflammatory Cytokines Contribute to DEP-Induced Permeability of Capillary-like Endothelial Tubes

ABSTRACT

Inhalation of diesel exhaust particles (DEP) is associated with pulmonary and cardiovascular disease. This effect may result from inhaled particles reaching lung capillaries and gaining access to the blood stream. Using *in vitro* endothelial tubes as a simplified model of a capillary to study this process, it was previously shown that DEP induce the redistribution of vascular endothelial cell-cadherin (VE-Cad) away from the plasma membrane to intracellular locations, making the tubes permeable, and allowing DEP into the cell cytoplasm and tube lumen. Here the mechanisms activated by DEP to induce such permeability are examined. The results demonstrate that endothelial tube cells mount an oxidative stress response to DEP exposure. Particles induced relocalization of Nrf2 from the cytoplasm to the nucleus, upregulating the expression of the enzyme heme oxygenase-1 (HO-1). Hydrogen peroxide and oxidized proteins were detected after 24 hr of exposure to DEP. Vascular endothelial cell growth factor-A (VEGF-A), initially termed "vascular permeability factor" (VPF), was found to be up-regulated in response to the HO-1 expression induced by DEP. In addition, the levels of cytokines TNF-α and IL-6 were increased after DEP exposure. These also induced upregulation of VEGF-A, but in a manner that was not apparently dependent on HO-1. These data suggest that the DEP-induced permeability of capillary-like endothelial tubes is, in part, a consequence of antioxidant and pro-inflammatory responses ultimately increasing secreted VEGF-A levels.

INTRODUCTION

Epidemiological studies have demonstrated a connection between exposure to diesel exhaust particles (DEP) and adverse health effects (Pope and Dockery 2006; Riedl and Diaz-Sanchez 2005; Sydbom *et al.* 2001). While many effects on cardiovascular health come from long term exposures (Pope *et al.* 2004), there are also consequences of short term exposures, where ambient air levels of DEP can be linked to myocardial infarctions and other cardiovascular incidents (Brook 2008; Peters *et al.* 2001; Peters *et al.* 2004; Pope and Dockery 2006). The particulate components of DEP associated with increased cardiovascular morbidity and mortality are the fine particles (sizes ≤ 2.5 μm, i.e. $PM_{2.5}$) and the ultrafine particles ($PM_{0.1}$ sizes are ≤ 0.1 μm, i.e., ≤ 100 nm) which are a subset within $PM_{2.5}$ (Pope and Dockery 2006).

There is much interest in understanding how DEP cause adverse health effects. Several mechanisms have been proposed, such as inducing production of harmful ROS (Bai *et al.* 2001; Becker *et al.* 2005), initiating inflammatory responses (Salvi *et al.* 1999); disrupting autonomic balance (Pope *et al.* 2008), and disrupting vascular function (Mills *et al.* 2007). It is likely that all are involved in contributing to the final pathology. Support for endothelial dysfunction as a DEP-induced mechanism has come from many venues. Notably, vasoconstriction has been demonstrated in humans who inhaled ambient $PM_{2.5}$ and ozone for 2 hr (Brook *et al.* 2002), and impairment of vasodilatation was observed 24 hr after a 1 hr diesel exhaust inhalation study (Tornqvist *et al.* 2007). Also, 24 hr after intratracheal installation of DEP or DEP extracts, the water content of mouse lungs increased (Inoue *et al.* 2006), suggesting an increase in pulmonary endothelial permeability. Permeability may occur in part because particles injury alveolar epithelia,

which then release cytotoxic components that injure the capillaries, and it may also occur because alveolar macrophages become activated and secrete factors potentially harmful to endothelia. DEP, however, are also likely to have direct effects on capillary endothelia. Inhaled particles have been shown to reach the circulation (Geiser *et al.* 2005; Kreyling *et al.* 2002; Kreyling *et al.* 2009; Nemmar *et al.* 2005; Nemmar *et al.* 2002; Nemmar *et al.* 2004b; Nemmar *et al.* 2001). While this data is largely based on TiO_2 and iridium particle inhalation studies (Geiser *et al.* 2005; Kreyling *et al.* 2002; Nemmar *et al.* 2002; Nemmar *et al.* 2001; Oberdorster 2002), a more recent report used labeled 80 nm and 20 nm carbon nanoparticles, and found them 24 hr after inhalation in many organs, including blood (Kreyling *et al.* 2009). This is of particular interest because carbon is a major constituent of DEP.

Because DEP have been implicated in gaining access to the circulation, and may have a direct effect on endothelial permeability, *in vitro*-assembled capillary-like endothelial tubes were recently used to model the translocation of particles into capillaries. The permeabilizing effect of DEP on endothelial tubes was visualized with confocal microscopy, demonstrating that the adherens junction component VE-cadherin moved from cell-cell junctions to intracellular locations, and that particles ended up in the cells' cytoplasm as well as in the luminal space of tubes (Chao et al., submitted). The DEP-induced redistribution of VE-cadherin was highly similar to that which occurs to endothelial monolayers in response to hydrogen peroxide (H_2O_2) exposure (Kevil *et al.* 2001), suggesting that perhaps one effector of DEP-induced endothelial permeability is the generation of H_2O_2.

HO-1 is a ROS-induced antioxidant enzyme that facilitates anti-apoptotic responses in endothelial cells (Brouard *et al.* 2002; Silva *et al.* 2006; Wang *et al.* 2007). HO-1 is known to induce expression of vascular endothelial cell growth factor (VEGF-A) (Dulak *et al.* 2008). This molecule was first discovered functionally, and named vascular permeability factor (VPF) (Connolly *et al.* 1989; Ferrara and Henzel 1989; Keck *et al.* 1989; Senger *et al.* 1990; Senger *et al.* 1983). As a result of its effect in promoting permeability, cancer-related edema is often treated with inhibitors of VEGF-A (Gerstner *et al.* 2009). DEP-induced HO-1 activity is therefore a candidate facilitator of endothelial permeability via induction of VEGF-A secretion.

Interleukin-6 is a cytokine demonstrated to increase the permeability of endothelial monolayers (Maruo *et al.* 1992), and DEP were found to upregulate IL-6 and TNF-α in the plasma of volunteers 24 hr after controlled exposure inhalations (Tornqvist *et al.* 2007). Thus, pro-inflammatory cytokines may also contribute to permeability.

These several correlations prompted the work reported here, where the endothelial tube model system, a system free of the confounding effects of inflammatory cells, was used to examine how DEP might modulate endothelial permeability. Mechanisms examined were induction of endothelial proinflammatory cytokines, reactive oxygen species, such as H_2O_2, and HO-1-dependent VEGF-A secretion. The results obtained indicate that, in capillary-like endothelial tubes, DEP do, in fact, induce antioxidative and pro-inflammatory responses that are linked to VEGF-A levels. These data suggest a possible set of pathways initiated by DEP exposure that result in vascular permeability.

MATERIALS AND METHODS

Cell culture

Human umbilical vein endothelial cells (HUVECs) were cultured in endothelial cell growth medium EBM-2 Bulletkit (Lonza) as previously described (Chao et al., submitted). Medium was supplemented with phosphate buffered saline and Tween-80 to make a final concentration of 1X PBS, 0.05% Tween-80 (1X PBS is 137 mM NaCl, 2.7 mM KCl, 10 mM Sodium Phosphate dibasic, 2 mM Potassium Phosphate monobasic, pH 7.4). This was done to minimize differences between non-DEP-exposed controls and DEP-treated samples, since DEP are suspended in 1X PBS, 0.05% Tween-80. Thus, medium always means that containing PBS-Tween-80. HUVECs at passage 5 to 15 were used to assemble tubes on 10 mg/ml Matrigel, LDEV-free (BD Biosciences), solidified onto 2-well chamber slides (120 µl Matrigel/well) or 6-well (150 µl Matrigel/well) plastic plates. The Matrigel was solidified for at least 30 min before adding cells. HUVECs were plated at 156 cells/mm^2 on both 2-well chamber slides (6 X 10^4 cells/well), and on 6-well plastic dishes (1.5 X 10^5 cells/well). Endothelial tubes were allowed to form for 12 hr prior to adding DEP. Medium was changed daily. Well characterized DEP (Bai *et al.* 2001; Singh *et al.* 2004) were a gift from Dr. Masaru Sagai, Aomori Univeristy of Health and Welfare, Japan. Particles were prepared as previously described to create a suspension resulting in sizes of PM$_{2.5}$, of which a portion is PM$_{01}$ (Chao et al., submitted). Since the density of the cells is the same on both types of wells used, 1 ml of either medium alone (i.e., 0 µg DEP/ml), or 1, 10, or 100 µg DEP/ml was applied to each well, and unless otherwise indicated, analysis was performed after a 24 incubation at 37°C.

Reagents

N-Acetyl Cysteine was obtained from Sigma-Aldrich (St. Louis, MO). Cytokines TNF-α and IL-6 were purchased from R&D Systems, Inc (Mineapolis, MN). Tin protoporphyrin IX (SnPP) was bought from Frontier Scientific, Inc. (Logan, UT). Other reagents employed are incorporated into the appropriate method sections below.

Lactate dehydrogenase cytotoxicity assay

The CytoTox-Homogeneous membrane integrity assay kit (Promega) was used to assess the number of cells surviving DEP exposure by assessing the amount of cytosolic lactate dehydrogenase (LDH) released from any cells not killed by the exposure. HUVEC tubes (6 X 10^4 cells/well) were treated with DEP (0, 1, 10, 100 μg/ml) in the presence or absence of 10 mM NAC for 24 hr. After exposure to DEP, cells were rinsed with cold PBS to remove any LDH released from dead cells. The remaining live cells were lysed by a 1 hr incubation in 200 μl of the lysis buffer provided in the kit. The relative fluorescence (described in relative fluorescence units) of LDH at 490 nm was then measured. Endothelial tubes not exposed to DEP were used as the positive control, defining the maximum amount of LDH released as 100%. The absorbance of test samples was expressed as a percentage of this maximum, representing the percentage of cells surviving DEP exposure relative to the number of surviving unexposed cells.

Analysis of intracellular ROS accumulation

The ROS detection studies were performed using an Image-iT^{TM} Live Green Reactive Oxygen Species Detection Kit (Molecular Probes/Invitrogen). The method involved analyzing the intracellular accumulation of ROS due to H_2O_2 generation, based on the conversion of the non-fluorescent probe carboxy-H_2DCFDA (2', 7'-dichlorohihydrofluorescein diacetate) to green-fluorescent carboxy-DCF. Endothelial tubes were treated with 0, 1, 10 and 100 μg DEP/ml for 24 hr. DEP were then washed away with 37°C 1X PBS, and the samples were incubated for 25 min at 37°C with fresh medium containing 25 μM carboxy-H_2DCFDA, which penetrates cells. After washing again with 37°C 1 X PBS, ROS detection was visualized with epifluorescence microscopy at 200X magnification (emission at 495-529 nm, Olympus IX71 Inverted Microscope), examining the carboxy-DCF which could not be transported out of the cells.

Measurement of H_2O_2 production

H_2O_2 production was assessed with (10-acetyl-3,7-dihydroxyphenoxazine) using a commercially available Amplex Red Hydrogen Peroxide/Peroxidase Assay Kit (Molecular Probes/ Invitrogen), with some protocol modifications. First a standard curve was prepared using serial dilutions of H_2O_2. Endothelial tubes were treated with various concentrations of DEP (0, 1, 10, and 100 μg/ml) for 24 hr, then were scraped from wells and collected in pH adjusted SDS-PAGE buffer (25 mM Tris, 192 mM glycine, pH 7.4, 0.1% SDS) to which 1/100 volume of Sigma's protease inhibitor cocktail (cat. # P2714, containing AEBSF, Aprotinin, bestatin hydrochloride, E-64, EDTA and Leupeptin) was added. (The buffer contained no azide, so as not to interfere with the Amplex Red.) The protein in the lysate was quantitated, and made 4000 μg/ml. A 2.5 μl aliquot of lysate was added to 47.5

μl 1X PBS, then 50 μl of Amplex Red reagent/0.2 U/ml horse radish peroxidase, 0.5 mM

NADPH solution was added, and the mixture was incubated at room temperature for 30

min. The absorbance of samples was read on an HTS 7000 Plus Bio Assay Reader (540 nm

excitation, 590 nm emission-- Perkin Elmer Life Sciences). The amount of H_2O_2 was

determined by comparison to the standard curve.

Assessment of oxidative modifications of proteins

ROS-induced oxidative modification of proteins (i.e., amino acid side chains

modified with carbonyl groups by ROS) was detected using an OxyBlot Protein Oxidation

Detection kit (Chemicon). Briefly, the HUVEC tubes were scraped from wells, sonicated

for 1 min with pH adjusted SDS-PAGE buffer (as above) containing a final concentration

of 1% Sigma's P2714 protease inhibitor cocktail, then cell debris was removed by

centrifugation at 10,000 x g for 10 min. Protein concentrations were determined using the

bicinchoninic acid method (BCA Protein Assay, Pierce) at absorbance 540 nm. Lysate

proteins (5 μg/sample) were derivatized with 1,3-dinitro-phenyl-hydrazine (DNP)

following the manufacturer's protocol, and subjected to SDS-PAGE on 12% gels. Proteins

were then electrotransferred to 0.22 μm nitrocellulose membranes (Bio-Rad). Blots were

incubated for 1 hr at room temperature in blocking buffer (3% BSA with 0.02% NaN_3 in

TBST [25 mM Trizma base, pH 7.3, 3.0 mM KCl, 140 mM NaCl and 0.05% Tween-20,]),

then incubated with the kit's polyclonal DNP antibody (diluted 1:150) for 1 hr at room

temperature, followed by incubation with goat anti-rabbit HRP-conjugated IgG secondary

antibody (Bio-Rad cat. #170-6515), diluted 1-5000, for 1 hr at room temperature. The

nitrocellulose membrane was treated with Super Signal West Pico chemiluminescence

reagent (Pierce) for visualizing immunoreactive proteins on X-ray film. The band intensities of the many carbonyl-modified proteins in DEP-exposed sample lanes was visually compared with that of the negative control (i.e., endothelial tubes not exposed to DEP) to make a qualitative evaluation, but differences were not quantitated.

Protein preparation and Western Blot analysis

For Western blots of cell lysates, HUVEC tubes were collected and lysed by sonication for 1 min in pH adjusted SDS-PAGE buffer supplemented with 1% Sigma's protease inhibitor cocktail, then cell debris was separated out by centrifugation at 10,000 x g for 10 min. The concentration of protein in each sample was measured using the bicinchoninic acid method (BCA Protein Assay, Pierce). Cell lysate proteins were loaded (30 µg per well) onto SDS polyacrylamide gels for electrophoresis.

Nuclear protein extracts were prepared from the endothelial tube cells by adapting a one hour minipreparation technique (Deryckere and Gannon 1994). Briefly, cells were collected and sonicated 1 min in a relatively low salt lysis buffer (0.6 % Nonidet P-40 [NP-40], 150 mM NaCl, 10 mM HEPES pH 7.9, 1 mM EDTA, 0.5 mM phenylmethylsulfonyl fluoride [PMSF]), then centrifuged for 30 sec at 2500 rpm. The supernatant, which contained the nuclei, was next incubated for 5 min on ice, then centrifuged for 5 min at 5000 rpm. The pelleted nuclei were resuspended in a higher salt lysis solution (25% glycerol, 20 mM HEPES pH 7.9, 420 mM NaCl, 1.2 mM $MgCl_2$, 0.2 mM EDTA, 0.5 mM DTT, 0.5 mM PMSF, 2 mM benzamidine, and 5 µg/ml of aprotinin), and incubated on ice for 20 min. Insoluble nuclear debris was pelleted by a 30 sec centrifugation. The protein concentration of the supernatant containing the nuclear extract

was determined using a BCA Assay (Pierce), and the samples were frozen in liquid nitrogen and stored at -80°C until used for SDS-PAGE, when 20 μg protein per lane was applied to the gels.

Because endothelial tubes are always plated at the same density and incubated in the same relative volume of medium, for secreted products, 40 μl of medium was used directly for SDS-PAGE. For all of the three protein preparations mentioned (whole cell, nuclear, and medium), after electrophoresis the proteins were electrophoretically transferred to 0.22 μm nitrocellulose membrane. A 1 hr incubation at room temperature was performed in blocking buffer (3% BSA with 0.02% NaN_3 in TBST) to reduce non-specific reactivity of antibodies. All primary antibodies were diluted 1 to 1000 for use. These were: rabbit anti-rat HO-1 antibody (SPA-895, Stressgen); rabbit anti-human anti-Nrf2 peptide antibody (ab31163, Abcam); rabbit anti-human VEGF-A polyclonal antibody (ab46154, Abcam); rabbit anti-mouse GAPDH antibody (G9547, Sigma). The respective companies all indicated that the non-human antibodies used cross react with the corresponding human proteins, and this was, indeed, the case. Incubations were at $4^{\circ}C$, overnight. The secondary antibody for each was goat anti-rabbit IgG (H+L) conjugated to horseradish peroxidase (HRP) (Bio-Rad cat # 170-6515), diluted 1 to 5000, and blots were incubated 1 hr at room temperature. Blots were enhanced with Super Signal West Pico chemiluminescence reagent (Pierce), and exposed to X-ray film.

Immunofluorescence

HUVECs were seeded onto Matrigel-coated 2-well chamber slides for tube formation prior to DEP exposure. After DEP treatment for 24 hr, the HUVEC tubes were

fixed with 4% paraformaldehyde for 10 min, and then permeabilized with 0.05% Triton X-100 for 10 min at room temperature. Nonspecific reactivity was blocked by incubation with 2% normal goat serum plus 0.02% NaN_3 in PBS for 1 hr at room temperature. Endothelial tubes were incubated with primary polyclonal antibody against Nrf2 (Abcam ab31163) at a 1:100 dilution for 1 hr at room temperature, followed by a 1 hr room temperature incubation with goat anti-rabbit secondary antibody labeled with Alexa 488 (Molecular Probes/ Invitrogen cat # A11008), diluted 1 to 200. To the sections, Prolong Gold anti-fade mounting media including DAPI (Invitrogen) was added, and slides were covered for an overnight incubation at $4^{o}C$. All images were observed at 630X magnification on a Leica TCS SP5 Spectral Confocal Microscope.

Measurement of Cytokines IL-6 and TNF-α

Human TNF-α and IL-6 were evaluated using the Human TNF-α Ready-SET-Go! ELISA Kit with Pre-Coated Plates, and the Human IL-6 Ready-SET-Go! ELISA Kit with Pre-Coated Plate (eBioscience), following the manufacturer's instructions. Briefly, triplicate six well plates were seeded with 1.5 X 10^5 HUVEC cells/well, and, after tubes were formed, various concentrations of DEP (0, 1, 10, 100 μg/ml) with or without NAC (10 mM) were added for a 24 hr exposure. After this, 200 μl medium was collected and added to the kit's plate wells, purchased pre-coated with cytokine "capture" antibody. The plate was incubated overnight at $4^{o}C$, and the next day, medium was aspirated, and wells were washed with 2% normal goat serum with 0.02% NaN_3 in PBS for 1 hr at room temperature. After aspirating off the wash, a biotin-conjugated "detecting" primary antibody against either IL-6 or TNF-α was added for a room temperature incubation of 1 hr

duration. Once this was done, the supernantant solution was aspirated off, and the wells were washed several times. Avidin conjugated-horse radish peroxidase (HRP) was added for a 1 hr room temperature incubation. Finally, substrate solution (tetramethylbenzidine) was added for a 15 min room temperature incubation, then plates were read at 450 nm. The levels of IL-6 and TNF-α were determined by comparison to a standard curve that was graphed from analyzing the 450 nm readings of 2 fold serial dilutions of each cytokine. For this, plates whose wells were pre-coated with capture antibody were used, and the procedure outlined above was used with the serial dilutions rather than sample medium.

Statistics

For statistical analysis, each experiment was performed at least 2 times, and in each case, samples were always run in triplicate. The results were expressed as means $\pm$ SD and were analyzed using Student t-tests. $p < 0.05$ and $p < 0.01$ indicated by * and **, respectively, were considered statistically significant.

RESULTS

DEP are cytotoxic and induce generation of ROS in endothelial tubes

Our previous work used LDH assays to demonstrate that a 24 hr DEP exposure is cytotoxic to HUVEC tubes. To evaluate whether cytotoxicity was a consequence of oxidative stress, as is true with monolayer cultures (Bai *et al.* 2001; Furuyama *et al.* 2006), assays were repeated with the addition to medium of 10 mM N-acetyl cysteine (NAC) along with the 0, 1, 10, or 100 μg DEP/ml employed. NAC has been shown to increase

endogenous glutathione levels and reduce the effects of oxidative stress and cytotoxicity (Furuyama *et al.* 2006; Olivieri *et al.* 2001; Pocernich *et al.* 2000). As seen in Fig 3-1 (black bars), cell death was detectible in particle-exposed cells at all DEP concentrations. However, in the presence of NAC (white bars), endothelial tube cells were unaffected by DEP at 1 and 10 μg/ml concentrations. Without NAC, at 100 μg DEP/ml, only 40% of the cells survived the 24 hr treatment, but when NAC was added, 80% of the cells survived. These findings support the idea that DEP induce oxidative stress.

Generation of ROS by the HUVEC tubes in response to DEP was evaluated using an ROS detection kit for live cells (Image-iT Live Green ROS Detection kit, Molecular Probes/ Invitrogen) coupled with visualization by microscopy (Fig. 3-2A). This method also allowed evaluation of changes in structural integrity of the capillary-like tubes. As seen in the left panels, HUVEC tube integrity is unaffected by DEP at 1 μg/ml, and only slightly affected by 10 μg/ml. At 100 μg/ml the tube cells remain in the same position on the plate, but round up and lose cell-cell contacts. The right panels of Fig 3-2A shows ROS generated in response to DEP. The ROS were detected by adding to HUVEC tube cells non-fluorescent carboxy-DCFH after DEP exposure, and visualizing the amount of compound converted to fluorescent carboxy-DCF. When 1 μg DEP/ml was used, ROS production was minimal, with only 5-10 small green punctate areas indicating ROS generation. Samples treated with 10 μg/ml DEP showed slightly more fluorescence. In the wells treated with 100 μg DEP/ml for 24 hr, ROS generation was very abundant, with nearly all the cells fluorescing.

To identify if H_2O_2 is among the ROS generated in response to particles, endothelial tube cells were exposed to 0, 1, 10 or 100 μg DEP/ml for 24 hr, then incubated

with Amplex Red and spectrophotometrically assayed at 540 nm. Comparison to a standard curve determined the amount of H_2O_2 generated per well (each containing 1.5 x 10^5 cells). As shown in Fig 3-2B, cells exposed to 1 μg DEP/ml generated only 1.1 times more H_2O_2 (0.18 nmol) than untreated cells (0.16 nmol). At the 10 μg/ml and 100 μg/ml concentrations of DEP, production of H_2O_2 in the tube cells was 2.8 times higher (0.51 nmol, $p < 0.05$) and 12.8 times higher (2.05 nmol), respectively, than controls.

Oxidative modifications to proteins were detected by an OxyBlot assay. HUVEC tube extracts were made after DEP exposure, and protein carbonyl groups were derivatized to 2,4-dinitrophenylhydrazone (DNP) moieties using dinitro-phenyl-hydrazine. Proteins were separated on SDS-polyacrylamide gels, and blotted onto nitrocellulose membrane. An antibody against DNP was used to detect the level of derivatized carbonyls (Fig. 3-2C). Compared to cells not exposed to particles, DEP caused increased protein oxidation as assessed by the intensity of the immunoreactivity against the equal amounts of protein loaded in each well. The two lower DEP exposures (1 and 10 μg/ml) were not significantly different from each other, however, the 100 μg DEP/ml exposure greatly increased the immunoreactivity, indicating increased levels of carbonyl groups in endothelial tube cell proteins.

Effect of DEP on Nrf2 expression and activation

Detection of H_2O_2 and oxidative modifications of proteins suggested that cells would likely mount a detoxification response to enhance their chance of survival. Nuclear factor erythroid 2-related factor 2 (Nrf2) is a transcription factor known to regulate detoxification enzymes. This factor responds to oxidative stress by translocating from the

cytoplasm to the nucleus, where it binds to gene promoter regions, enhancing transcription. HO-1 gene expression is one that is enhanced by Nrf2 (Buckley *et al.* 2003; Hsieh *et al.* 2009). To evaluate whether this occurs in the 3D HUVEC model, endothelial tubes were assessed for their expression of Nrf2 in response to DEP. Immunoblots of Nrf2 from two kinds of protein extracts were performed. One was a whole cell extract of DEP-treated tubes: this blot demonstrated that the overall level of Nrf2 does not change in response to DEP exposure (Fig 3-3A, lower blot). A separate set of DEP-treated tubes was used to isolate and prepare a nuclear protein extract. The levels of Nrf2 in the nuclear extract increased with increasing DEP concentration (Fig 3-3A, upper blot). At 1 and 10 μg DEP/ml, the amount of nuclear Nrf2 is 3.0 and 5.2 times higher than that of the control, respectively. At the highest concentration of DEP, it was 9.0 times greater. The shuttling of the transcription factor from the cytoplasm to the nucleus is shown *in situ* in Fig. 3-3B, where the Nrf2 immunofluorescence pattern of untreated endothelial tubes is compared to those treated with 100 μg DEP/ml. In unexposed capillary-like tubes, Nrf2 (green) was present predominantly in the cytoplasm after 24 hr in culture. Following a 24 hr exposure to 100 μg DEP/ml, the transport of Nrf2 to the nucleus was dramatic. Merging the Nrf2 and DAPI nuclear images clearly shows much of the green Nrf2 colocalizing with the blue nuclei. These data place Nrf2 in the correct location after DEP exposure for enhancing the expression of detoxification enzymes.

Expression of antioxidant protein HO-1

The production of ROS and nuclear localization of Nrf2 suggested that endothelial tubes employ detoxification enzymes, such as heme oxygenase-1 (HO-1), to mount a

defense against DEP-induced toxicity. Therefore, levels of HO-1 were evaluated as a representative of ROS-minimizing enzymes. After a 24 hr exposure to DEP, HUVEC tube proteins were analyzed for HO-1 levels by Western analysis (Fig 3-4A). A strong increase was observed at the 10 μg/ml exposure, and an extreme response was observed at 100 μg/ml. The presence of NAC in the cultures attenuated the induction of HO-1 expression, and the more specific inhibitor of HO-1, tin protoporphyrin (SnPP), totally inhibited HO-1 expression. Fig 3-4B shows a quantification of the blots, and accentuates that HO-1 is around 3.8 times higher after exposure to 10 μg DEP/ml, and 9 times higher after exposure to 100 μg DEP/ml. NAC and SnPP significantly reduced the HO-1 response, with the specific HO-1 inhibitor SnPP having more effect at the 100 μg DEP/ml concentration than NAC did.

To examine the timing of HO-1 expression, HUVEC tubes were treated with 10 μg DEP/ml for 6, 12 and 24 hr, and HO-1 was evaluated by Western analysis. To attenuate ROS, 10 mM NAC was added to sister cultures at the same time the 10 μg DEP/ml treatment was started. DEP caused an increase in HO-1 by 6 hr, which grew stronger at 12 and at 24 hr (Fig 3-4C). Again, NAC totally inhibited the induction of HO-1 in tubes exposed to 10 μg DEP/ml. Quantification of the blots in histogram form (Fig 3-4D) shows HO-1 was increased over controls by 1.2 fold at 6 hr, by 1.6 fold at 12 hr, and by ~3.5 fold at 24 hr. This is in good agreement with the previous experiment, where the 24 hr response value was 3.8 fold higher than controls. These results suggest that exposure to 10 μg DEP/ml causes HO-1 induction to begin slowly, taking between 6 and 12 hr to get a 60% increase over controls, but that the response intensifies by 24 hr, being 350% higher than controls.

Affect of DEP on cytokines TNF-α and IL-6

The respiratory system and capillaries have been shown to respond to DEP exposure by secreting pro-inflammatory cytokines TNF-α and IL-6 (Alfaro-Moreno *et al.* 2002; Hartz *et al.* 2008; Inoue *et al.* 2006; Ulrich *et al.* 2002). To examine whether this was true for endothelial tubes, cultures were treated for 24 hr with 1, 10, or 100 μg DEP/ml plus or minus NAC (10 mM). As determined by comparison to an ELISA-generated standard curve (not shown), unexposed control HUVEC tubes released 16.6 pg/ml of TNF-α and 11.8 pg/ml IL-6 into the medium (Fig 3-5A). No significant difference was observed in cytokine levels when HUVEC tubes were exposed to 1 μg/ml DEP. However, at 10 μg/ml DEP, 22.7 ± 0.6 pg/ml TNF-α and 21.8 ± 0.6 pg/ml IL-6 was found in medium, and with a 24 hr exposure to 100 μg DEP/ml, the HUVEC tube cells expressed 47.5 ± 2.3 pg/ml TNF-α and 42.4 ± 3.6 pg/ml IL-6, about 3-4 times the control levels. The presence of NAC significantly suppressed expression of both cytokines. With this ROS inhibitor, 100 μg DEP/ml induced secretion of only 20.4 ± 5.2 pg/ml TNF-α and 20.2 ± 0.84 pg/ml IL-6. These values are comparable to those of samples exposed to 10 μg DEP/ml without any added NAC, and strongly indicate that ROS generated by particle exposure mediate the secretion of the cytokines from endothelial cells.

TNF-α has been shown to induce expression of HO-1 in HUVEC monolayer cultures, whereas IL-6 did not (Terry *et al.* 1998, 1999). Curious about whether this would be true for cytokine expression in HUVEC tubes after a 24 hr exposure, each cytokines was tested for how it modulated endothelial tube HO-1 expression. The amount of each cytokine secreted after a 24 hr exposure to 100 μg/ml DEP (i.e., 47.5 pg/ml TNF-α and

42.4 pg/ml IL-6) was added to endothelial tubes for a 24 hr incubation, and the level of HO-1 was assessed. (In this experiment, no DEP was added, just the amount of cytokine that 100 µg/ml DEP would have induced.) Neither cytokine changed the level of HO-1 expression after 24 hr (Fig. 3-5B). A quantification of the blot is shown in Fig. 3-5C. The lack of HO-1induction by IL-6 was expected. The fact that TNF-α did not induce HO-1 may be because its effect does not persist for 24 hr in culture unless there is an agent present, such as DEP, to continuously induce TNF-α expression.

DEP stimulate secretion of VEGF into the culture medium

HO-1 expression has been shown to induce secretion of vascular endothelial cell growth factor (aka VEGF-A, referred to as VEGF throughout) (Bussolati *et al.* 2004; Dulak *et al.* 2008; Lin *et al.* 2008). Therefore, to assess whether DEP-induced HO-1 increases secretion of endothelial VEGF, HUVEC tubes were treated for 24 hr with 0, 1, 10 or 100 µg/ml concentrations of DEP, with or without 10 mM NAC, or with and without SnPP. VEGF-A levels were then assayed by western analysis. As shown in Fig 3-6A, the level of VEGF-A was increased by DEP treatment, but addition of NAC totally diminished the effect and SnPP mostly diminished it. This strongly suggests that the effect of DEP is mediated by ROS, and that HO-1 expression is one of the major effectors of the VEGF-A secretion. However, the fact that SnPP could not totally inhibit VEGF-A secretion indicates that factors other than HO-1 must be involved in the elevated DEP-induced secretion of VEGF-A. Quantification of the VEGF-A levels is shown graphically in Fig. 3-6B.

Finally, assays were performed to test whether cytokines TNF-α and IL-6 were factors influencing VEGF-A levels after 24 hr was tested. The amount of each cytokine produced after tubes are exposed to 100 μg DEP/ml (47.5 pg/ml TNF-α and 42.4 pg/ml IL-6) was applied to HUVEC tubes, and allowed to incubate for 24 hr (with no added DEP). As seen in Fig. 3-7A, both cytokines independently upregulate VEGF-A, and together their 24 hr effect is slightly increased compared to each individually. The quantification of the blot is shown in Fig. 3-7B. The results indicate that VEGF-A secretion is also regulated by a DEP-induced proinflammatory mechanism.

DISCUSSION

The many similarities between *in vitro* endothelial capillary tubes and *in vivo* capillary structures (Donovan *et al.* 2001; Grant *et al.* 1991; Zimrin *et al.* 1995) prompted the use of HUVEC tube cultures as a simplified way to gain an understanding of the effects DEP might have on lung capillaries. This model system cannot target any particular area of the lung, and is lacking other cell types adversely influenced by DEP, which subsequently release components injurious to the endothelium. The model system can only evaluate what may occur if inhaled DEP are translocated to the endothelia. There is significant evidence in the literature indicating that particles with similarities to DEP do, indeed, reach the capillaries (Geiser *et al.* 2005; Kreyling *et al.* 2002; Kreyling *et al.* 2009; Nemmar *et al.* 2002; Nemmar *et al.* 2004b; Nemmar *et al.* 2001; Oberdorster 2002). Thus, it is likely that HUVEC tubes can be effectively employed to model potential effects of DEP on the vasculature.

Previous work compared HUVEC monolayers and the HUVEC tube model, and suggested that endothelial tubes are perhaps a more biologically relevant model system. (The data on tubes and the discussion of both cultures is presented in Chao et al., submitted). The most notable behavioral property that endothelial tubes have in common with *in vivo* capillaries is strict negative regulation on proliferation, even while large areas of the culture dish are empty. Therefore, a three dimensional conformation appears to confer a more biological context for study. When tubes were exposed to DEP, the simulated vessels clearly became permeable, as demonstrated by redistribution of the adherens junction component VE-cadherin to an intracellular location (Chao et al., submitted). The aim of the present study was to examine how DEP induce endothelial tube permeability.

DEP have been shown to induce ROS in animal models, monolayer endothelial cell cultures (Bai *et al.* 2001; Sagai *et al.* 1993), and now from this work, in capillary-like endothelial tubes. This was determined by (i) demonstrating that N-acetyl cysteine attenuated DEP cytotoxicity, (ii) observing an increase in protein oxidation, and (iii) by measuring a DEP-induced generation of H_2O_2. The importance of H_2O_2 generation cannot be underestimated because it has been shown to induce VE-cadherin internalization in endothelial cell monolayer cultures, causing cell-cell gaps that make the monolayers permeable (Kevil *et al.* 1998). Thus, the permeabilization of endothelial tubes via the DEP-induced reorganization of VE-cadherin (Chao et al., submitted) is, in part, likely due to the generation of H_2O_2.

VEGF-A is also known to affect permeability (Connolly *et al.* 1989; Ferrara and Henzel 1989; Keck *et al.* 1989; Senger *et al.* 1983), and VEGF-A inhibitors are used to

decrease edema in cancers (Gerstner *et al.* 2009; Strugar *et al.* 1994). Thus, another mechanism warranting consideration was a possible DEP-induced influence on VEGF-A levels. VEGF-A has been shown to be induced by HO-1 (Cisowski *et al.* 2005; Dulak *et al.* 2008; Jozkowicz *et al.* 2003). Therefore, whether DEP induced HO-1 was investigated. Nrf2 is a factor controlling expression of HO-1 (Buckley *et al.* 2003; Hsieh *et al.* 2009), and endothelial tubes exposed to DEP transported Nrf2 from the cytoplasm to the nucleus. In addition, HO-1 expression was induced within 6-12 hr. The link between HO-1 and VEGF-A secretion was investigated by exposing endothelial tubes to DEP in the presence and absence of NAC and the HO-1 inhibitor SnPP, followed by measuring the amount of VEGF-A in the culture medium after 24 hr. VEGF-A secretion was induced by DEP, and the levels were attenuated by the addition of NAC and SnPP, indicating that DEP-induced HO-1 is a factor contributing to endothelial VEGF-A secretion.

Several years ago it was demonstrated that IL-6 regulates permeability in endothelial cells in monolayer culture (Maruo *et al.* 1992). Pro-inflammatory cytokines, including IL-6 are stimulated by DEP exposure, whether by intratracheal installation of DEP into mouse lungs (Inoue *et al.* 2006), by involuntary whole particle aspiration (Singh *et al.* 2004), or by direct application of particles in medium of macrophages *in vitro* (Bachoual *et al.* 2007). To further identify mechanisms for DEP-induced vascular permeability, the effect of DEP on TNF-α and IL-6 secretion was tested, as was the effect of these cytokines on VEGF-A secretion. TNF-α and IL-6 secretion by endothelial tubes was up-regulated by DEP exposure, and this up-regulation was inhibited by NAC. In addition, the amount of each cytokine induced by 100 µg/ml DEP was capable of increasing secreted VEGF-A levels in the absence of DEP. However, while TNF-α and

IL-6 elevated VEGF-A, they did not accomplish this by enhancing the expression of HO-1. A 24 hr incubation of endothelial tubes with the cytokines had no effect on HO-1 levels. Times shorter than 24 hr were not tested. Thus, after exposre to DEP for 24 hr, endothelial permeability was facilitated by the ROS induction of TNF-α and IL-6 cytokines, and this upregulation is possibly via a mechanism independent of HO-1.

The experiments performed indicated that VEGF-A produced by the endothelial tubes in response to DEP does not induce angiogenesis, since there was no sprouting of tubes after DEP addition. Nor did the VEGF-A induce endothelial cell proliferation when assessed by MTS assays (data not shown). VEGF-A has splice variants, and the factor's effects can be mediated by several signaling pathways, one of which leads to chronic permeability and vasodilation. In any particular instance, the pathway affected may be modulated by the balance of VEGF-A splice variants present (Harper and Bates 2008), although other evidence suggests the persistent expression of total VEGF-A is more important than which variants are used (Esser et al., 1998).

In summary, the *in vitro* model system of capillary-like endothelial tubes was used to illucidate how DEP increase the permeability of endothelia. The experiments revealed that DEP are cytotoxic and cause oxidative stress, and in turn, the ROS that are generated induce H_2O_2 production, HO-1 expression and pro-inflammatory cytokines. These are all components known to contribute to endothelial permeability. HO-1 expression and pro-inflammatory cytokines may accomplish this by induction of VEGF-A secretion, which in many situations, particularly cancers, enhances endothelial permeability. A schematic of how DEP affect permeability is provided in Fig 8. To the figure is added a feed back loop, based on evidence that VEGF-A also induces HO-1 (Bussolati *et al.* 2004;

Fernandez and Bonkovsky 2003; Siner *et al.* 2007). If VEGF-A were to increase the amount of HO-1 in endothelia, this would ultimately serve to further induce additional VEGF-A secretion, and potentially promote endothelial permeability to a greater extent. Were these phenomena to occur to even a small degree in lung capillaries after exposure to DEP, it becomes possible to understand how particles might gain access to the bloodstream and contribute toward precipitation of adverse cardiovascular affects.

FIGURES

Fig 3-1. Cell survival is decreased by increasing concentrations of DEP (black bars), as assessed by LDH assays. The cytotoxicity of DEP is attenuated when 10 mM NAC is added to the cultures with the DEP (white bars). The LDH absorbances are expressed as relative percent of the untreated control tubes, defined as the 100% survival level. Values represent means $\pm$ SD, n = 3. Statistical analysis was by Student t-tests.
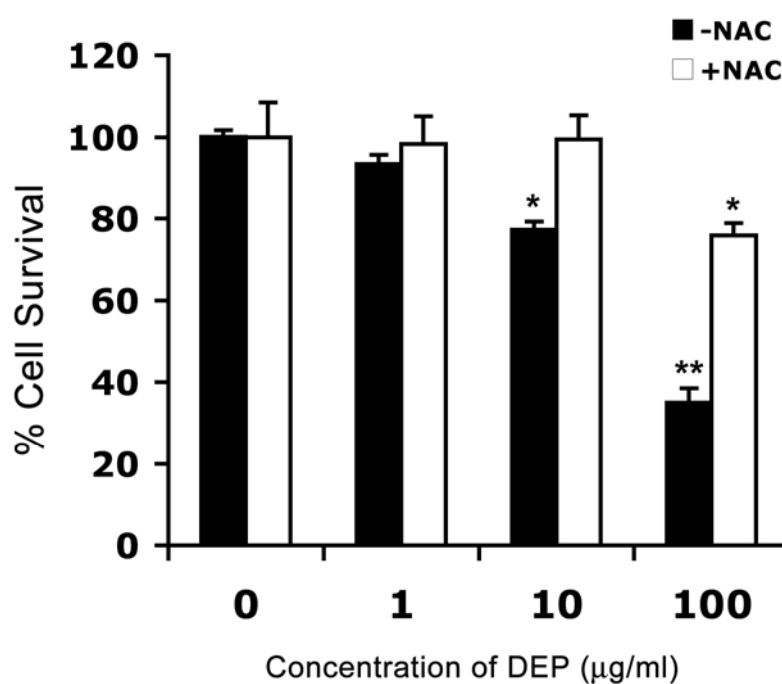
Fig 3-2. DEP cause generation of ROS in endothelial tubes. (A) HUVEC tubes were treated with no DEP, or 1, 10, or 100 μg DEP/ml for 24 hr. ROS detection was accomplished with the Image-iT^{TM} Live Green Reactive Oxygen Species Detection Kit. Tubes were visualized at 200X magnifications on an Olympus IX71 Inverted Microscope. Phase contrast images are shown on the left, and the epifluorescence is shown on the right. The green punctuate fluorescence represents conversion of non-fluorescent DCFH-DA (2', 7'-dichlorohihydrofluorescein diacetate) to fluorescent DCF by ROS. (B) H_2O_2 production generated in endothelial tube cells in response to 0, 1, 10 and 100 μg DEP/ml was assessed by Amplex Red assays, graphed as relative light units (left Y-axis). The nmol amount of H_2O_2 was experimentally determined by comparison to a standard curve (right Y-axis), calculated from assays run with known nmol amounts of H_2O_2 from serial dilutions (not shown). Values are means $\pm$ SD (n = 3). A Student t-tests statistical analysis was performed. (C) Further evidence of ROS was found by detecting an increase in carbonyl groups, indicating oxidization of proteins in endothelial tubes treated with increasing concentrations of DEP. Protein lysates were made from HUVEC tubes after exposure to DEP for 24 hr. Lysates were quantitated, and equal amounts of protein from each treatment group were used to derivatize carbonyl groups with dinitro-phenyl hydrazine (DNP). Samples were then electrophoresed and blotted for reaction with a DNP-specific antibody.

(A)

0 µg/ml

1 µg/ml

10 µg/ml

100 µg/ml
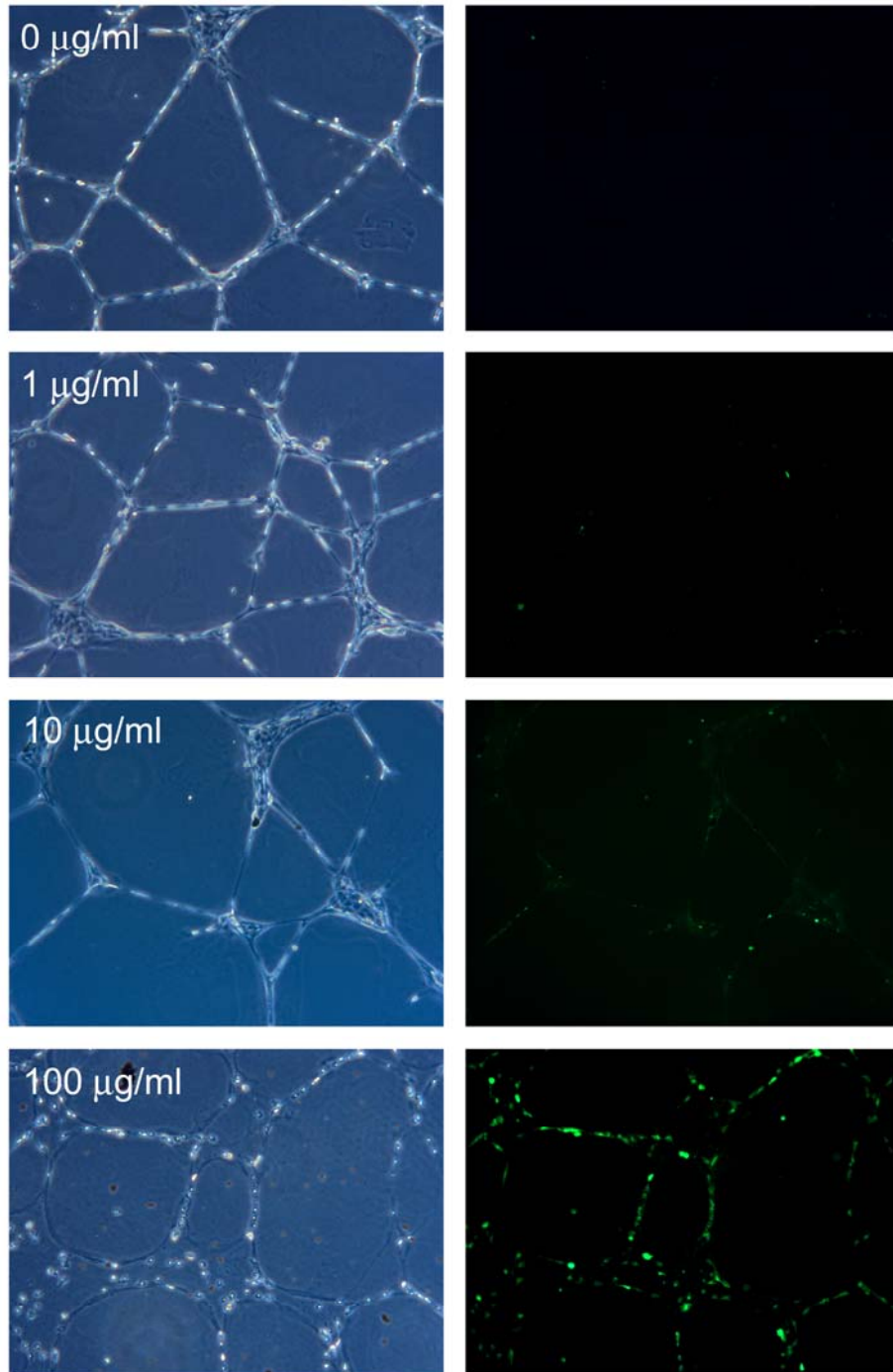
(B)
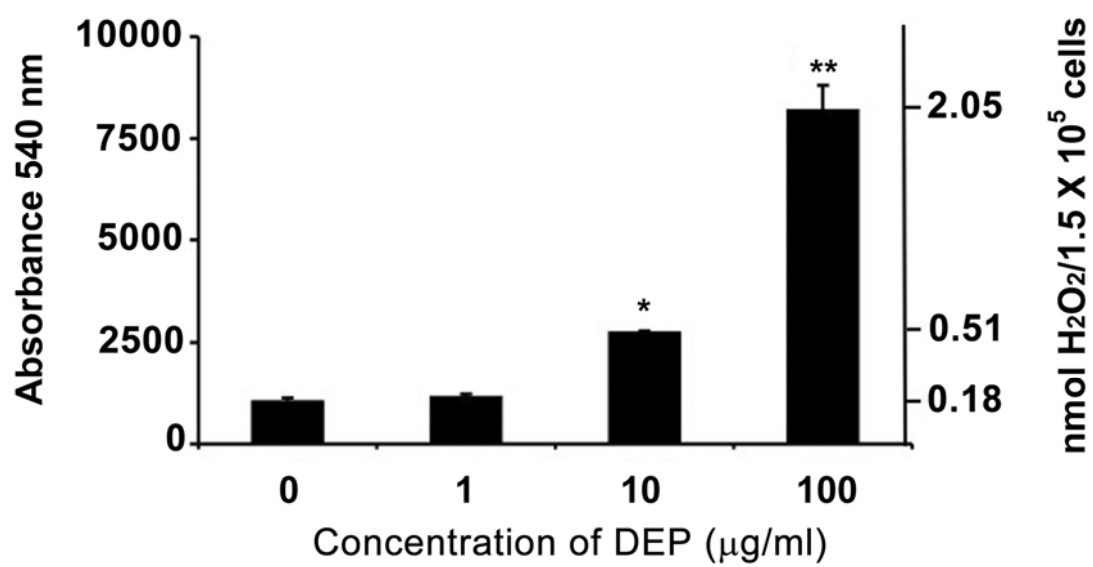
(C)
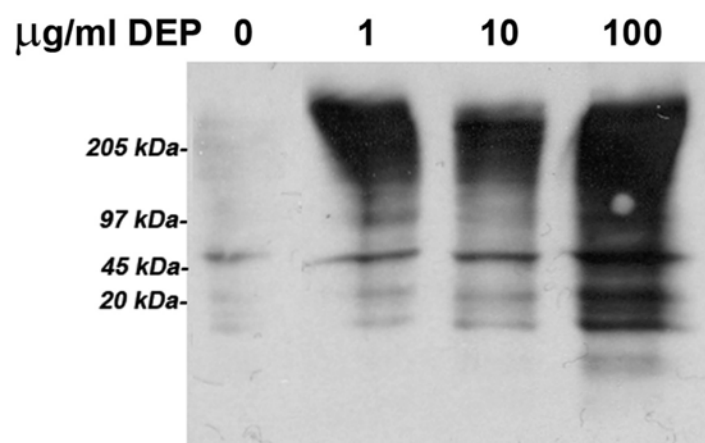
Fig 3-3. DEP induce translocation of Nrf2 from the cytoplasm to the nucleus. (A) Capillary-like endothelial tubes were incubated with no DEP, or 1, 10 or 100 μg DEP/ml for 24 hr. Two western blots are shown, one of Nrf2 in extracts of isolated nuclei (top), and the other of Nrf2 from whole cell protein isolates (bottom). The blots indicate that increasing amounts of DEP increase the Nrf2 levels that are translocated to the nucleus. (B) Confocal microscopy of Nrf2 plus or minus DEP: With no DEP, Nrf2 immunofluorescence is seen mostly in the cytoplasm. With exposure to 100 μg DEP/ml for 24 h, Nrf2 is found to be translocated to the nucleus. The magnification (630X) in all panels is same. Scale bar = 50 μm).

(A)
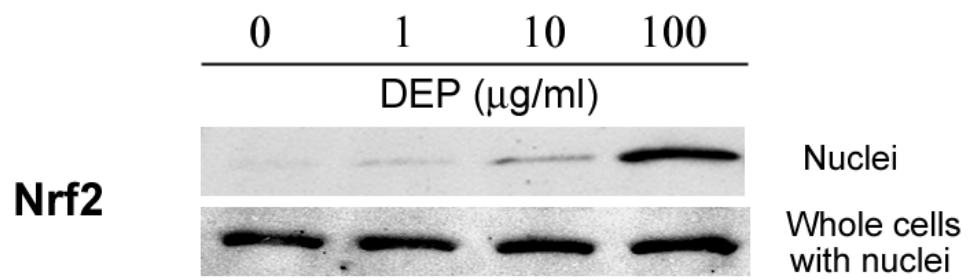
(B)
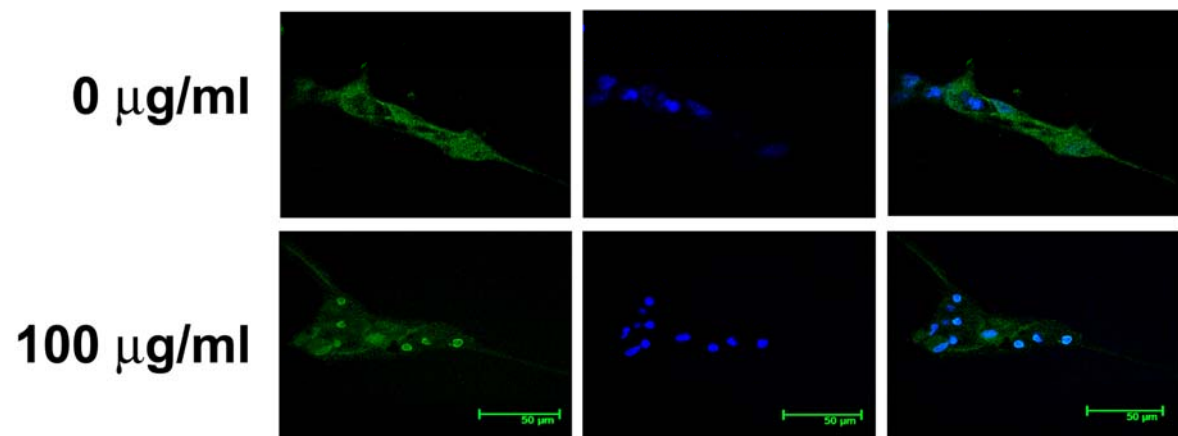
Fig 3-4. DEP induce endothelial expression of HO-1. (A) After a 24 hr exposure to no DEP or 1, 10 or 100 μg/ml, plus or minus 10 mM NAC or 25 μM SnPP, endothelial tubes were lysed and proteins extracted for Western analysis. Immunoblotting shows HO-1 is induced by DEP in a dose dependent manner, and that ROS is an intermediary for HO-1 induction, since HO-1 levels are reduced when NAC is added. Furthermore, SnPP totally inhibits the HO-1 expression induced by DEP. Equal protein loading was confirmed with GAPDH Westerns. (B) Histograms show a quantification of HO-1 levels after 24 hr exposure to DEP. Bars are the relative fold change compared to the control with no added DEP. (C) Western blotting was performed to determine the timing of HO-1 expression after addition of 10 μg DEP/ml to tubes, plus and minus NAC. Equal protein loading was confirmed by GAPDH immunoreactivity. (D) Quantification of HO-1 expression at 0, 6, 12, and 24 hr, derived from the Western blots. The HO-1 band intensity for the 0 time point was defined as one, and all other time points are shown as the fold-change relative to this point. *$p <$ 0.05 indicates significance. Values are means $\pm$ SD, n = 3. Statistical analysis was by Student t-tests.

(A)

NAC (10 mM)	−	−	−	−	+	+	+	+	−	−	−	−	
SnPP (25 μM)	−	−	−	−	−	−	−	−	+	+	+	+	
DEP (μg/ml)	0	1	10	100	0	1	10	100	0	1	10	100	

HO-1   33 kD

GAPDH   35 kD

(B)

(C)

| DEP (10 μg/ml) | − | + | + | + | − | + | + | + |
| NAC (10 mM) | − | − | − | − | + | + | + | + |

| Time (hr) | 0 | 6 | 12 | 24 | 0 | 6 | 12 | 24 |

HO-1

GAPDH
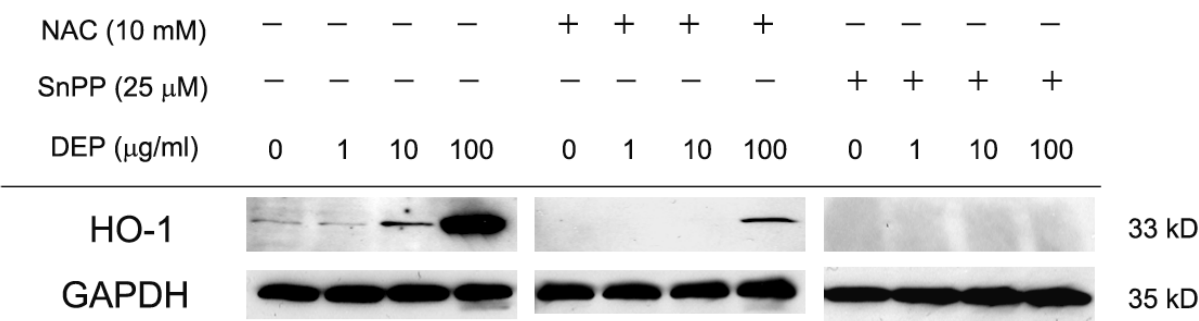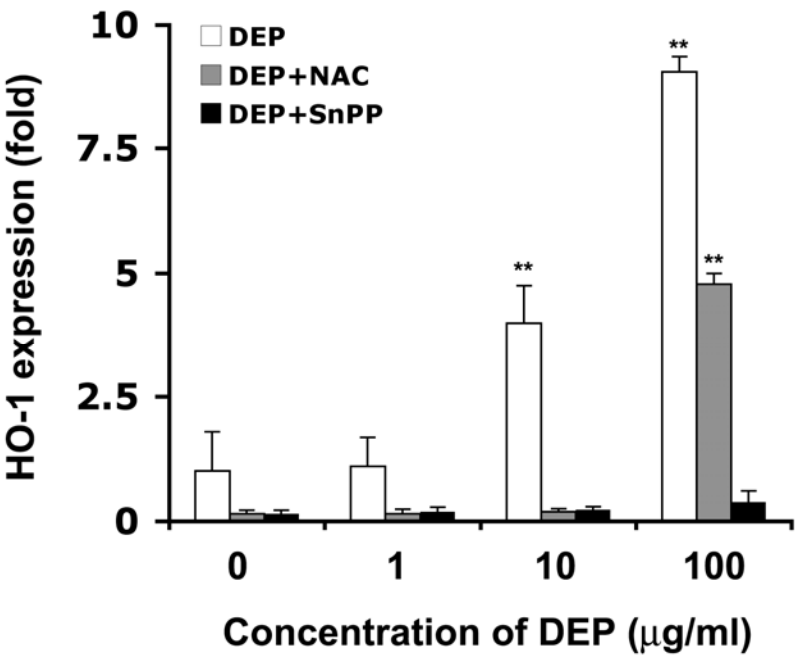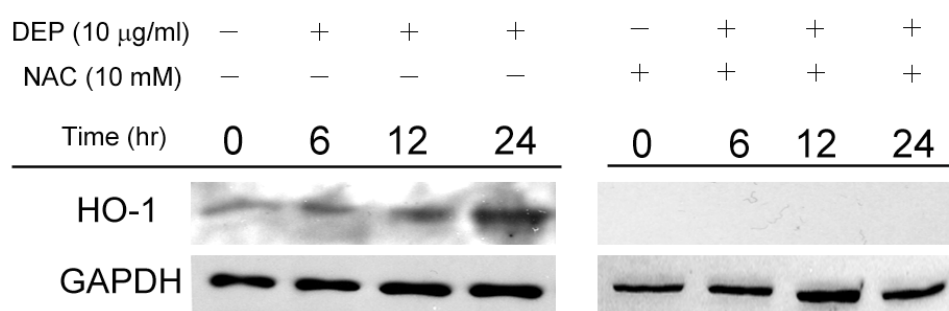
(D)
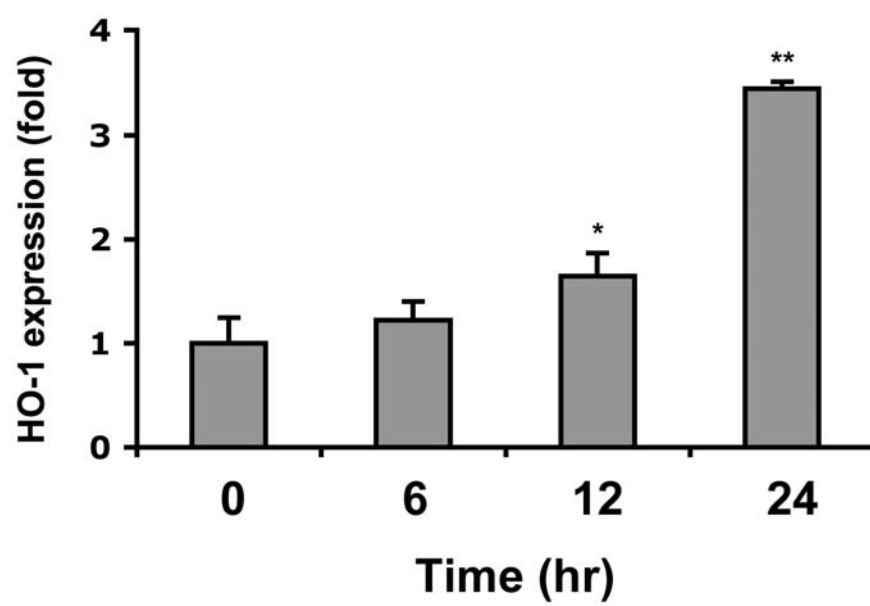
Fig 3-5. ELISAs demonstrate that DEP increase secretion of pro-inflammatory cytokines TNF-α and IL-6. (A) After exposing endothelial tubes to no DEP or 1, 10, or 100 μg DEP/ml, plus and minus 10 mM NAC, medium was collected and was evaluated by ELISA. Concentrations of TNF-α and IL-6 were found in the pg/ml range as determined by comparison to a standard curve (not shown). Increasing DEP concentrations increased cytokine secretion. NAC attenuated the increase of cytokine secretion. Significance was reached at *$p < 0.05$ and **$p < 0.01$ in samples treated with 10 and 100 μg DEP/ml compared to the same amount of DEP plus NAC. Values represent means ± SD (n = 6). Statistical analysis was by student t-test. (B) TNF-α and IL-6 do not affect HO-1 levels. The amount of cytokines secreted after a 24 hr exposure to 100 μg DEP/ml was previously determined by ELISA. This amount of TNF-α (47.5 pg/ml) and IL-6 (42.4 pg/ml) was added to endothelial tube cultures to evaluate whether the cytokines had a direct effect on HO-1 levels. After treatment of endothelial tubes with exogenous cytokines for 24 hr, Western analysis of HUVEC tube lysates was performed using HO-1 antibody. No significant increase in HO-1 was observed. Equal protein loading was confirmed with GAPDH immunoreactivity. (C) HO-1 response to TNF-α and IL-6 was quantificiated by normalizing the Western band intensities to those of GAPDH. HO-1 expressed by the no treatment control was defined as 1. Values are expressed as means ± SD (n = 3). Statistical analysis was by Student t-tests.

(A)
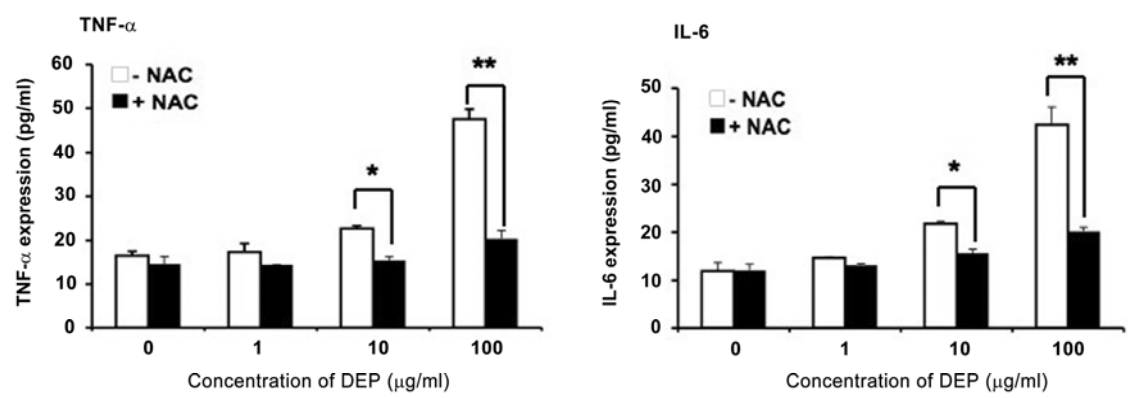
(B)

(C)
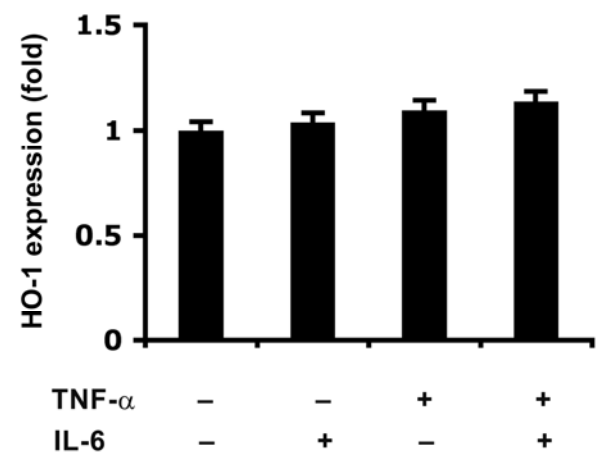
Fig 3-6. DEP induce VEGF-A secretion. (A) Secretion of VEGF from capillary endothelial tubes is related to DEP-induced HO-1 expression. HUVEC tubes were exposed to no DEP or 1, 10 or 100 µg DEP/ml plus or minus NAC (10 mM) or plus or minus SnPP for 24 hr. Medium was collected and run on gels for immunoblotting. Without NAC and SnPP, VEGF-A secretion increased in a dose dependent manner. NAC totally blocked VEGF-A secretion, and SnPP partially blocked it, indicating that, while HO-1 is partially an effector of VEGF-A secretion, factors other that HO-1 are also responsible. To assure that equal amounts of protein were loaded in each lane, half of each gels was used for the blot and the other half, loaded in the same order with the same amount of protein, was stained with Coomassie blue, and is indicated as "loading control". (B) Semi-quantification of VEGF-A secretion from the blots: The relative intensity of VEGF-A bands from the Western was graphed, with the value of the no DEP treatment sample set as 1. The data show that inhibiting HO-1 with SnPP does not totally block VEGF-A secretion as NAC does. Values of $*p < 0.05$ and $**p < 0.01$ compared with the control were considered significant. Values are mean $\pm$ SD, n = 3. Statistical analysis was by Student t-tests.

(A)

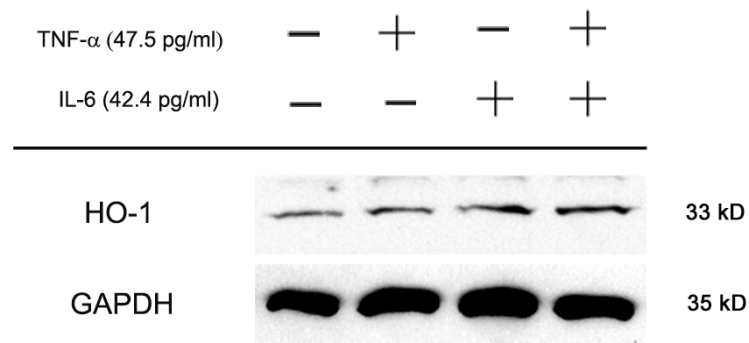| NAC (10 mM) | – | – | – | – | + | + | + | + | – | – | – | – | – |
| SnPP (25 μM) | – | – | – | – | – | – | – | – | – | + | + | + | + |
| DEP (μg/ml) | 0 | 1 | 10 | 100 | 0 | 1 | 10 | 100 | 0 | 0 | 1 | 10 | 100 |

VEGF-A   43 kD

Loading Control   -75 kD
-50 kD
-25 kD
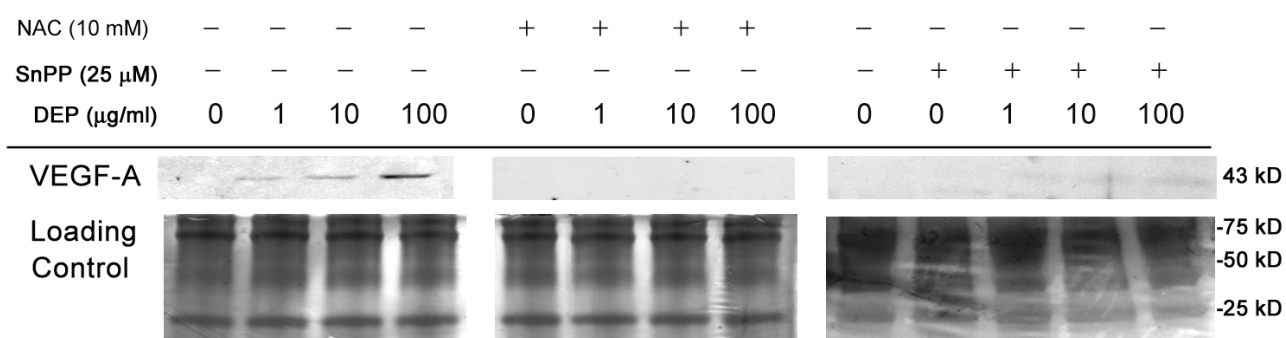
(B)
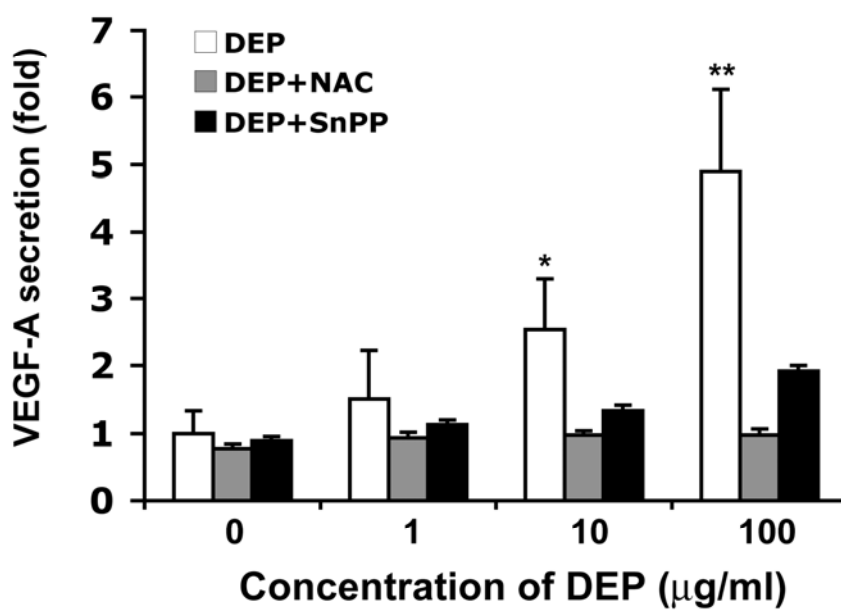
Fig 3-7. Exogenous cytokines TNF-α and IL-6 increase VEGF-A secretion by endothelial tubes. (A) To medium of HUVEC tubes (not exposed to DEP) was added exogenous TNF-α (47.5 pg/ml) and IL-6 (42.4 pg/ml) for a 24 hr incubation. After the treatment, the medium was collected and subjected to SDS-PAGE. Half the gel was used for Western analysis, probing with VEGF antibody, and the other identically loaded half served as a loading control, stained with Coomassie blue. (B) Semi-quantification of the intensity of VEGF-A bands from the blot indicates that both cytokines together have more effect on VEGF-A secretion than each individually, although the response to both is not perfectly addititive.

(A)
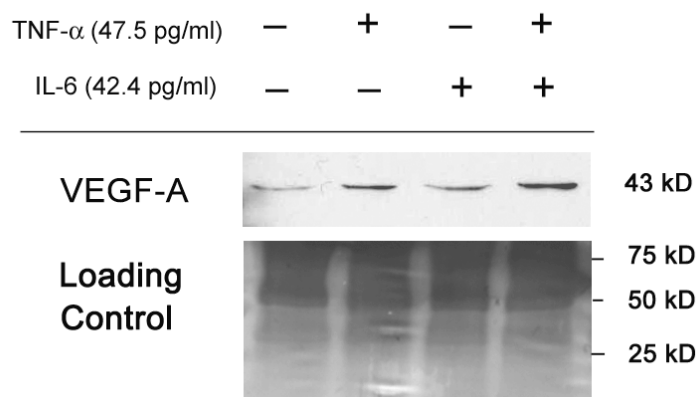
(B)
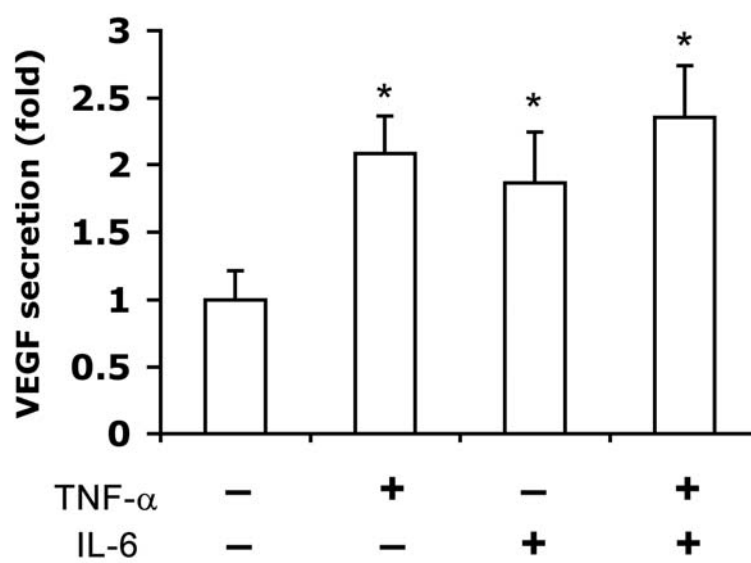
Fig 3-8. Schematic diagram depicting mechanisms potentially inducing vascular permeability. DEP cause capillary-like endothelial tubes to produce ROS. This increases vascular permeability by upregulating H_2O_2, which internalizes the cell-cell junctional VE-cadherin. Also, translocation of Nrf2 to the nucleus, upregulates HO-1 expression, and DEP trigger the release of pro-inflammatory cytokines TNF-α and IL-6. Both the antioxidant enzyme HO-1 and the proinflammatory cytokines increase secretion of VEGF-A, a factor known to increase endothelial permeability. Other reports indicate that VEGF-A induces the expression of HO-1 (Bussolati *et al.* 2004; Fernandez and Bonkovsky 2003; Siner *et al.* 2007), thus a feed back loop is included in the schematic.
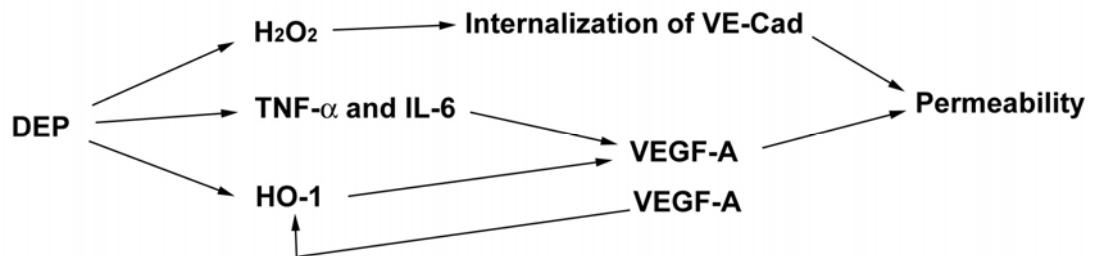
Chapter III

Diesel Exhaust Particles Induce HUVEC Tube Apoptosis by Inhibition of the Akt Pathway and activation of p53

ABSTRACT

A small percentage of inhaled diesel exhaust particles (DEP) reach the circulatory system (Nemmar *et al.* 2002; Nemmar *et al.* 2004b). Because DEP are implicated in the acute onset of cardiovascular events, such as myocardial infarction (Brook 2008), we have been exploring how DEP gain access to the lumen of endothelia by using *in vitro* cultures of pre-assembled endothelial tubes. In previous experiments, the factors involved in DEP-induced permeability were found to be redistribution of VE-cadherin from endothelial cell membranes to the cytoplasm, and pro-inflammator and pro-oxidative induction of VEGF-A secretion. In addition to inducing permeability, VEGF-A is often associated with cell survival. However, in DEP exposed samples, permeability has been correlated with cell death as assessed by MTS and LDH assays. Here we show that, while DEP cause VEGF-A levels to rise, they also induce the dissociation of VEGFR-2 from VE-cadherin in endothelial adherens junctions, an event that disfavors cell survival. The Akt-1 signaling pathway, often a player in permeability, was not activated by DEP. Our results indicate that DEP-induced cell death occurs by p53-mediated apoptosis. At low DEP concentrations, Mdm2 is expressed and likely helps offset the pro-apoptotic effects of p53, but at high concentrations, Mdm2 expression is absent and apoptosis is extensive.

Abbreviations: DEP, diesel exhaust particles; VEGFR-2, vascular endothelial growth factor receptor 2

INTRODUCTION

Epidemiological studies have demonstrated that vehicle emissions from diesel engines are a major source of ambient air particulate matter (PM), which can cause acute cardiovascular problems within 48 hr of exposure (Pope and Dockery 2006; Samet *et al.* 2000). PM is composed of solid and liquid particles which are predominantly produced from vehicle exhaust (Nel 2005). These particles and have a large surface area and contain a high content of potentially toxic components (Oberdorster and Utell 2002). Fine PM diesel exhaust particles (DEP, diameter ≤ 2.5 μm, $PM_{2.5}$) have been observed to reach the alveoli, and a small percentage of the particles are translocated to the systemic circulation (Mills *et al.* 2006). Our previous work using *in vitro* endothelial tubes has shown that DEP induce endothelial permeabilty. Permeability occurs by disruption of adherens junctions, and by pro-inflammatory and pro-oxidative induction of VEGF-A. Usually VEGF-A is also associated with cell survival, but in our system, MTS and LDH assays have shown that DEP are cytotoxic to HUVEC tubes. Since Akt-1 activation is involved in both cell survival and endothelial permeability, whether this was true at least for DEP-induced permeability was tested. In this report we show that it is not. In addition, we have identified the DEP-induced mechanism responsible for apoptosis: disruption of the association of VEGF receptor-2 from VE-cadherin and activation of the p53 pro-apoptotic pathway.

MATERIALS AND METHODS

Cell culture

Human umbilical vein endothelial cells (HUVECs) were cultured in endothelial cell growth medium EBM-2 Bulletkit (Lonza) with 2% FBS. Subculturing was performed when cell confluence has reached approximately 85%. Cell at passages 5 to 15 were used for assays. Medium was changed everyday. For endothelial capillary tube cell cultures, 10 mg/ml Matrigel (LDEV-free, BD Biosciences), a basement membrane extracellular matrix, was coated onto each well of 2-well chamber slides (120 μl/well) and 6-well (150 μl/well) plastic plates on ice, respectively. The Matrigel was allowed to solidify at 37°C for 30 min before adding cells. HUVECs were plated at 156 cells/mm^2 onto 2-well chamber slides (6 X 10^4 cells/well) and 6-well (1.5 X 10^5 cells/well) plastic plates for 12 hr before DEP exposure. Cells were grown in a 5% CO_2 atmosphere at 37°C.

Reagents

DEP were collected from a Japanese automobile diesel engine by Dr. Masaru Sagai (Aomori University of Health and Welfare, Aomori, Japan). DEP were dispersed by vortexing for 3 min then sonicating at 60 Hz for 5 min in Tween 80/PBS solution. Various concentrations of DEP dispersed in medium were applied to the tube cells for the assays. To verify inactivation of PI3-kinase and Akt, the pathway inhibitors Wortmannin (1 μM final concentration, Alexis) and LY294002 (20 μM final concentration, Alexis) were added to the medium of HUVEC tubes, and the resulting phenotypes were compared with the phenotype induced by DEP exposure.

Western analysis

For total protein extraction, 24 hours after DEP treatment HUVEC tubes were collected and sonicated for 1 min in 1 ml lysis buffer [25 mM Tris, pH 7.4, 0.1% SDS, 192 mM glycine, 1% protease inhibitor (Sigma)]. Debris was pellet by centrifuging at 10,000 x g for 10 min and the supernatant collected. Protein concentrations were measured using the bicinchoninic acid method (BCA protein assay, Pierce) and read at 540 nm. After denaturation for 5 min at 95°C, 40 μg protein was loaded in the wells of SDS polyacrylamide gels for electrophoresis.

For secreted proteins, medium from HUVEC capillary tubes was collected after DEP treatment. Because cell density and medium volume were constant across all samples, 40 μl of medium from each treatment condition was incubated at 95°C for 5 min before being loaded onto SDS polyacrylamide gels for electrophoresis. Coomassie blue was used to stain gels to verify equal loading of wells.

For immunoprecipitation, 1.5 mg/50 μl Dynabeads (Immunoprecipitation kit-Dynabeads Protein A, Invitrogen) were incubated with primary rabbit monoclonal anit-human VE-Cadherin antibody (1:80 dilution, Abcam) at 4°C, overnight. The conjugated Dynabeads-antibody were placed on a magnet, the supernatant was removed, then cell extracts were added. The protein in the extract was quantitated, and made 4 mg/ml, and a 250 μl aliquot was added to the beads (= 1 mg) for a 10 min incubation with rotation at room temperature. The Dynabeads-antibody-extracts were then washed and the immunotargeted protein was eluted from the Dynabead sample following the manufacturer's instructions. The eluates were denatured by heating at 95°C for 5 min and

loaded onto 7.5% SDS polyacryamide gels for electrophoresis. Dynabeads conjugated with rabbit IgG (cat # 011-000-003, Jackson ImmunoResearch) were incubated with cell lysates as negative controls.

Proteins separated electrophorectically on acrylamide gels were transferred to nitrocellulose membranes. Nonspecific reactivity of the membranes was reduced by incubation of the blot in blocking buffer (3% BSA with 0.02% NaN$_3$ in TBST) for 1 hr at room temperature. (TBST = 25 mM Tris, pH 7.4, 3.0 mM KCl, 140 mM NaCl and 0.05% Tween 20). Primary antibodies were: mouse monoclonal anti-human VE-cadherin (1:250, BD Biosciences), rabbit polyclonal anti-human VEGF-A (1:500, Abcam), rbbit polyclonal anti-human VEGF-B (1:1000, Abcam), rabbit polyclonal anti-rat VEGF-C (1:1000, Abcam), rabbit polyclonal anti-human VEGF-D (1:250, Abcam), rabbit monoclonal anti-human VEGFR-1 (1:10000, Abcam), rabbit polyclonal anti-human-VEGFR-2 (1:200, Abcam), mouse monoclonal anti-murine p53 (1:1000, Abcam), rabbit monospecific anti-human p21 (1:1000, Cell signaling Technology), rabbit monospecific anti-human PI3-kinase p110 (1:500, Abcam), mouse polyclonal anti-mouse Mdm2 (1:500, Abnova), rabbit polyclonal anti-mouse Akt (1:1000, Cell signaling Technology), rabbit polyclonal anti-mouse phospho-Akt (1:1000, Cell signaling Technology), and rabbit polyclonal anti-mouse GAPDH (1:5000, Sigma). All were verified as reacting with human proteins. Primary antibodies were added to blots at the appropriate dilutions for a 4°C incubation overnight. The appropriate secondary antibody conjugated to horseradish peroxidase (HRP) (i.e., either goat anti-mouse IgG or goat anti-rabbit IgG, Bio-Rad) was diluted 1:5000 in 5% non-fat dry milk, 1X TBST and incubated with blots for 1 hr at room temperature. The protein products on the blots were visualized after chemilluminescent treatment

(containing the HRP substrate luminol, fromPierce) by exposure to X-ray film. Protein preparations made from unexposed cells were use as controls.

The films of Westerns were subjected to identical exposure conditions for normalization purposes. For cell lysate analyses, the band density of immunodetected proteins were measured. These were normalized to density to the band from GAPDH immunoreactivity. The band intensity of secreted proteins were normalized to the density of the Coomassie blue-stained ~150 kD band in the loading control.

Immunofluorescence

After DEP treatment (0, 1, 10, and 100 μg/ml) for 24 hr, the tube cells were fixed with 4% paraformaldehyde for 10 min at room temperature. Nonspecific reactivity was blocked by addition of 2% normal goat serum with 0.02% sodium azide (NaN$_3$) in PBS for 1 hr at room temperature. The capillary tube cells were incubated with primary mouse monoclonal anti-human VE-cadherin (BD Biosciences), rabbit polyclonal anti-human VEGFR-2, rabbit polyclonal anti-human p53 (Abcam), and mouse monoclonal anti-mouse Mdm2 (Abnova) antibodies at a 1:100 dilution (10 μl in 1 ml blocking buffer, i.e., 2% normal goat serum) for 1 hr at room temperature. This was followed by incubation with goat anti-mouse secondary antibody labeled with Alexa 488 (green, cat # A21121, Invitrogen) or TRITC (red, cat # 115-025-146, Jackson ImmunoResearch) of goat anti-rabbit secondary antibody labeled with Alexa 488 (green, cat # A11008, Invitrogen) or Alexa 594 (red, cat # A11012, Invitrogen), used at a 1:200 dilution, incubating at room temperature for 1 hr. Slides were covered with Prolong Gold (Invitrogen) anti-fade mounting media with DAPI and stored at 4°C overnight. Images were observed at 400X

magnifications on an epifluorescent microscope (Olympus IX71 Inverted Microscope) or at 630X magnification on a Leica TCS SP5 Spectral Confocal Microscope.

Quantitation of apoptosis

HUVECs were cultured on 2-well chamber slides precoated with 120 µl Matrigel per well, incubated 12 hours to allow for tube formation, then tubes were exposed to various concentrations of DEP (0, 1, 10, 100 µg/ml) for 24 hours. As a positive control for apoptosis, cells were exposed to UV lights (5 mJ/min) for 10 minutes. Samples were fixed in 4% paraformaldehyde, 1X PBS for 10 minutes, and apoptosis was detected using a fluorometric TdT-mediated dUTP Nick End labeling assay kit (TUNEL, Promega). The samples were incubated in 100 µl Equilibration buffer for 10 min at room temperature, then 100 µl of TdT (Terminal Deoxynucleotidyl Transferase) buffer was added (98 µl Equilibration buffer, 1 µl Biotinylated Nucleotide Mix, and 1 µl TdT Enzyme) for a 60 min incubation at 37°C. Nuclei were stained with DAPI. The incorporation of fluorescein-12-dUTP at the 3′-OH ends of the HUVEC tube DNA was visualized by immunofluorescence microscopy (Olympus IX71 Inverted Microscope). Magnification was at 100X. The percentage of apoptotic cells was calculated by dividing the number of cells stained with dUTP fluorescein by the total number of DAPI stained nuclei (i.e., the total number of cells) in the field.

Measurement of Caspase 3 activity

Caspase 3 activity was assessed using the Caspase-Glo 3/7 assay kit (Promega). HUVEC tube cells were plated onto Matrigel precoated 12-well plates at a density of 156

cells/mm^2 (6 x 10^4 cells/well). After treatment with 100 µg/ml DEP for 1, 3, 6, 12 and 24 hr,

the plates were removed from the incubator and allowed to equilibrate to room temperature

for approximately 30 min, then the Caspase-Glo 3/7 assay reagent (200 µl/well) was

applied according to the manufacturer's instructions. Relative light units (RLU) emited by

the product were measured using a luminometer (HTS 7000 Plus Bio Assay Reader Perkin

Elmer Life Sciences, Shelton, CT). The absorbance values were compared with that of

non-treated controls and are expressed as the average fold difference from these controls.

Statistics

For statistical analysis, each experiment was performed in triplicate and repeated 2

or 3 times. The results were expressed as means ± SD for three independent experiments.

Differences between groups were analyzed by using Student t-tests and One-Way ANOVA

with GraphPad statistics software. * and ** are representative of $p < 0.05$ and $p < 0.01$,

respectively, and indicated a statistically significant difference.

RESULTS

Increasing concentrations of DEP increase VEGF-A secretions, while VEGFR-2 expression is unchanged

Our previous results have shown that increasing DEP levels induce secretion of

VEGF-A, making endothelial tubes more permeable. To identify which VEGF-A receptor

is involved in mediating the VEGF-A response, and to examine whether other VEGFs are

involved in a DEP-induced response, these proteins were analyzed by Western blots. Endothelial tubes were exposed for 24 hr to either no DEP, or to 1, 10 or 100 μg/ml DEP. After exposure medium was collected for VEGF isoform analysis and protein extracts were prepared from the HUVEC tubes for receptor analysis. As seen in Fig 4-1, endothelial tubes do not express VEGF-B or VEGF-C. VEGF-D is expressed, but is unchanged by DEP exposure. Only VEGF-A responds to DEP. As the DEP exposure concentrations rise, VEGF-A secretion is increased as well. Of VEGFR-1 and VEGFR-2, only VEGFR-2 is present, and it does not significantly change in amount after DEP exposure.

DEP disrupt the association of VEGR-2 and VE-cadherin

VEGFR-2 is associated with VE-Cad in the plasma membrane of healthy, functional endothelial cells. Because we previously demonstrated that VE-Cad is redistributed in response to DEP, we examined by pull down assays whether the association of these two molecules was disrupted by exposure to low concentrations of DEP (1 and 10 μg/ml). By first immunoprecipitating VE-Cad from HUVEC tube lysates, running the immunoprecipitated product on a gel, then using Western analysis to determine how muchVEGFR-2 was associated with the VE-Cad, it was observed that the amount of detectible VEGFR-2 decreased with increasing DEP concentration (Fig 4-2A). This would be expected if the VE-Cad-VEGFR-2 interaction is broken when VE-Cad is internalized or if the levels of VE-Cad decreased. As shown previously (Chao *et al*, submitted), VE-Cad levels were not significantly altered by DEP exposures, although the molecule was redistributed in cells. Fig 4-2B quantitates the blot, normalizing the VEGFR-2 levels to those of VE-Cad, and shows that 10 μg/ml DEP significantly reduced the association of the

2 molecules. In Fig 2C this is clearly visible by confocal microscopy. Without DEP exposure, The VEGFR-2 signal (green) overlaps with the VE-Cad signal (red), as shown in the merged panel. HUVEC tubes exposed to 10 µg/ml, however, show areas in the merged images where green does not overlap with red, indicating that the internalization of some VE-Cad with VEGFR-2 remaining at the cell surface.

DEP induce endothelial tube cell apoptosis

The association of VEGFR-2 with VE-Cad has been shown to enhance cell survival. The loss of association between the molecules should therefore result in cell death. To examine this, HUVEC tubes exposed to various concentrations of DEP were examined by fluorescent *in situ* end labeling (TUNEL) assay to evaluate apoptosis. As seen in Fig 4-3A, apoptosis is detectible at 10 µg/ml DEP, but is very extensive at 100 µg/ml. Quantitation of apoptosis is shown in Fig 4-3B. At 10 µg/ml DEP, about 18% of the cells have died, but at 100 µg/ml, 90% are dead. To examine apoptosis in another way, caspase 3 activity was evaluated at 1, 3, 6, 12 and 24 hr by using a Caspase Glo-3/7 Assay. As shown in Fig 4-3C, 100 µg/ml DEP induced capase 3 activity, reaching a maximum of about 2.5 times the control at 12 hr. However, the activation decreased between 12 and 24 hr after DEP treatment.

DEP exposure diminishes Akt-1 activation

The PI3 kinase/Akt pathway is implicated in both cell survival and increased endothelial permeability. DEP increase permeability, yet cause apoptosis. To examine how the PI3 kinase/Akt pathway responds to DEP exposure, Western analyses were performed.

PI3 kinase decreased with increasing DEP concentrations. Total Akt-1 levels remained constant with increasing DEP levels, but phosphorylated Akt-1 was decreased (Fig 4-4A). This data is shown as histograms in Fig 4-4B, and suggests that cells undergo apoptosis probably because Akt-1 is not activated by phosphorylation. This downregulation of PI3 kinase/Akt signaling by DEP was confirmed by comparing the Fig 4-4A blot with one made from HUVEC tubes treated with the Akt inhibitors Wormannin and LY294002 a blot. However, DEP did not depress the levels of PI3 kinase and Akt-1 as effectively as the amount of inhibitors used in the experiment.

Apoptosis occurs via p53 activation

DEP-induced apoptosis was further studied by examining the p53 and p21 pathways using Western analysis. As indicated in Fig 4-5A, p53 levels increase with increasing DEP concentrations, whereas p21 levels are unchanged (data not shown). Interestingly, Mdm2 is upregulated in HUVEC tube cells by the 2 lower doses of DEP, but is not in the highest dose. Mdm2 interaction with p53 likely plays a role in why 1 and 10 µg/ml DEP induce less apoptosis than the 100 µg/ml DEP dose. The histogram representation of the blot shown in Fig 4-5B indicates that with 0 and 1 µg/ml DEP, Mdm2 levels (white bars) are equivalent to p53 levels (black bars). With 10 µg/ml DEP, the amount of Mdm2 is about 30% lower than p53, and at 100 µg/ml, it is less than 10% of the p53 level. This is further highlighted in Fig 4-6, where colocalization of Mdm2 and p53 is observed with a low DEP concentration (10 µg/ml), but not with 100 µg/ml DEP, where no Mdm2 is apparent.

DISCUSSION

The present study demonstrated that, of the VEGF isoforms, only VEGF-A is responsive to DEP, increasing in amount with increasing DEP concentrations. The VEGF receptor in endothelial tubes is VEGFR-2, unlike endothelial monolayers where VEGFR-1 is the receptor (data not shown). The level of VEGFR-2 in endothelial tubes remained relatively constant after 24h exposure to varying concentrations of DEP. VEGFR-2 is associated with VE-Cadherin in endothelial membranes, and serves to enhance cell survival (Dejana 2004). Although VEGFR-2 levels did not change in response to DEP, the fact that VE-cadherin relocalized from the membrane to the cytoplasm reduced the amount of VEGFR-2 involved in survival-promoting complexes. This was shown both by pull down assays as well as confocal microscopy. At 10 µg/ml DEP, there was 25% less VEGFR-2 complexed with VE-Cadherin. As a consequence, endothelial tube cells underwent apoptosis in response to DEP, also shown by confocal microscopy.

Previously, we demonstrated that DEP made endothelial tubes permeable, which allowed particles to gain access to the endothelial tube lumen. The mechanisms contributing to this were (1) increased permeability from VE-cadherin internalization, and (2) increased permeability due to VEGF-A secretion that was stimulated by pro-oxidative and pro-inflammatory responses to DEP. Activation of the PI3-linase/Akt pathway has been implicated in vascular permeability (Kilic et al., 2006), but in our system, Akt-1 was not activated. Rather, DEP served to inactivate the Akt pro-survival pathway, inducing Western patterns that resemble those of normal endothelial tubes treated with Akt inhibitors Wortmannin and LY294002. Furthermore, the pro-apoptotic p53 pathway

(Levine 1997; Vousden and Prives 2009) was activated by DEP. However, p21, a known regulator of cell cycle, was unaffected by DEP exposure.

Phosphorylation of Akt has also been associated with an increased nuclear localization of Mdm2 (Ogawara *et al.* 2002). Although in our system Akt-1 was disabled, Mdm2 levels did increase with the 2 lower concentrations of DEP, as assessed by immunoblotting and confocal microscopy. Mdm2 is a negative regulator of p53 (Alarcon-Vargas and Ronai 2002; Honda *et al.* 1997; Oliner *et al.* 1993). Mdm2 and p53 form an autoregulatory feedback loop in which p53 positively regulates Mdm2 at the transcriptional level and Mdm2 negatively controls p53 expression at the posttranslational level (Mayo and Donner 2001). Our findings showed that both p53 and Mdm2 have a fairly equivalent dose dependent increase at 1 μg/ml DEP. At 10 μg/ml DEP, Mdm2 levels are somewhat lower than p53, but at the high DEP dose, Mdm2 were a fraction of p53 levels, and apoptosis levels were very high. It is possible that at low concentrations, DEP induces p53, which increases Mdm2, which then in turn negatively regulates the p53 activity. However, the 100 μg/ml DEP appear to inhibit any Mdm2 expression.

In summary, DEP induces changes in endothelial cell-cell junctions that disconnect the association between VEGFR-2 and VE-cadherin in the membrane. In addition, TUNEL assays and caspase 3 activity assay indicate that high concentrations of DEP induce apoptosis. The pathway used likely involves p53, since this molecule is upregulated by DEP exposure.

FIGURES

Fig 4-1. Western analysis of VEGF isoforms secreted into culture medium and VEGF receptors 1 and 2 in protein extracts of HUVEC tube cells. Only VEGF-A is responsive to DEP concentrations. Equal loading of samples was assured by using ~50 kDa band as a normalizer from medium proteins, and the GAPDH antibody signal for proteins from cell lysates.
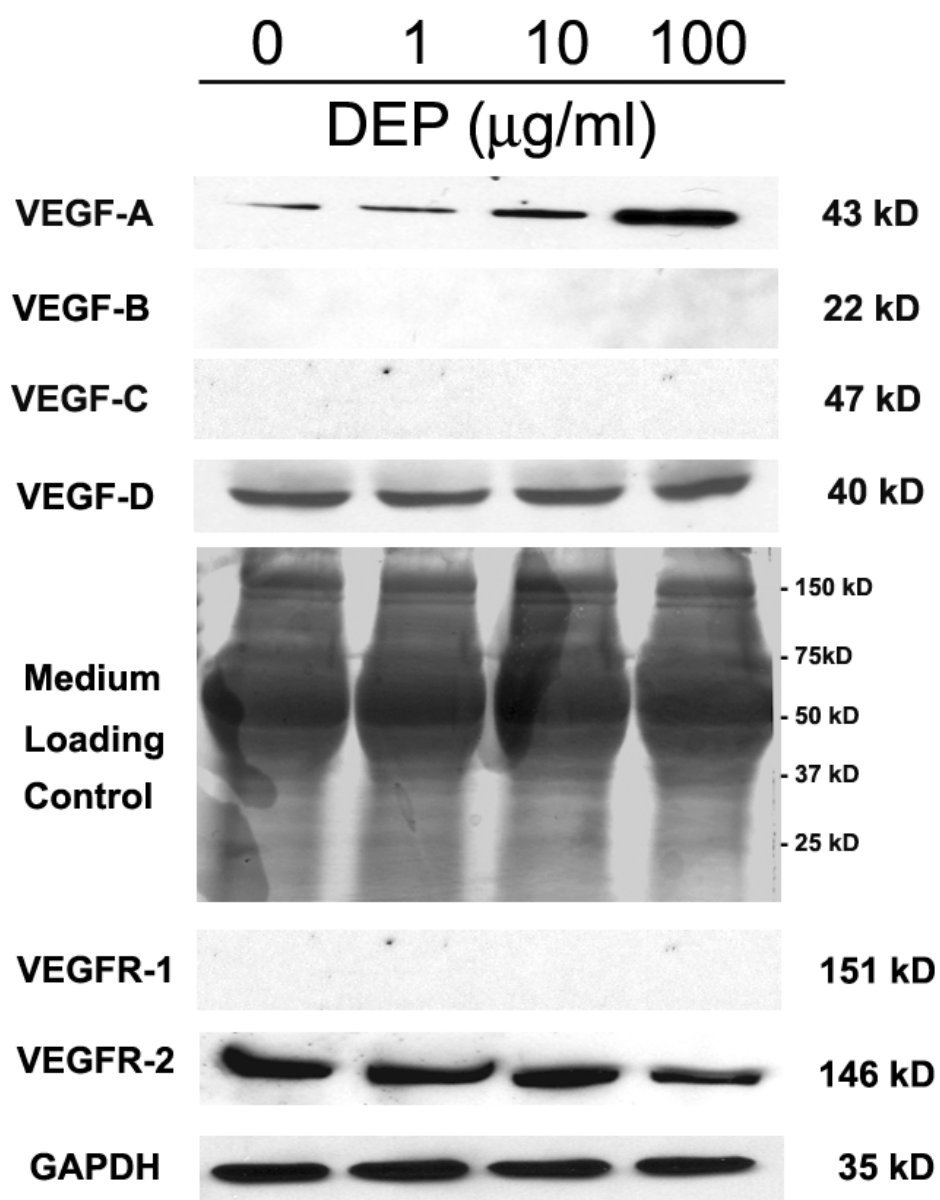
Fig 4-2. Effects of DEP on VEGFR-2 colocalization with VE-cadherin. (A) Pull down assays with VE-Cadherin antibody, followed by Westerns probed with VEGFR-2 antibody indicate that much of the cells VEGFR-2 is disassociated from VE-cadherin by DEP exposure. (B) A quantitation of the Western blots is shown as histograms. *$p < 0.05$ compared with the control, means ± SD, n = 3. (C) Confocal microscopy of VEGFR-2 (green) and VE-cadherin (red) show localization of the two molecules in control HUVEC tubes (upper panels). In those treated with 10 μg/ml (lower panels), merging the red and green signals demonstrates a decrease in colocalization, since individual green fluorescence is easily detectible. Shown are representative images from three independent experiments. Scale bar = 15 μm.

(A)

IP: VE-Cad
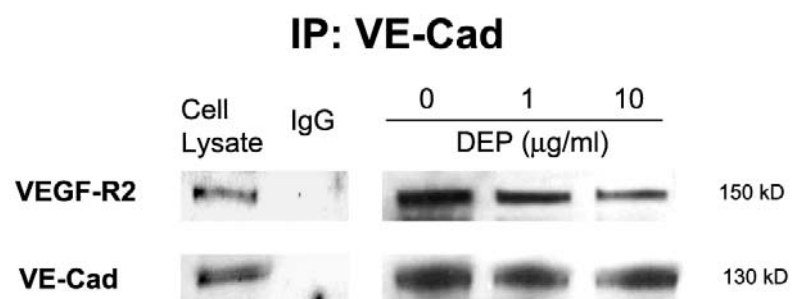
(B)
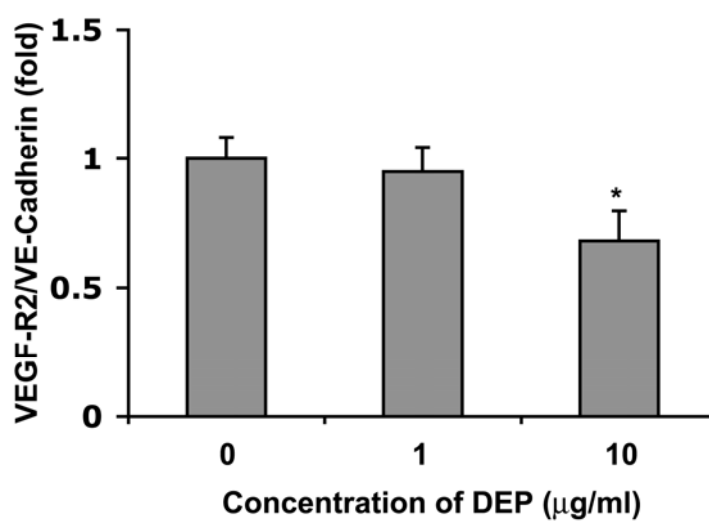
(C)
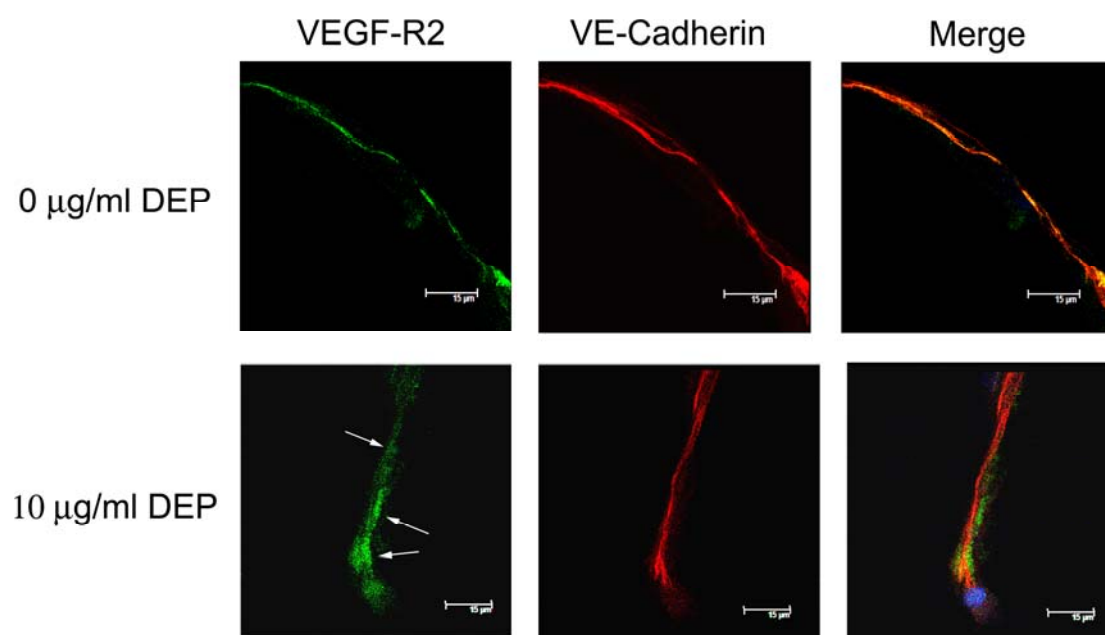
Fig 4-3. DEP induce endothelial tube cell apoptosis. HUVEC tubes were treated with 0, 1, 10 and 100 μg/ml DEP for 24 hr. (A) Left panel photos are stained for nuclei with DAPI (blue). Right panels detect apoptosis using *in situ* end labeling (TUNEL) of fragmented DNA with fluorescent dUTP (green). The assays were visualized by immunofluorescence microscopy at 100X magnifications (Olympus IX71 Inverted Microscope) with emission at 495-529 nm. HUVEC tubes exposed to UV (5 mJ/min) were used as a positive control for apoptosis. Shown are representative images from three independent experiments. (B) Semi-quantitation of the TUNEL assays after DEP exposure. The number of green apoptotic cells were counted, and divided by the total number of blue nuclei in the field of view. Histograms indicate the number of apoptotic cells per 100 nuclei. Values were normalized to the control and showed as the percentage-change relative to control. (C) Measurement of caspase 3 activitiy in tube cells treated with 100 μg/ml DEP using a Caspase Glo-3/7 assay kit. Endothelial tube cells were treated with DEP for 1, 3, 6, 12, and 24 hr prior to measuring caspace 3. Values were normalized to the untreated control (0 hr) and are shown as the fold-change relative to the control. *$p < 0.05$ and **$p < 0.01$ compared with the control, means ± SD, n = 3. Statistical analysis was by Student t-tests.

(A)

Nuclear Stain   Apoptosis

(+) Control

Untreated Control

1 µg/ml DEP

10 µg/ml DEP

100 µg/ml DEP
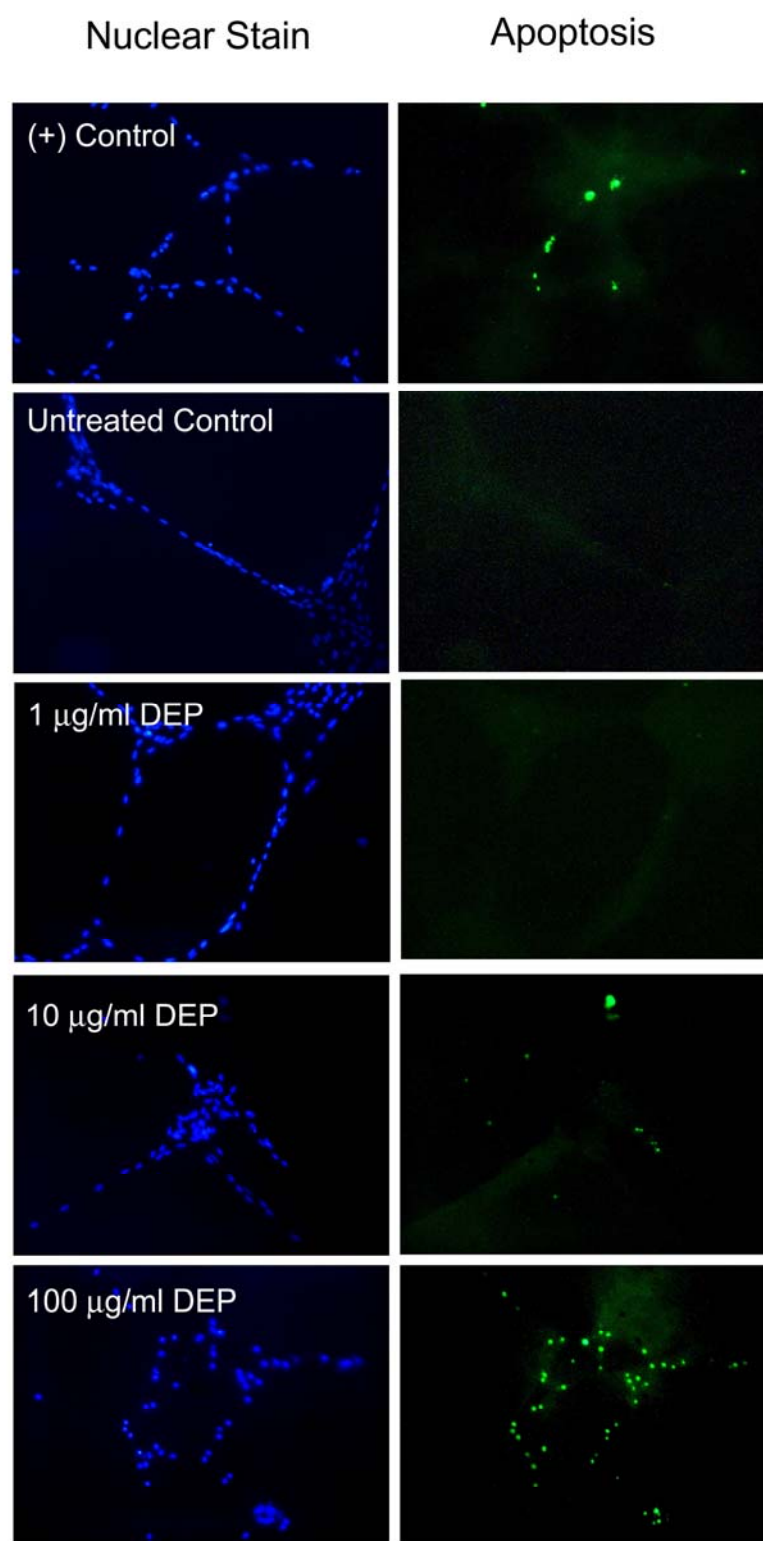
(B)
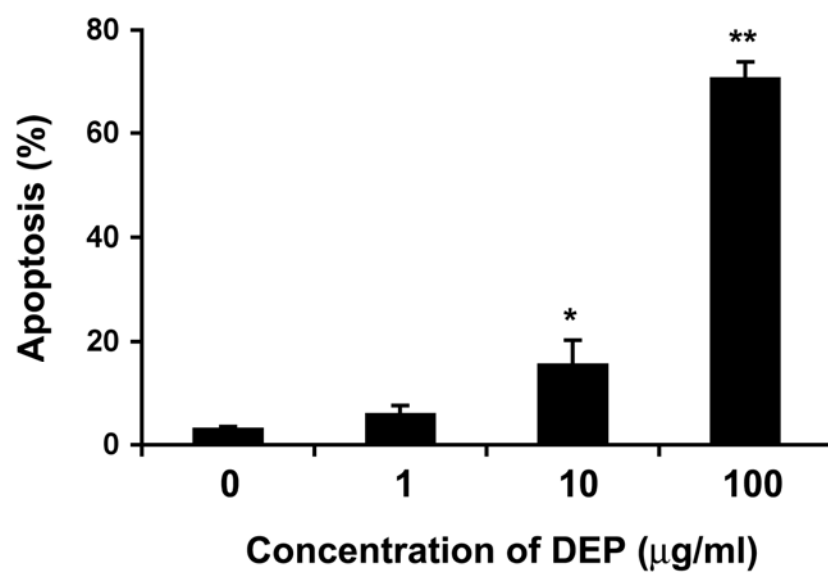
(C)
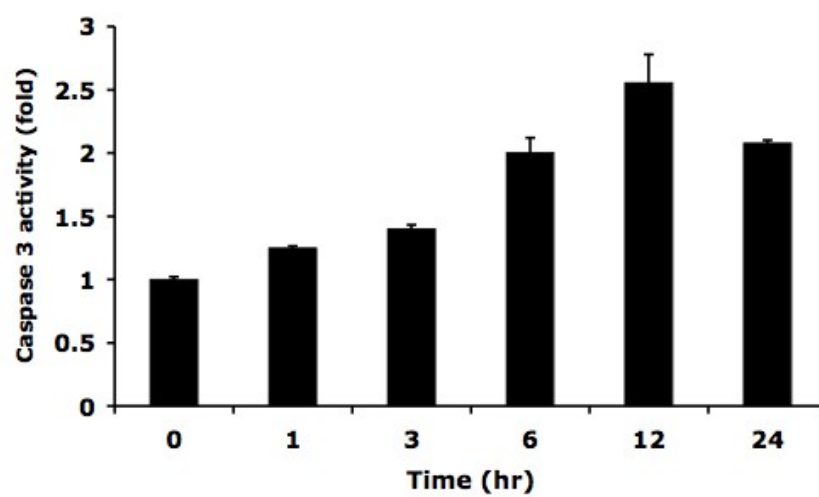
Fig 4-4. Effects of DEP on PI3-kinase/Akt expression. (A) After 24 hr exposures to DEP (0, 1, 10 or 100 μg/ml), HUVEC tube cells were harvested and lysed. The levels of PI3-kinase, Akt and p-Akt were determined by Western blot. Equal amount of protein loading was confirmed based on GAPDH immunoreactivity. (B) Quantitation showed PI3-kinase and p-Akt were decreased in a dose dependent manner as the relative fold change to the control. Total Akt was unaffected by DEP. *$p < 0.05$ and **$p < 0.01$ compared with the control, means ± SD, n = 3. Statistical analysis was by student t-test. (C) To compare the effects of DEP with PI3-kinase/Akt pathway inhibitors, HUVEC tube cells were treated with Wortmannin (1 μM) and LY294002 (20 μM) for 24 hr, then harvested and lysed. The level of PI3-kinase, Akt and p-Akt were determined by Western blot. Equal amount of protein loading was confirmed based on total GAPDH expression.

(A)

(B)

(C)

Wortmannin	—	+	—
LY294002	—	—	+

PI3K   110 kD

Akt   60 kD

pAkt   60 kD

GAPDH   35 kD
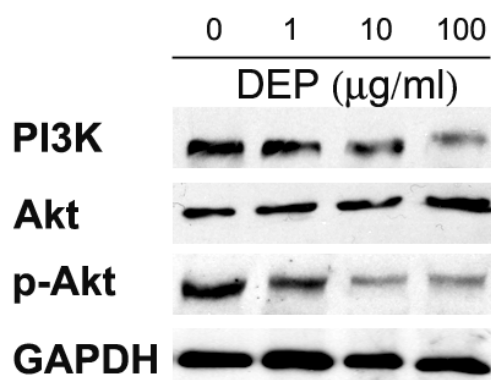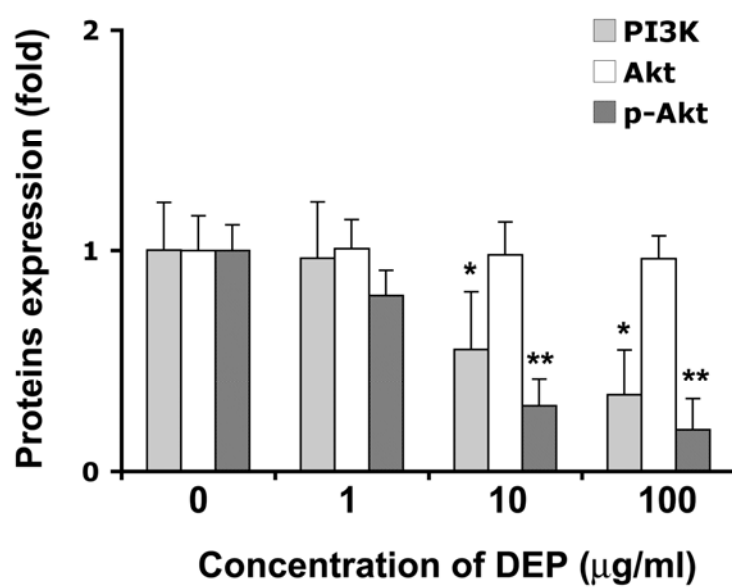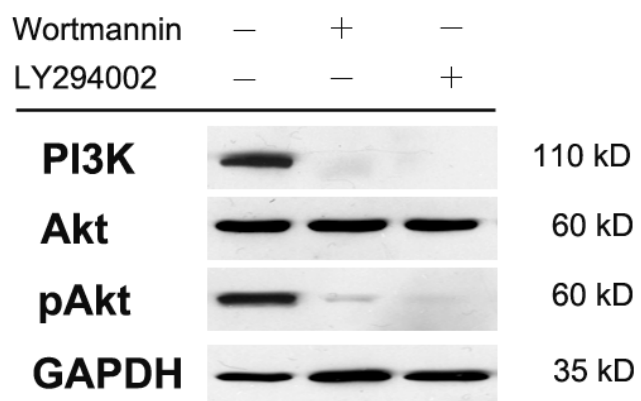
Fig 4-5. DEP-mediated activation of p53 and Mdm2 in endothelial tube cells. (A) After 24 hr exposure to DEP (0, 1, 10 and 100 μg/ml), HUVEC tube proteins were obtained by cell lysis. Levels of p53 and Mdm2 were determined by Western analysis. Equal amount of protein loading was confirmed based on total GAPDH immunoreactivity. (B) Quantitation showed a dose dependent increase of p53 and Mdm2 at 1 and 10 μg/ml as the relative fold change compared to the control. DEP also induced p53 at 100 μg/ml; Mdm2 was not induced at this DEP concentration. *$p < 0.05$ and **$p < 0.01$ compared with the control, means ± SD, n = 3. Statistical analysis was by student t-test.

(A)
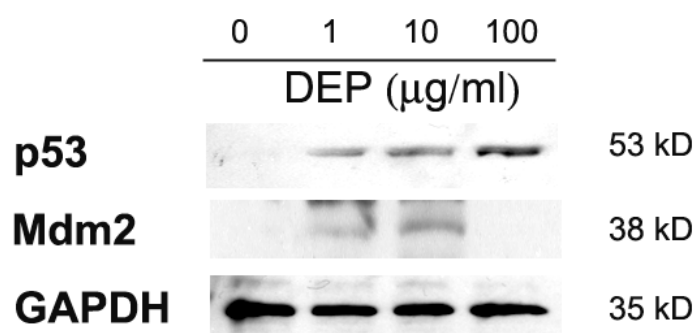
(B)
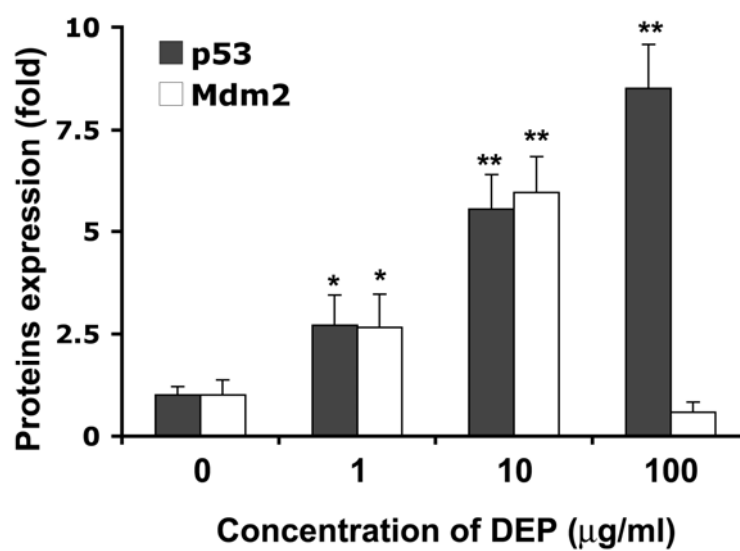
Fig 4-6. Effects of DEP on p53/Mdm2 localization. Images show the distribution of Mdm2 and p53 in response to 24 hr exposures to DEP (0, 10 and 100 μg/ml). HUVEC tube cells were visualized on a Leica spectral confocal microscopy (TCS, SP5, with water lens, N.A. 1.3) using anti-Mdm2 and anti-p53 primary antibodies and secondary antibodies labeled with Alexa Fluor 488 (red) and Alexa 594 (green), respectively. Mdm2 is not present in untreated HUVEC tubes, nor in those exposed to 100 μg/ml DEP. Nuclei were stained blue with DAPI. Shown are representative images from three independent experiments. Scale bar = 5 μm. Magnification is 630X.
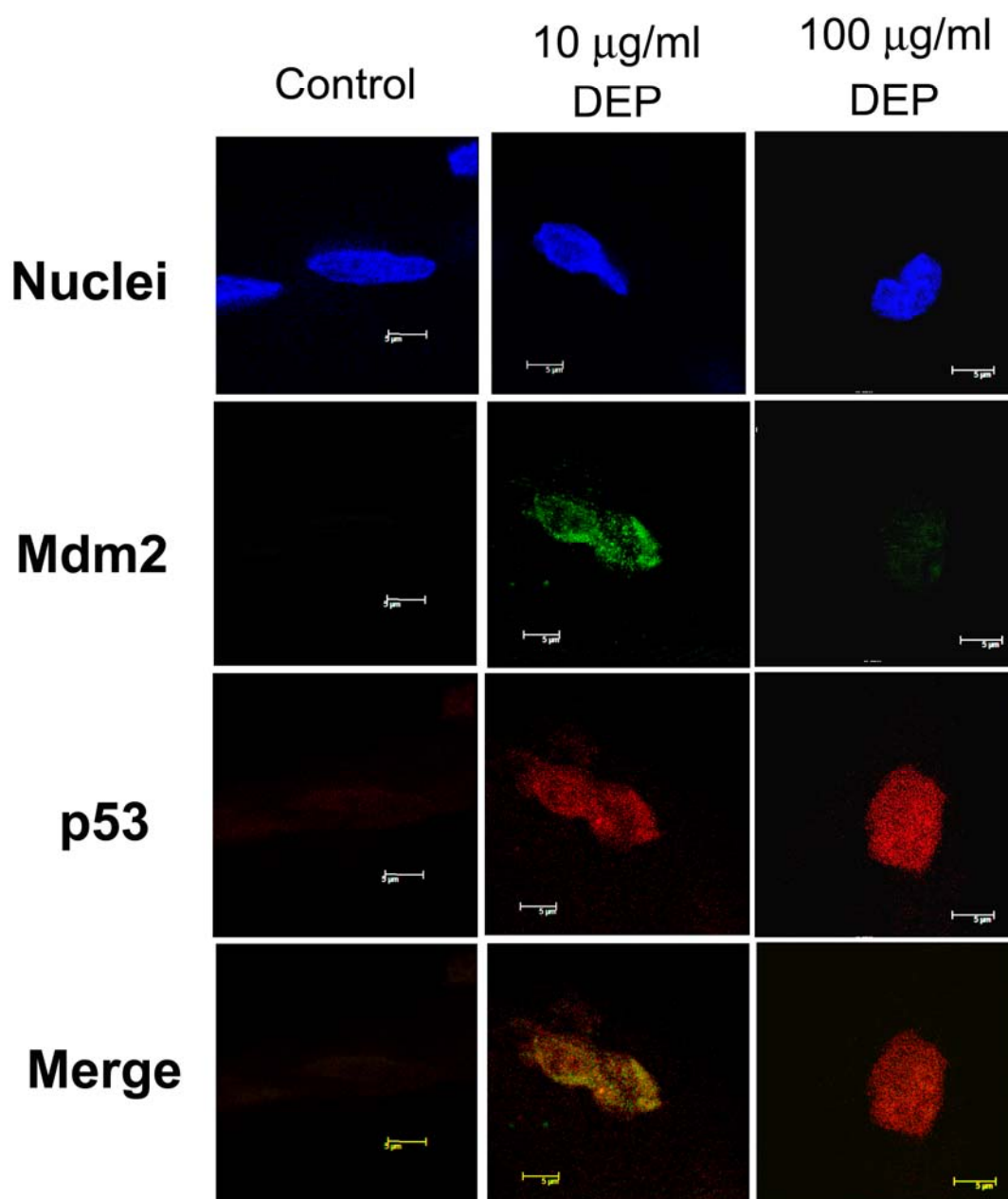
Conclusion

To determine how DEP alters endothelial function, thereby contributing to adverse cardiovascular events, will require epidemiological studies, coupled with human, animal and cell culture exposure studies. Exposure chambers have verified diesel-induced increases in thrombus formation in humans (Lucking *et al.* 2008), as have hamster exposure studies (Nemmar *et al.* 2002; Nemmar *et al.* 2004b), but these are directed at blood components more than at the capillary endothelium itself. To date, endothelial responses to DEP have consisted mostly of assessment of vascular leakage or blood pressure measurements *in vivo*, or of studies on monolayer cultures of endothelial cells (Bai *et al.* 2001; Furuyama *et al.* 2006; Li *et al.* 2009; Sumanasekera *et al.* 2007). *In vivo*, an alveolar capillary that would encounter DEP would be a three dimensional tubular structure with a lumen. To mimic the organizational level of the capillary, we have used *in vitro* assembled endothelial tubes. This allowed us to obtain data in the context of a simulated capillary structure, and thus allowed us to visualize DEP within luminal spaces. The *in vitro* capillary-like tube structure is not a perfect model: It cannot reveal blood flow or blood pressure-induced responses; it cannot model any specific area of the vasculature other than the capillary in the most general sense; and it has no mural cells which are always present to some degree *in vivo*. Future work in the Gordon laboratory will attempt to add mural cells to the endothelial tubes in culture.

The ways in which endothelial tubes are more like capillaries than monolayers are, (1) the proliferation profile of endothelial tube cells is restricted as is that of *in vivo* capillary endothelial cells (Hadley *et al.* 1985). Networks of *in vitro* capillary tubes remain

healthy and vital for up to 8 days without any sign of net proliferation (although homeostasis may be occurring). Monolayers of HUVECs, however, doubled every 24 h until their substratum's surface was confluent; and (2) *In vitro* HUVEC tubes are also a more *in vivo*-like model because they express VEGFR-2, the main signaling VEGFR used by *in vivo* capillary endothelial cells. To be more specific, our data demonstrate that HUVEC tubes express VEGFR-2, but not VEGFR-1, while HUVEC monolayers express VEGFR-1, but not VEGFR-2. *In vivo*, both receptors are present, but VEGFR-1 levels are usually low compared to VEGFR-2. Their functions have mostly been studied in the context of angiogenesis, so their roles after vessels are fully formed is not as well investigated. What is known is that VEGFR-2 is the predominant receptor used by quiescent endothelial cells. It controls cell proliferation, migration, cell survival and vascular permeability. VEGFR-1 appears to act as a positive or negative regulator of VEGFR-2 and also contributes to vascular permeability control (Holmes *et al.* 2007; Olsson *et al.* 2006). The fact that VEGFR-2 is present on endothelial tubes suggests that the tube phenotype resembles the *in vivo* capillary phenotype better than monolayers do.

Our studies used DEP generated by a Japanese automobile engine (Sagai *et al.* 1993). These particles have been characterized and used in several other studies (Bai *et al.* 2001; Inoue *et al.* 2006; Ito *et al.* 2000; Kumagai *et al.* 1997). Because $PM_{2.5}$ is considered injurious, DEP were dispersed to biologically relevant sizes. By light microscopy after dispersion, particles were found to be as large as 2.5 μm and as small as 0.1 μm (100 nm). Since 100 nm is limit of light microscopy, smaller particles could not be seen, but were assumed to be present. Zeta potential sizing of particles demonstrated that the average diameter of our dispersed DEP was 254 nm. Using the fact that the largest particles are 10

times larger in diameter than the average to predict a bell shaped curve, the smallest

particles would be about 10 times smaller than the average, being 25 nm in diameter. This

is well within the size range believed to have physiological consequences.

Applying these particles to endothelial tubes allowed determinations of

cytotoxicity and permeability with relation to DEP dose. Capillary leakiness (i.e.,

permeability) has been related to disruption of the adherens junctions (Gallicano *et al.*

2001). VE-cadherin is required for the proper assembly of adherens junctions and

development of normal endothelial barrier function. Deletion of VE-cadherin in mice

(*VE-cadherin* $^{-/-}$) was embryonically lethal due to immature vascular development

(Carmeliet *et al.* 1999; Vittet *et al.* 1997). Ectopic expression of a VE-cadherin mutant

lacking the cadherin extracellular domain, whether in human dermal microvascular cells

(Venkiteswaran *et al.* 2002) or in endothelial cells (Nawroth *et al.* 2002), resulted in a

leaky junctional barrier (Nawroth *et al.* 2002; Venkiteswaran *et al.* 2002). Our data in

chapter 1 showed that exposure to increasing DEP concentrations caused increased

redistribution of VE-cadherin away from the HUVEC cell membranes to the cytoplasm, a

phenotype like that observed in leaky capillaries *in vivo*. If the data can be extrapolated to

alveolar capillaries, it suggests that when particles encounter the endothelium, they may

alter the adherens junction, causing the capillary cell-cell junctions to become permeable.

Animal models and endothelial cells in monolayer cultures (Sagai *et al.* 1993;

Sumanasekera *et al.* 2007) have been used to show that DEP induce of ROS. In Chapter II

we show this is also true for capillary-like endothelial tubes. The ROS-induced lethality of

DEP is attenuated by N-acetyl cysteine (NAC) as assessed by LDH assays. Protein

oxidation also was observed in response to DEP, with H_2O_2 representing at least a portion

of the ROS generated. H_2O_2 generation has been shown to induce VE-cadherin internalization in endothelial cell monolayer cultures, causing cell-cell gaps that make the monolayer permeable (Kevil *et al.* 1998). Therefore, the endothelial tube cultures reorganizing VE-cadherin and becoming permeable in response to DEP may be, in part, due to the generation of H_2O_2. Furthermore, the antioxidant enzyme HO-1 was generated in response to DEP, and specific inhibitors of HO-1 demonstrated that the increased level of this enzyme was linked to increased VEGF-A secretion. Thus, oxidative stress induces VEGF-A secretion and favors permeability of HUVEC tubes. Also, several studies have reported that pro-inflammatory cytokines can be stimulated by DEP exposure in both *in vitro* monolayers of endothelial cells (Terada *et al.* 1999) and *in vivo* models (Nemmar *et al.* 2004a). We have shown that endothelial tube cells secrete TNF-α and IL-6 in response to DEP exposure, and that these are correlated with an increase in VEGF-A secretion. If the data described in chapter 2 were to also be true in *in vivo* capillaries, a DEP-induced induction of VEGF-A can be predicted as a mechanism contributing to capillary permeability.

Activation of the PI3 kinase/Akt signaling pathway is known to increase vascular permeability (Chen *et al.* 2005) and to enhance endothelial cell survival (Amaravadi and Thompson 2005). Our results presented a dilemma for Akt as a potential signaling pathway. This is because DEP caused endothelial tube permeability with apoptosis, not with survival. If the Akt pathway were activated at all, it could contribute to only the permeability phenotype in the model system used. Therefore, we initially hypothesized that DEP activated Akt to favor permeability. Our hypothesis was incorrect, since increasing levels of DEP reduced phosphorylation of Akt, and failed to stimulate this powerful survival

pathway. At low concentrations of DEP, the anti-apoptotic protein Mdm2 was expressed. It was not expressed in untreated HUVEC tubes. Mdm2 can bind the pro-apoptotic protein p53 and inactivate its activity, facilitating survival. This was observed after exposure to the two low concentrations of DEP. In contrast, at the high dose of DEP, Mdm2 expression was not maintained. The apoptosis observed likely resulted from p53 activity, facilitated by the down regulation of Mdm2.

Finding that VE-cadherin and VEGF-A induction were involved in DEP-induced permeability surprised us. However, in the endothelial literature (but not in the DEP literature) such a link between the molecules has been described: VEGFR-2 is in close proximity to VE-cadherin in the membrane. A connection between the two was found experimentally, and was initially schematicized as a β-catenin-PI3 kinase interaction (i.e., a β-catenin bound to the intracellular domain of VE-Cad, interacted with PI3kinase bound to the intracellular domain of VEGFR-2, Carmeliet *et al.* 1999). This allowed binding of VEGF-A to VEGFR-2 to influence endothelial permeability by disrupting VE-cadherin interactions between individual cells. More recently it was found that Src is bound to VE-cadherin but does not phosphorylate it (see Fig 1-7). When VEGF-A binds VEGFR-2, the receptor associates with a distal domain of Src, linking and phosphorylating both VEGFR-2 and VE-cadherin. (One of these phosphorylations may be through "scr homology and β cell protein" aka shb.) Phosphorylation of VE-cadherin causes molecular uncoupling of adjacent cells via disruption of the adherens junctions. This makes the vessel permeable (Chou *et al.* 2002; Lambeng *et al.* 2005; Wallez *et al.* 2006).

Why should permeability through disruption of adherens junctions be coupled with endothelial cell survival? Such a system is necessary because separation of the endothelial

cells is an initial step in angiogenesis. By creating a space between adjacent endothelia, cells can bud from the vessel to begin forming a vascular branch. Shortly after the bud is formed, proliferation of the cells is enabled. If separation between endothelial cells were invariably linked restricted proliferation or to cell death, the forming new vessels, angiogenesis, could not occur.

The results we present in Chapter III indicate that survival and permeability are not coupled in DEP-exposed endothelia. Instead, adheren junction separation occurs and apoptosis is induced, with Akt signaling being attenuated. Another schematic review of VEGF-A induced VEGFR-2 signaling (without considering VE-cadherin) is shown in Figure 5.1 (from Kowanetz and Ferrara, et al., 2006). This model separated VEGF-A-VEGFR-2 mediated activation of PI3 kinase into 3 pathways, all via Shb2 (src homology and β-cell protein). Two of these pathways lead to activation of Akt, one ending in cell survival, the other ending in vascular permeability. In addition, there is pathway toward vascular permeability via Src, mediated by phosphorylation of a different VEGFR-2 tyrosine than the one interacting with Shb (Kowanetz and Ferrara, 2006). While details are still sparse, it is important to push forward our understanding of the ways that endothelial survival and permeability may occur in an unlinked fashion. It is also important to recognize there are many ways to achieve endothelial permeability.

Fig 5-1. VEGF-A-VEGFR-2 signaling pathways (from Kowanetz and Ferrara, 2006).
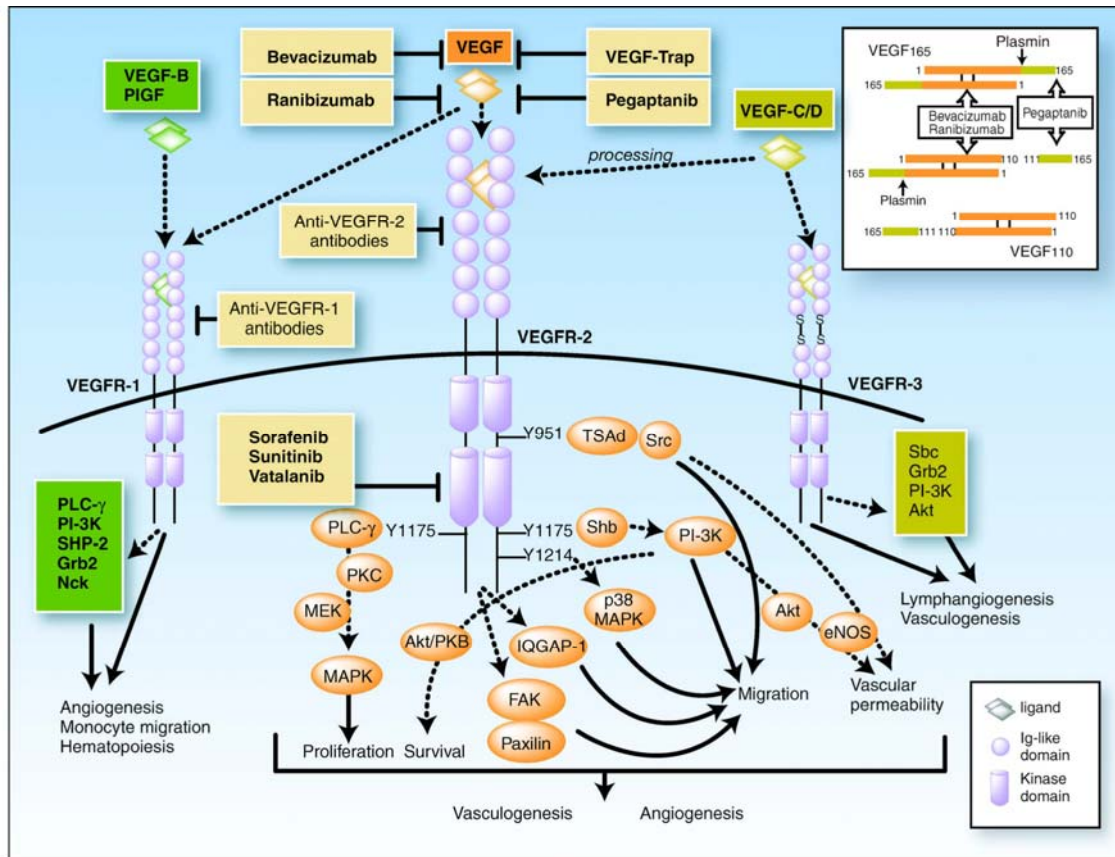
In summary, this thesis demonstrates that DEP are able to interrupt the adherens junctions of HUVEC tubes, causing VE-cadherin to become internalized. This makes the cell junctions permeable. In addition, particles can be found within endothelial cells and within the lumen of HUVEC tubes. If inhalation of DEP were to cause similar events in lung capillaries, it suggests that, *in vivo*, DEP may gain access into the bloodstream. Once inside the vessel, DEP could interact with platelets or initiate an immune or oxidative stress response. In HUVEC tubes, the endothelial cells themselves mount these responses in the absence of blood components. These responses lead to the secretion of VEGF-A, which is a vascular permeability factor. Increasing levels of DEP caused increasing levels of

endothelial cell apoptosis. In most studies, increases in VEGF-A have been shown to signal cell survival though the PI3K/Akt pathway, but in the presence of DEP this pathway was not activated. Overall, the results suggest that the lower amounts of DEP used in these studies may approach a biologically relevant exposure level since, *in vivo* after DEP inhalation, alveolar endothelial cell death has never been reported, but a small number of particles do appear to gain access to the circulation.

VE-cadherin associates with VEGFR-2 to regulate cell survival and vascular permeability i*n vivo* and in monolayer cultures of endothelial cells. When VEGF-A binds to VEGFR-2, the adherens junctions are disrupted. VEGFR-2 is phosphorylated and dissociated from VE-cadherin, which also becomes phosphorylated. Internalization of VE-cadherin increases vascular permeability. Cell survival is dependent on the membrane association of VE-cadherin with VEGFR-2, therefore internalization of these molecules also disrupts the cell's survival mechanism, favoring pathways to cell death. Our data highlights this from several directions. DEP induces ROS generation in endothelial tube cells, increasing H_2O_2 production with VE-cadherin internalization. Furthermore, DEP-induced ROS upregulates HO-1 expression and cytokines TNF-α and IL-6 secretion, which lead to the induction of VEGF-A secretion. This is another pathway to permeability. Fig 5-2, shows a model of the events that occur as described by our results. 1. DEP increases vascular permeability by inducing generation of ROS and cytokines, which result in secretion of VEGF-A. 2. DEP-induced VEGF-A binds to VEGFR-2. This results in dissociation of VEGFR-2 and VE-Cad. VE-Cad internalizes, which also causes permeability by disrupting the adherens junctions. 3. In angiogenesis, the Akt pathway is

used to induce permeability, however, DEP inhibit the Akt pathway. Therefore the Akt pathway activation is not a contributor to DEP-induced endothelial permeability.

Fig 5-2. Schematic diagram depicting mechanisms leading to permeability identified by the thesis.
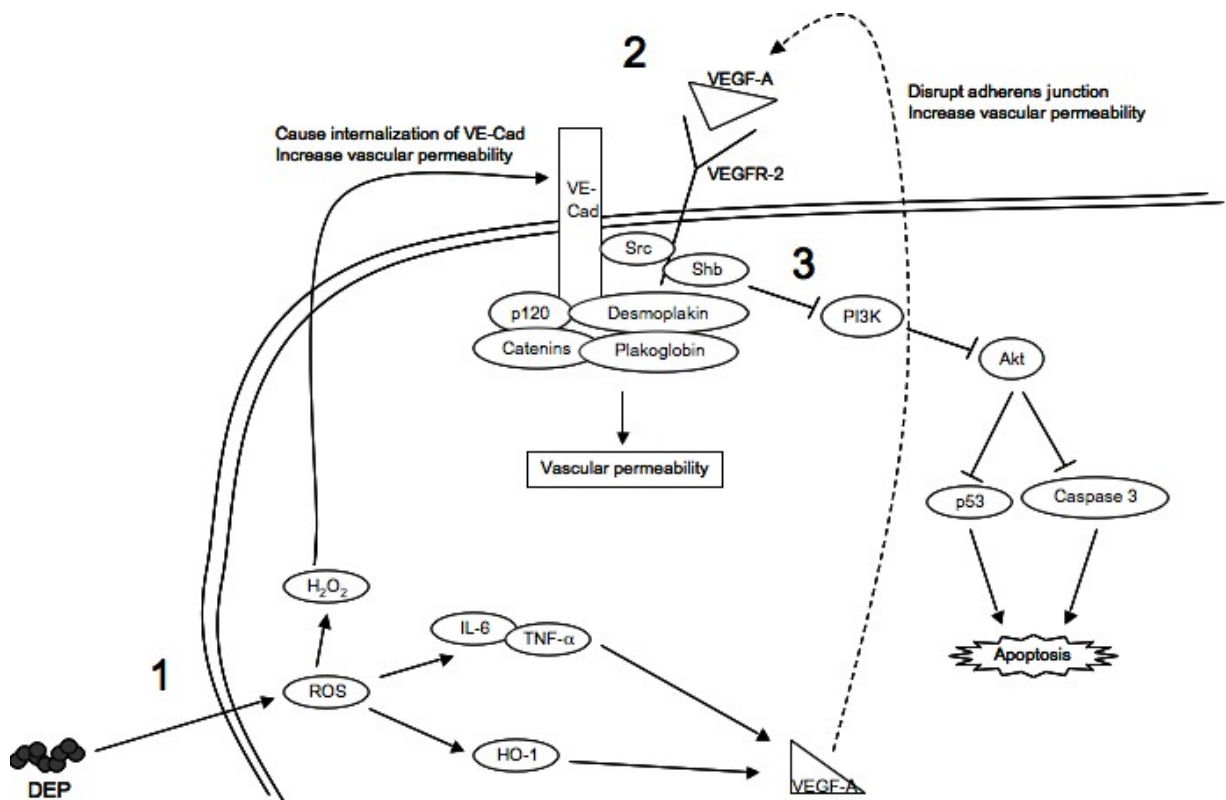
We conclude that *in vitro* endothelial tubes are a useful and informative model system to gain clues about the DEP-induced mechanisms that adversely affect cardiovascular health. Endothelial tube cultures can provide additional and different information from what can be obtained using endothelial cells in monolayer culture.

Regardless of the system used, future work is needed to reveal why DEP-induced VEGF-A secretion does not activate the Akt survival pathway, as occurs when VEGF-A secretion is induced by other factors.

Future Work

Examination of the effect of other types of PMs or extracts of DEP on endothelial tubes

PM air pollution is an air-suspended mixture containing solid and liquid particles, which vary in size, number, and chemical composition. The size distribution of these suspended particles includes coarse particles, fine particles, and ultrafine particles. Fine and ultrafine particles, including DEP, and various heterogeneous chemicals are derived mainly from the emission of combustion reactions. Although short-term DEP exposure has been experimentally correlated with adverse cardiovascular events, there is not much epidemiological evidence to show that cardiovascular effects are the consequence of acute DEP exposure for residents. Most epidemiology studies show that PM is the main air pollutant that causes adverse health effects. Thus, other types of particles could be used to examine what are the specific responses induced by DEP in endothelial tubes, verus what responses are due to a particulate being a specific size. Carbon nanopartices can be obtained in very specific diameters, and could be used for such a comparison.

In addition, DEP could be extracted with aqueous or organic solvents to separate elemental carbon from soluble components. Treatment of endothelial tubes with the

extracted particles and soluble components could determine what is important for causing endothelial tube permeability and redistribution of adherens junctional proteins. Furthermore, it is well known that the composition of DEP varies from region to region due to the different types of the diesel engines used in specific areas. It might be useful to perform extractions on DEP generated by several types of engines and perform experiments that would identify which ones are more likely to cause endothelial permeability. This could then be correlated with the epidemiology of acute cardiovascular events reported in the area.

Examination of lower doses of DEP

From our findings, the concentration of DEP (100 μg/ml) is too high to be biologically relevant, since it kills the endothelial cells. In vivo, there is no evidence that DEP inhalation causes endothelial cell death. Future work should address using lower DEP concentrations (between 0.1 and 10 μg/ml), which should be much less harmful to the cells, but could still show symptoms of inducing permeability.

Some of our work suggested that, not only does particle translocation occur by penetrating cell-cell junctions, but also by transversing endothelial cells (not shown). Future work can address translocation by diffusion or endocytosis and exocytosis.

Translocation studies using fluorescently-labeled particles

Our data have indicated that particles can be found within the *in vitro* capillary-like endothelial tube lumen and that DEP upregulate factors that result in endothelial permeability. However, we only directly measured the permeability of endothelial

monolayers (not shown). This was accomplished by using 70 kDa dextran, which cannot reach the lower compartment of a trans well chamber when monolayers of endothelial cells are confluent (i.e., when dextran is placed on top of cells, if junctions are intact, it cannot pass between the cells to reach a lower chamber). We found that DEP at 1, 10, and 100 µg/ml caused HUVEC monolayer cultures plated on transwell dishes to become permeable, and allow dextran to reach the lower chamber. However, tube permeability was not directly measured. Future work in the laboratory will include such experiments, and will employ fluorescently-labeled dextran to determine whether the material can end up in the lumen of tubes. The dextran will be left on tubes for various times, aspirated off, then tubes will be fixed for analysis by confocal microscopy.

Reduction of DEP-induced ROS generation by tocopherols or other antioxidants

Our results show that the endothelial tubes are a useful and informative model system to study how DEP might gain access to the alveolar capillary lumen, where they can potentially lead to adverse prothrombotic effects. The model may also serve to indicate whether antioxidants offset the ability of DEP to induce endothelial permeability. Vitamin E tocopherols (α-, β-, δ-, and γ-tocopherol) are an important group of dietary antioxidants. Not only has γ-tocopherol been shown to have antioxidant activity, but also anti-inflammatory activity (Hensley et al, 2004). Mixed tocopherols have been suggested as effective cardiovascular disease deterents because of their ability to inhibit apoptosis, and because of their anti-inflammatory and anti-oxidative activities (Jihyeung et al, 2009; Liu, 2003). Preliminary work in the Gordon laboratory has pre-treated endothelial tubes with various concentrations of mixed tocopherols, and has determined that DEP apoptosis

is reduced. Experiments are being designed to examine whether ROS generation is decreased and whether factors that favor permeability are attenuated by tocopherol pre-treatment prior to DEP exposure.

Other uses for the in vitro endothelial tube model system

In vivo, pericytes cover capillary endothelia and contribute to the control of endothelial proliferation as well as permeability. In general, the more extensively the capillary is covered with pericytes, the less permeable the capillary is. Future experiments should include assembling endothelial tubes, followed by attempting to get pericytes to cover them. This type of system could be used as a more biological representation of alveolar capillaries. In addition, smooth muscle cells might be added to tubes to possibly model arterioles, or leukocytes or macrophages could be added to see if co-culturing altered DEP-induced effects such a permeability. Any type of experiment that would include other cell types encountered by endothelial cells could add biological relevance to the model system.

The model system might also be adapted to further study the effect of DEP on specific adherens junction molecules. Endothelial cells could be stably transfected with plasmid constructs that would encode junctional proteins tagged with green fluorescent protein (GFP). Care would be needed to ensure that interactive sites in the junctional proteins are still functional with the GFP tag, then endothelial cells could be assembled into tubes for treatment with DEP. The dynamic movement of VE-cadherin, β-catenin, desmoplakin, or plakoglobin within endothelial tube cells might be possible with this type

of experiment. This is especially possible now that the Pharmacology and Toxicology Department has obtained a microscope that can do live cell imaging.

References

Al-Humadi, N. H., Siegel, P. D., Lewis, D. M., Barger, M. W., Ma, J. Y., Weissman, D. N., and Ma, J. K. (2002). Alteration of intracellular cysteine and glutathione levels in alveolar macrophages and lymphocytes by diesel exhaust particle exposure. *Environmental health perspectives* **110**, 349-53.

Alarcon-Vargas, D., and Ronai, Z. (2002). p53-Mdm2--the affair that never ends. *Carcinogenesis* **23**, 541-7.

Alfaro-Moreno, E., Martinez, L., Garcia-Cuellar, C., Bonner, J. C., Murray, J. C., Rosas, I., Rosales, S. P., and Osornio-Vargas, A. R. (2002). Biologic effects induced in vitro by PM10 from three different zones of Mexico City. *Environmental health perspectives* **110**, 715-20.

Amaravadi, R., and Thompson, C. B. (2005). The survival kinases Akt and Pim as potential pharmacological targets. *The Journal of clinical investigation* **115**, 2618-24.

Anselme, F., Loriot, S., Henry, J. P., Dionnet, F., Napoleoni, J. G., Thuillez, C., and Morin, J. P. (2007). Inhalation of diluted diesel engine emission impacts heart rate variability and arrhythmia occurrence in a rat model of chronic ischemic heart failure. *Archives of toxicology* **81**, 299-307.

Auger, F., Gendron, M. C., Chamot, C., Marano, F., and Dazy, A. C. (2006). Responses of well-differentiated nasal epithelial cells exposed to particles: role of the epithelium in airway inflammation. *Toxicology and applied pharmacology* **215**, 285-94.

Baccarelli, A., Zanobetti, A., Martinelli, I., Grillo, P., Hou, L., Giacomini, S., Bonzini, M., Lanzani, G., Mannucci, P. M., Bertazzi, P. A., and Schwartz, J. (2007). Effects of exposure to air pollution on blood coagulation. *J Thromb Haemost* **5**, 252-60.

Bachoual, R., Boczkowski, J., Goven, D., Amara, N., Tabet, L., On, D., Lecon-Malas, V., Aubier, M., and Lanone, S. (2007). Biological effects of particles from the paris subway system. *Chemical research in toxicology* **20**, 1426-33.

Bai, Y., Suzuki, A. K., and Sagai, M. (2001). The cytotoxic effects of diesel exhaust particles on human pulmonary artery endothelial cells in vitro: role of active oxygen species. *Free radical biology & medicine* **30**, 555-62.

Barcellos-Hoff, M. H., Aggeler, J., Ram, T. G., and Bissell, M. J. (1989). Functional differentiation and alveolar morphogenesis of primary mammary cultures on reconstituted basement membrane. *Development (Cambridge, England)* **105**, 223-35.

Baulig, A., Garlatti, M., Bonvallot, V., Marchand, A., Barouki, R., Marano, F., and Baeza-Squiban, A. (2003). Involvement of reactive oxygen species in the metabolic

pathways triggered by diesel exhaust particles in human airway epithelial cells. *American journal of physiology* **285**, L671-9.

Bazzoni, G., and Dejana, E. (2001). Pores in the sieve and channels in the wall: control of paracellular permeability by junctional proteins in endothelial cells. *Microcirculation* **8**, 143-52.

Bazzoni, G., and Dejana, E. (2004). Endothelial cell-to-cell junctions: molecular organization and role in vascular homeostasis. *Physiological reviews* **84**, 869-901.

Becker, S., Dailey, L. A., Soukup, J. M., Grambow, S. C., Devlin, R. B., and Huang, Y. C. (2005). Seasonal variations in air pollution particle-induced inflammatory mediator release and oxidative stress. *Environmental health perspectives* **113**, 1032-8.

Bellacosa, A., Kumar, C. C., Di Cristofano, A., and Testa, J. R. (2005). Activation of AKT kinases in cancer: implications for therapeutic targeting. *Advances in cancer research* **94**, 29-86.

Block, M. L., Wu, X., Pei, Z., Li, G., Wang, T., Qin, L., Wilson, B., Yang, J., Hong, J. S., and Veronesi, B. (2004). Nanometer size diesel exhaust particles are selectively toxic to dopaminergic neurons: the role of microglia, phagocytosis, and NADPH oxidase. *Faseb J* **18**, 1618-20.

Bonvallot, V., Baeza-Squiban, A., Baulig, A., Brulant, S., Boland, S., Muzeau, F., Barouki, R., and Marano, F. (2001). Organic compounds from diesel exhaust particles elicit a proinflammatory response in human airway epithelial cells and induce cytochrome p450 1A1 expression. *American journal of respiratory cell and molecular biology* **25**, 515-21.

Breen, E. C. (2007). VEGF in biological control. *Journal of cellular biochemistry* **102**, 1358-67.

Brook, R. D. (2008). Cardiovascular effects of air pollution. *Clin Sci (Lond)* **115**, 175-87.

Brook, R. D., Brook, J. R., and Rajagopalan, S. (2003). Air pollution: the "Heart" of the problem. *Current hypertension reports* **5**, 32-9.

Brook, R. D., Brook, J. R., Urch, B., Vincent, R., Rajagopalan, S., and Silverman, F. (2002). Inhalation of fine particulate air pollution and ozone causes acute arterial vasoconstriction in healthy adults. *Circulation* **105**, 1534-6.

Brook, R. D., Franklin, B., Cascio, W., Hong, Y., Howard, G., Lipsett, M., Luepker, R., Mittleman, M., Samet, J., Smith, S. C., Jr., and Tager, I. (2004). Air pollution and cardiovascular disease: a statement for healthcare professionals from the Expert Panel on Population and Prevention Science of the American Heart Association. *Circulation* **109**, 2655-71.

Brouard, S., Berberat, P. O., Tobiasch, E., Seldon, M. P., Bach, F. H., and Soares, M. P. (2002). Heme oxygenase-1-derived carbon monoxide requires the activation of transcription factor NF-kappa B to protect endothelial cells from tumor necrosis factor-alpha-mediated apoptosis. *The Journal of biological chemistry* **277**, 17950-61.

Brown, J. S., Zeman, K. L., and Bennett, W. D. (2002). Ultrafine particle deposition and clearance in the healthy and obstructed lung. *American journal of respiratory and critical care medicine* **166**, 1240-7.

Buckley, B. J., Marshall, Z. M., and Whorton, A. R. (2003). Nitric oxide stimulates Nrf2 nuclear translocation in vascular endothelium. *Biochemical and biophysical research communications* **307**, 973-9.

Burchiel, S. W., Lauer, F. T., McDonald, J. D., and Reed, M. D. (2004). Systemic immunotoxity in AJ mice following 6-month whole body inhalation exposure to diesel exhaust. *Toxicology and applied pharmacology* **196**, 337-45.

Bussolati, B., Ahmed, A., Pemberton, H., Landis, R. C., Di Carlo, F., Haskard, D. O., and Mason, J. C. (2004). Bifunctional role for VEGF-induced heme oxygenase-1 in vivo: induction of angiogenesis and inhibition of leukocytic infiltration. *Blood* **103**, 761-6.

Calderon-Garciduenas, L., Azzarelli, B., Acuna, H., Garcia, R., Gambling, T. M., Osnaya, N., Monroy, S., MR, D. E. L. T., Carson, J. L., Villarreal-Calderon, A., and Rewcastle, B. (2002). Air pollution and brain damage. *Toxicologic pathology* **30**, 373-89.

Calderon-Garciduenas, L., Reed, W., Maronpot, R. R., Henriquez-Roldan, C., Delgado-Chavez, R., Calderon-Garciduenas, A., Dragustinovis, I., Franco-Lira, M., Aragon-Flores, M., Solt, A. C., Altenburg, M., Torres-Jardon, R., and Swenberg, J. A. (2004). Brain inflammation and Alzheimer's-like pathology in individuals exposed to severe air pollution. *Toxicologic pathology* **32**, 650-8.

Carmeliet, P., Lampugnani, M. G., Moons, L., Breviario, F., Compernolle, V., Bono, F., Balconi, G., Spagnuolo, R., Oostuyse, B., Dewerchin, M., Zanetti, A., Angellilo, A., Mattot, V., Nuyens, D., Lutgens, E., Clotman, F., de Ruiter, M. C., Gittenberger-de Groot, A., Poelmann, R., Lupu, F., Herbert, J. M., Collen, D., and Dejana, E. (1999). Targeted deficiency or cytosolic truncation of the VE-cadherin gene in mice impairs VEGF-mediated endothelial survival and angiogenesis. *Cell* **98**, 147-57.

Chen, J., Somanath, P. R., Razorenova, O., Chen, W. S., Hay, N., Bornstein, P., and Byzova, T. V. (2005). Akt1 regulates pathological angiogenesis, vascular maturation and permeability in vivo. *Nature medicine* **11**, 1188-96.

Chao, M. W., Kozlosky, J., Po I. P., Svoboda, K. K. H., Cooper, K., Laumbach, R., and Gordon, M. K. Vascular Endothelial Cell-Cadherin is Redistributed Away From the Plasma Membranes of Endothelial Tubes in Response to Diesel Exhaust Particles. *Submitted*.

Chao, M. W., Po I. P., Laumbach, R., Kozlosky, J., Cooper, K., Gordon, M. K. ROS and Pro-inflammatory Cytokines Contribute to DEP-Induced Permeability of Capillary-like Endothelial Tubes. *Submitted*.

Chen, X. L., Varner, S. E., Rao, A. S., Grey, J. Y., Thomas, S., Cook, C. K., Wasserman, M. A., Medford, R. M., Jaiswal, A. K., and Kunsch, C. (2003). Laminar flow induction of antioxidant response element-mediated genes in endothelial cells. A novel anti-inflammatory mechanism. *The Journal of biological chemistry* **278**, 703-11.

Chou, M. T., Wang, J., and Fujita, D. J. (2002). Src kinase becomes preferentially associated with the VEGFR, KDR/Flk-1, following VEGF stimulation of vascular endothelial cells. *BMC biochemistry* **3**, 32.

Cisowski, J., Loboda, A., Jozkowicz, A., Chen, S., Agarwal, A., and Dulak, J. (2005). Role of heme oxygenase-1 in hydrogen peroxide-induced VEGF synthesis: effect of HO-1 knockout. *Biochemical and biophysical research communications* **326**, 670-6.

Clement, B., Musso, O., Lietard, J., and Theret, N. (1999). Homeostatic control of angiogenesis: A newly identified function of the liver? *Hepatology (Baltimore, Md* **29**, 621-3.

Connolly, D. T., Heuvelman, D. M., Nelson, R., Olander, J. V., Eppley, B. L., Delfino, J. J., Siegel, N. R., Leimgruber, R. M., and Feder, J. (1989). Tumor vascular permeability factor stimulates endothelial cell growth and angiogenesis. *The Journal of clinical investigation* **84**, 1470-8.

Cormier, S. A., Lomnicki, S., Backes, W., and Dellinger, B. (2006). Origin and health impacts of emissions of toxic by-products and fine particles from combustion and thermal treatment of hazardous wastes and materials. *Environmental health perspectives* **114**, 810-7.

De Biase, L., Pignatelli, P., Lenti, L., Tocci, G., Piccioni, F., Riondino, S., Pulcinelli, F. M., Rubattu, S., Volpe, M., and Violi, F. (2003). Enhanced TNF alpha and oxidative stress in patients with heart failure: effect of TNF alpha on platelet O2- production. *Thrombosis and haemostasis* **90**, 317-25.

Dejana, E. (2004). Endothelial cell-cell junctions: happy together. *Nat Rev Mol Cell Biol* **5**, 261-70.

Dejana, E., and Del Maschio, A. (1995). Molecular organization and functional regulation of cell to cell junctions in the endothelium. *Thrombosis and haemostasis* **74**, 309-12.

Dejana, E., Orsenigo, F., and Lampugnani, M. G. (2008). The role of adherens junctions and VE-cadherin in the control of vascular permeability. *Journal of cell science* **121**, 2115-22.

Deramaudt, B. M., Braunstein, S., Remy, P., and Abraham, N. G. (1998). Gene transfer of human heme oxygenase into coronary endothelial cells potentially promotes angiogenesis. *Journal of cellular biochemistry* **68**, 121-7.

Deryckere, F., and Gannon, F. (1994). A one-hour minipreparation technique for extraction of DNA-binding proteins from animal tissues. *BioTechniques* **16**, 405.

Devalia, J. L., Bayram, H., Rusznak, C., Calderon, M., Sapsford, R. J., Abdelaziz, M. A., Wang, J., and Davies, R. J. (1997). Mechanisms of pollution-induced airway disease: in vitro studies in the upper and lower airways. *Allergy* **52**, 45-51; discussion 57-8.

Diaz-Sanchez, D. (1997). The role of diesel exhaust particles and their associated polyaromatic hydrocarbons in the induction of allergic airway disease. *Allergy* **52**, 52-6; discussion 57-8.

Diaz-Sanchez, D., Dotson, A. R., Takenaka, H., and Saxon, A. (1994). Diesel exhaust particles induce local IgE production in vivo and alter the pattern of IgE messenger RNA isoforms. *The Journal of clinical investigation* **94**, 1417-25.

Dolk, H., and Vrijheid, M. (2003). The impact of environmental pollution on congenital anomalies. *British medical bulletin* **68**, 25-45.

Donovan, D., Brown, N. J., Bishop, E. T., and Lewis, C. E. (2001). Comparison of three in vitro human 'angiogenesis' assays with capillaries formed in vivo. *Angiogenesis* **4**, 113-21.

Dudek, S. M., and Garcia, J. G. (2001). Cytoskeletal regulation of pulmonary vascular permeability. *J Appl Physiol* **91**, 1487-500.

Dulak, J., Loboda, A., and Jozkowicz, A. (2008). Effect of heme oxygenase-1 on vascular function and disease. *Current opinion in lipidology* **19**, 505-12.

Dvorak, H. F. (2002). Vascular permeability factor/vascular endothelial growth factor: a critical cytokine in tumor angiogenesis and a potential target for diagnosis and therapy. *J Clin Oncol* **20**, 4368-80.

Eleuteri, E., Magno, F., Gnemmi, I., Carbone, M., Colombo, M., La Rocca, G., Anzalone, R., Genta, F. T., Zummo, G., Di Stefano, A., and Giannuzzi, P. (2009). Role of oxidative and nitrosative stress biomarkers in chronic heart failure. *Front Biosci* **14**, 2230-7.

Esser, S., Wolburg, K., Wolburg, H., Breier, G., Kurzchalia, T., and Risau, W. (1998). Vascular endothelial growth factor induces endothelial fenestrations in vitro. *The Journal of cell biology* **140**, 947-59.

Fan, Z. T., Meng, Q., Weisel, C., Laumbach, R., Ohman-Strickland, P., Shalat, S., Hernandez, M. Z., and Black, K. (2008). Acute exposure to elevated PM(2.5) generated by

traffic and cardiopulmonary health effects in healthy older adults. *Journal of exposure science & environmental epidemiology*.

Ferin, J., and Oberdorster, G. (1992). Polymer degradation and ultrafine particles: potential inhalation hazards for astronauts. *Acta astronautica* **27**, 257-9.

Fernandez, M., and Bonkovsky, H. L. (2003). Vascular endothelial growth factor increases heme oxygenase-1 protein expression in the chick embryo chorioallantoic membrane. *British journal of pharmacology* **139**, 634-40.

Ferrara, N., and Henzel, W. J. (1989). Pituitary follicular cells secrete a novel heparin-binding growth factor specific for vascular endothelial cells. *Biochemical and biophysical research communications* **161**, 851-8.

Ferrara, N., Mass, R. D., Campa, C., and Kim, R. (2007). Targeting VEGF-A to treat cancer and age-related macular degeneration. *Annual review of medicine* **58**, 491-504.

Ferrara, N., Winer, J., Burton, T., Rowland, A., Siegel, M., Phillips, H. S., Terrell, T., Keller, G. A., and Levinson, A. D. (1993). Expression of vascular endothelial growth factor does not promote transformation but confers a growth advantage in vivo to Chinese hamster ovary cells. *The Journal of clinical investigation* **91**, 160-70.
Finkelstein, M. M., Verma, D. K., Sahai, D., and Stefov, E. (2004). Ischemic heart disease mortality among heavy equipment operators. *American journal of industrial medicine* **46**, 16-22.

Folkman, J., and Hanahan, D. (1991). Switch to the angiogenic phenotype during tumorigenesis. *Princess Takamatsu symposia* **22**, 339-47.

Folkman, J., and Klagsbrun, M. (1987). Angiogenic factors. *Science (New York, N.Y* **235**, 442-7.

Franck, U., and Herbarth, O. (2002). Using scanning electron microscopy for statistical characterization of the diameter and shape of airborne particles at an urban location. *Environmental toxicology* **17**, 98-104.

Franke, T. F., Kaplan, D. R., and Cantley, L. C. (1997). PI3K: downstream AKTion blocks apoptosis. *Cell* **88**, 435-7.

Fredenburgh, L. E., Perrella, M. A., and Mitsialis, S. A. (2007). The role of heme oxygenase-1 in pulmonary disease. *American journal of respiratory cell and molecular biology* **36**, 158-65.

Fredricsson, B., Moller, L., Pousette, A., and Westerholm, R. (1993). Human sperm motility is affected by plasticizers and diesel particle extracts. *Pharmacology & toxicology* **72**, 128-33.

Freitas, A., Alves-Filho, J. C., Secco, D. D., Neto, A. F., Ferreira, S. H., Barja-Fidalgo, C., and Cunha, F. Q. (2006). Heme oxygenase/carbon monoxide-biliverdin pathway down regulates neutrophil rolling, adhesion and migration in acute inflammation. *British journal of pharmacology* **149**, 345-54.

Furuyama, A., Hirano, S., Koike, E., and Kobayashi, T. (2006). Induction of oxidative stress and inhibition of plasminogen activator inhibitor-1 production in endothelial cells following exposure to organic extracts of diesel exhaust particles and urban fine particles. *Archives of toxicology* **80**, 154-62.

Gabrys, D., Greco, O., Patel, G., Prise, K. M., Tozer, G. M., and Kanthou, C. (2007). Radiation effects on the cytoskeleton of endothelial cells and endothelial monolayer permeability. *International journal of radiation oncology, biology, physics* **69**, 1553-62.

Gallicano, G. I., Bauer, C., and Fuchs, E. (2001). Rescuing desmoplakin function in extra-embryonic ectoderm reveals the importance of this protein in embryonic heart, neuroepithelium, skin and vasculature. *Development (Cambridge, England)* **128**, 929-41.

Geiser, M., Rothen-Rutishauser, B., Kapp, N., Schurch, S., Kreyling, W., Schulz, H., Semmler, M., Im Hof, V., Heyder, J., and Gehr, P. (2005). Ultrafine particles cross cellular membranes by nonphagocytic mechanisms in lungs and in cultured cells. *Environmental health perspectives* **113**, 1555-60.

Gerber, H. P., McMurtrey, A., Kowalski, J., Yan, M., Keyt, B. A., Dixit, V., and Ferrara, N. (1998). Vascular endothelial growth factor regulates endothelial cell survival through the phosphatidylinositol 3'-kinase/Akt signal transduction pathway. Requirement for Flk-1/KDR activation. *The Journal of biological chemistry* **273**, 30336-43.

Gerstner, E. R., Duda, D. G., di Tomaso, E., Ryg, P. A., Loeffler, J. S., Sorensen, A. G., Ivy, P., Jain, R. K., and Batchelor, T. T. (2009). VEGF inhibitors in the treatment of cerebral edema in patients with brain cancer. *Nature reviews* **6**, 229-36.

Grant, D. S., Lelkes, P. I., Fukuda, K., and Kleinman, H. K. (1991). Intracellular mechanisms involved in basement membrane induced blood vessel differentiation in vitro. *In Vitro Cell Dev Biol* **27A**, 327-36.

Groten, T., Kreienberg, R., Fialka, I., Huber, L., and Wedlich, D. (2000). Altered subcellular distribution of cadherin-5 in endothelial cells caused by the serum of pre-eclamptic patients. *Molecular human reproduction* **6**, 1027-32.

Guo, R., Sakamoto, H., Sugiura, S., and Ogawa, M. (2007). Endothelial cell motility is compatible with junctional integrity. *Journal of cellular physiology* **211**, 327-35.

Hadley, M. A., Byers, S. W., Suarez-Quian, C. A., Kleinman, H. K., and Dym, M. (1985). Extracellular matrix regulates Sertoli cell differentiation, testicular cord formation, and germ cell development in vitro. *The Journal of cell biology* **101**, 1511-22.

Hanahan, D., and Folkman, J. (1996). Patterns and emerging mechanisms of the angiogenic switch during tumorigenesis. *Cell* **86**, 353-64.

Harper, S. J., and Bates, D. O. (2008). VEGF-A splicing: the key to anti-angiogenic therapeutics? *Nat Rev Cancer* **8**, 880-7.

Harren, M., Schonfelder, G., Paul, M., Horak, I., Riecken, E. O., Wiedenmann, B., and John, M. (1998). High expression of inducible nitric oxide synthase correlates with intestinal inflammation of interleukin-2-deficient mice. *Annals of the New York Academy of Sciences* **859**, 210-5.

Hartz, A. M., Bauer, B., Block, M. L., Hong, J. S., and Miller, D. S. (2008). Diesel exhaust particles induce oxidative stress, proinflammatory signaling, and P-glycoprotein up-regulation at the blood-brain barrier. *Faseb J* **22**, 2723-33.

Heinrich, U., Muhle, H., Takenaka, S., Ernst, H., Fuhst, R., Mohr, U., Pott, F., and Stober, W. (1986). Chronic effects on the respiratory tract of hamsters, mice and rats after long-term inhalation of high concentrations of filtered and unfiltered diesel engine emissions. *J Appl Toxicol* **6**, 383-95.

Hiura, T. S., Kaszubowski, M. P., Li, N., and Nel, A. E. (1999). Chemicals in diesel exhaust particles generate reactive oxygen radicals and induce apoptosis in macrophages. *J Immunol* **163**, 5582-91.

Hiura, T. S., Li, N., Kaplan, R., Horwitz, M., Seagrave, J. C., and Nel, A. E. (2000). The role of a mitochondrial pathway in the induction of apoptosis by chemicals extracted from diesel exhaust particles. *J Immunol* **165**, 2703-11.

Holmes, K., Charnock Jones, S. D., Forhead, A. J., Giussani, D. A., Fowden, A. L., Licence, D., Kempster, S., and Smith, G. C. (2008). Localization and control of expression of VEGF-A and the VEGFR-2 receptor in fetal sheep intestines. *Pediatric research* **63**, 143-8.

Holmes, K., Roberts, O. L., Thomas, A. M., and Cross, M. J. (2007). Vascular endothelial growth factor receptor-2: structure, function, intracellular signalling and therapeutic inhibition. *Cellular signalling* **19**, 2003-12.

Honda, R., Tanaka, H., and Yasuda, H. (1997). Oncoprotein MDM2 is a ubiquitin ligase E3 for tumor suppressor p53. *FEBS letters* **420**, 25-7.

Hsieh, C. Y., Hsiao, H. Y., Wu, W. Y., Liu, C. A., Tsai, Y. C., Chao, Y. J., Wang, D. L., and Hsieh, H. J. (2009). Regulation of shear-induced nuclear translocation of the Nrf2 transcription factor in endothelial cells. *Journal of biomedical science* **16**, 12.

Inoue, K., Takano, H., Sakurai, M., Oda, T., Tamura, H., Yanagisawa, R., Shimada, A., and Yoshikawa, T. (2006). Pulmonary exposure to diesel exhaust particles enhances coagulatory disturbance with endothelial damage and systemic inflammation related to lung inflammation. *Experimental biology and medicine (Maywood, N.J* **231**, 1626-32.

Iruela-Arispe, M. L., and Davis, G. E. (2009). Cellular and molecular mechanisms of vascular lumen formation. *Developmental cell* **16**, 222-31.

Ishinishi, N., Kuwabara, N., Nagase, S., Suzuki, T., Ishiwata, S., and Kohno, T. (1986). Long-term inhalation studies on effects of exhaust from heavy and light duty diesel engines on F344 rats. *Developments in toxicology and environmental science* **13**, 329-348.

Ito, T., Ikeda, M., Yamasaki, H., Sagai, M., and Tomita, T. (2000). Peroxynitrite formation by diesel exhaust particles in alveolar cells: Links to pulmonary inflammation. *Environmental toxicology and pharmacology* **9**, 1-8.

Iwai, K., Udagawa, T., Yamagishi, M., and Yamada, H. (1986). Long-term inhalation studies of diesel exhaust on F344 SPF rats. Incidence of lung cancer and lymphoma. *Developments in toxicology and environmental science* **13**, 349-60.

Jalava, P., Salonen, R. O., Halinen, A. I., Sillanpaa, M., Sandell, E., and Hirvonen, M. R. (2005). Effects of sample preparation on chemistry, cytotoxicity, and inflammatory responses induced by air particulate matter. *Inhalation toxicology* **17**, 107-17.

Jozkowicz, A., Huk, I., Nigisch, A., Weigel, G., Dietrich, W., Motterlini, R., and Dulak, J. (2003). Heme oxygenase and angiogenic activity of endothelial cells: stimulation by carbon monoxide and inhibition by tin protoporphyrin-IX. *Antioxidants & redox signaling* **5**, 155-62.

Keck, P. J., Hauser, S. D., Krivi, G., Sanzo, K., Warren, T., Feder, J., and Connolly, D. T. (1989). Vascular permeability factor, an endothelial cell mitogen related to PDGF. *Science (New York, N.Y* **246**, 1309-12.

Kevil, C. G., Okayama, N., and Alexander, J. S. (2001). H(2)O(2)-mediated permeability II: importance of tyrosine phosphatase and kinase activity. *Am J Physiol Cell Physiol* **281**, C1940-7.

Kevil, C. G., Payne, D. K., Mire, E., and Alexander, J. S. (1998). Vascular permeability factor/vascular endothelial cell growth factor-mediated permeability occurs through disorganization of endothelial junctional proteins. *The Journal of biological chemistry* **273**, 15099-103.

Kinney, P. L., Aggarwal, M., Northridge, M. E., Janssen, N. A., and Shepard, P. (2000). Airborne concentrations of PM(2.5) and diesel exhaust particles on Harlem sidewalks: a community-based pilot study. *Environmental health perspectives* **108**, 213-8.

Ko, F. W., and Hui, D. S. (2009). Outdoor air pollution: impact on chronic obstructive pulmonary disease patients. *Current opinion in pulmonary medicine* **15**, 150-7.

Kowanetz, M., and Ferrara, N. (2006). Vascular Endothelial Growth Factor Signaling Pathways: Therapeutic Perspective. *Clinical Cancer Research* **12**, 5018-5022.

Kreyling, W. G., Semmler, M., Erbe, F., Mayer, P., Takenaka, S., Schulz, H., Oberdorster, G., and Ziesenis, A. (2002). Translocation of ultrafine insoluble iridium particles from lung epithelium to extrapulmonary organs is size dependent but very low. *Journal of toxicology and environmental health* **65**, 1513-30.

Kreyling, W. G., Semmler-Behnke, M., Seitz, J., Scymczak, W., Wenk, A., Mayer, P., Takenaka, S., and Oberdorster, G. (2009). Size dependence of the translocation of inhaled iridium and carbon nanoparticle aggregates from the lung of rats to the blood and secondary target organs. *Inhalation toxicology* **21**, 55-60.

Krivoshto, I. N., Richards, J. R., Albertson, T. E., and Derlet, R. W. (2008). The toxicity of diesel exhaust: implications for primary care. *J Am Board Fam Med* **21**, 55-62.

Kumagai, Y., Arimoto, T., Shinyashiki, M., Shimojo, N., Nakai, Y., Yoshikawa, T., and Sagai, M. (1997). Generation of reactive oxygen species during interaction of diesel exhaust particle components with NADPH-cytochrome P450 reductase and involvement of the bioactivation in the DNA damage. *Free radical biology & medicine* **22**, 479-87.

Lambeng, N., Wallez, Y., Rampon, C., Cand, F., Christe, G., Gulino-Debrac, D., Vilgrain, I., and Huber, P. (2005). Vascular endothelial-cadherin tyrosine phosphorylation in angiogenic and quiescent adult tissues. *Circulation research* **96**, 384-91.

Lampugnani, M. G., Resnati, M., Raiteri, M., Pigott, R., Pisacane, A., Houen, G., Ruco, L. P., and Dejana, E. (1992). A novel endothelial-specific membrane protein is a marker of cell-cell contacts. *The Journal of cell biology* **118**, 1511-22.

Landvik, N. E., Gorria, M., Arlt, V. M., Asare, N., Solhaug, A., Lagadic-Gossmann, D., and Holme, J. A. (2007). Effects of nitrated-polycyclic aromatic hydrocarbons and diesel exhaust particle extracts on cell signalling related to apoptosis: possible implications for their mutagenic and carcinogenic effects. *Toxicology* **231**, 159-74.

Le, T. L., Joseph, S. R., Yap, A. S., and Stow, J. L. (2002). Protein kinase C regulates endocytosis and recycling of E-cadherin. *Am J Physiol Cell Physiol* **283**, C489-99.

Le, T. L., Yap, A. S., and Stow, J. L. (1999). Recycling of E-cadherin: a potential mechanism for regulating cadherin dynamics. *The Journal of cell biology* **146**, 219-32.

Levine, A. J. (1997). p53, the cellular gatekeeper for growth and division. *Cell* **88**, 323-31.

Li, N., Kim, S., Wang, M., Froines, J., Sioutas, C., and Nel, A. (2002). Use of a stratified oxidative stress model to study the biological effects of ambient concentrated and diesel exhaust particulate matter. *Inhalation toxicology* **14**, 459-86.

Li, R., Ning, Z., Cui, J., Khalsa, B., Ai, L., Takabe, W., Beebe, T., Majumdar, R., Sioutas, C., and Hsiai, T. (2009). Ultrafine particles from diesel engines induce vascular oxidative stress via JNK activation. *Free radical biology & medicine* **46**, 775-82.

Lim, M. J., Chiang, E. T., Hechtman, H. B., and Shepro, D. (2001). Inflammation-induced subcellular redistribution of VE-cadherin, actin, and gamma-catenin in cultured human lung microvessel endothelial cells. *Microvascular research* **62**, 366-82.

Lin, H. H., Chen, Y. H., Chang, P. F., Lee, Y. T., Yet, S. F., and Chau, L. Y. (2008). Heme oxygenase-1 promotes neovascularization in ischemic heart by coinduction of VEGF and SDF-1. *Journal of molecular and cellular cardiology* **45**, 44-55.

Lubarsky, B., and Krasnow, M. A. (2003). Tube morphogenesis: making and shaping biological tubes. *Cell* **112**, 19-28.

Lucking, A. J., Lundback, M., Mills, N. L., Faratian, D., Barath, S. L., Pourazar, J., Cassee, F. R., Donaldson, K., Boon, N. A., Badimon, J. J., Sandstrom, T., Blomberg, A., and Newby, D. E. (2008). Diesel exhaust inhalation increases thrombus formation in man. *European heart journal* **29**, 3043-51.

Mamessier, E., Nieves, A., Vervloet, D., and Magnan, A. (2006). Diesel exhaust particles enhance T-cell activation in severe asthmatics. *Allergy* **61**, 581-8.

Maruo, N., Morita, I., Shirao, M., and Murota, S. (1992). IL-6 increases endothelial permeability in vitro. *Endocrinology* **131**, 710-4.

Matsuo, M., Shimada, T., Uenishi, R., Sasaki, N., and Sagai, M. (2003). Diesel exhaust particle-induced cell death of cultured normal human bronchial epithelial cells. *Biological & pharmaceutical bulletin* **26**, 438-47.

Mayo, L. D., and Donner, D. B. (2001). A phosphatidylinositol 3-kinase/Akt pathway promotes translocation of Mdm2 from the cytoplasm to the nucleus. *Proceedings of the National Academy of Sciences of the United States of America* **98**, 11598-603.

McClellan, R. O. (1987). Health effects of exposure to diesel exhaust particles. *Annual review of pharmacology and toxicology* **27**, 279-300.

Mehta, D., and Malik, A. B. (2006). Signaling mechanisms regulating endothelial permeability. *Physiological reviews* **86**, 279-367.

Mills, N. L., Amin, N., Robinson, S. D., Anand, A., Davies, J., Patel, D., de la Fuente, J. M., Cassee, F. R., Boon, N. A., Macnee, W., Millar, A. M., Donaldson, K., and Newby, D. E. (2006). Do inhaled carbon nanoparticles translocate directly into the circulation in humans? *American journal of respiratory and critical care medicine* **173**, 426-31.

Mills, N. L., Tornqvist, H., Gonzalez, M. C., Vink, E., Robinson, S. D., Soderberg, S., Boon, N. A., Donaldson, K., Sandstrom, T., Blomberg, A., and Newby, D. E. (2007). Ischemic and thrombotic effects of dilute diesel-exhaust inhalation in men with coronary heart disease. *The New England journal of medicine* **357**, 1075-82.

Mills, N. L., Tornqvist, H., Robinson, S. D., Gonzalez, M., Darnley, K., MacNee, W., Boon, N. A., Donaldson, K., Blomberg, A., Sandstrom, T., and Newby, D. E. (2005). Diesel exhaust inhalation causes vascular dysfunction and impaired endogenous fibrinolysis. *Circulation* **112**, 3930-6.

Monks, T. J., and Lau, S. S. (1992). Toxicology of quinone-thioethers. *Critical reviews in toxicology* **22**, 243-70.

Nawroth, R., Poell, G., Ranft, A., Kloep, S., Samulowitz, U., Fachinger, G., Golding, M., Shima, D. T., Deutsch, U., and Vestweber, D. (2002). VE-PTP and VE-cadherin ectodomains interact to facilitate regulation of phosphorylation and cell contacts. *The EMBO journal* **21**, 4885-95.

Nel, A. (2005). Atmosphere. Air pollution-related illness: effects of particles. *Science (New York, N.Y* **308**, 804-6.

Nemmar, A., Hamoir, J., Nemery, B., and Gustin, P. (2005). Evaluation of particle translocation across the alveolo-capillary barrier in isolated perfused rabbit lung model. *Toxicology* **208**, 105-13.

Nemmar, A., Hoet, P. H., and Nemery, B. (2006). Translocation of ultrafine particles. *Environmental health perspectives* **114**, A211-2; author reply A212-3.

Nemmar, A., Hoet, P. H., Vanquickenborne, B., Dinsdale, D., Thomeer, M., Hoylaerts, M. F., Vanbilloen, H., Mortelmans, L., and Nemery, B. (2002). Passage of inhaled particles into the blood circulation in humans. *Circulation* **105**, 411-4.

Nemmar, A., Hoet, P. H., Vermylen, J., Nemery, B., and Hoylaerts, M. F. (2004a). Pharmacological stabilization of mast cells abrogates late thrombotic events induced by diesel exhaust particles in hamsters. *Circulation* **110**, 1670-7.

Nemmar, A., Hoylaerts, M. F., Hoet, P. H., and Nemery, B. (2004b). Possible mechanisms of the cardiovascular effects of inhaled particles: systemic translocation and prothrombotic effects. *Toxicology letters* **149**, 243-53.

Nemmar, A., Nemery, B., Hoet, P. H., Vermylen, J., and Hoylaerts, M. F. (2003). Pulmonary inflammation and thrombogenicity caused by diesel particles in hamsters: role of histamine. *American journal of respiratory and critical care medicine* **168**, 1366-72.

Nemmar, A., Vanbilloen, H., Hoylaerts, M. F., Hoet, P. H., Verbruggen, A., and Nemery, B. (2001). Passage of intratracheally instilled ultrafine particles from the lung into the systemic circulation in hamster. *American journal of respiratory and critical care medicine* **164**, 1665-8.

Oberdorster, G. (2001). Pulmonary effects of inhaled ultrafine particles. *International archives of occupational and environmental health* **74**, 1-8.

Oberdorster, G. (2002). Toxicokinetics and effects of fibrous and nonfibrous particles. *Inhalation toxicology* **14**, 29-56.

Oberdorster, G., Ferin, J., and Lehnert, B. E. (1994). Correlation between particle size, in vivo particle persistence, and lung injury. *Environmental health perspectives* **102 Suppl 5**, 173-9.

Oberdorster, G., and Utell, M. J. (2002). Ultrafine particles in the urban air: to the respiratory tract--and beyond? *Environmental health perspectives* **110**, A440-1.

Ogawara, Y., Kishishita, S., Obata, T., Isazawa, Y., Suzuki, T., Tanaka, K., Masuyama, N., and Gotoh, Y. (2002). Akt enhances Mdm2-mediated ubiquitination and degradation of p53. *The Journal of biological chemistry* **277**, 21843-50.

Ohyama, K., Ito, T., and Kanisawa, M. (1999). The roles of diesel exhaust particle extracts and the promotive effects of NO2 and/or SO2 exposure on rat lung tumorigenesis. *Cancer letters* **139**, 189-97.

Oliner, J. D., Pietenpol, J. A., Thiagalingam, S., Gyuris, J., Kinzler, K. W., and Vogelstein, B. (1993). Oncoprotein MDM2 conceals the activation domain of tumour suppressor p53. *Nature* **362**, 857-60.

Olivieri, G., Baysang, G., Meier, F., Muller-Spahn, F., Stahelin, H. B., Brockhaus, M., and Brack, C. (2001). N-acetyl-L-cysteine protects SHSY5Y neuroblastoma cells from oxidative stress and cell cytotoxicity: effects on beta-amyloid secretion and tau phosphorylation. *Journal of neurochemistry* **76**, 224-33.

Olk, S., Zoidl, G., and Dermietzel, R. (2009). Connexins, cell motility, and the cytoskeleton. *Cell motility and the cytoskeleton*.

Olsson, A. K., Dimberg, A., Kreuger, J., and Claesson-Welsh, L. (2006). VEGF receptor signalling - in control of vascular function. *Nat Rev Mol Cell Biol* **7**, 359-71.

Park, S., Nam, H., Chung, N., Park, J. D., and Lim, Y. (2006). The role of iron in reactive oxygen species generation from diesel exhaust particles. *Toxicol In Vitro* **20**, 851-7.

Peretz, A., Kaufman, J. D., Trenga, C. A., Allen, J., Carlsten, C., Aulet, M. R., Adar, S. D., and Sullivan, J. H. (2008). Effects of diesel exhaust inhalation on heart rate variability in human volunteers. *Environmental research* **107**, 178-84.

Peters, A., Frohlich, M., Doring, A., Immervoll, T., Wichmann, H. E., Hutchinson, W. L., Pepys, M. B., and Koenig, W. (2001). Particulate air pollution is associated with an acute phase response in men; results from the MONICA-Augsburg Study. *European heart journal* **22**, 1198-204.

Peters, A., von Klot, S., Heier, M., Trentinaglia, I., Hormann, A., Wichmann, H. E., and Lowel, H. (2004). Exposure to traffic and the onset of myocardial infarction. *The New England journal of medicine* **351**, 1721-30.

Peters, A., Wichmann, H. E., Tuch, T., Heinrich, J., and Heyder, J. (1997). Respiratory effects are associated with the number of ultrafine particles. *American journal of respiratory and critical care medicine* **155**, 1376-83.

Pocernich, C. B., La Fontaine, M., and Butterfield, D. A. (2000). In-vivo glutathione elevation protects against hydroxyl free radical-induced protein oxidation in rat brain. *Neurochemistry international* **36**, 185-91.

Pope, C. A., 3rd (2007). Mortality effects of longer term exposures to fine particulate air pollution: review of recent epidemiological evidence. *Inhalation toxicology* **19 Suppl 1**, 33-8.

Pope, C. A., 3rd, Burnett, R. T., Thurston, G. D., Thun, M. J., Calle, E. E., Krewski, D., and Godleski, J. J. (2004). Cardiovascular mortality and long-term exposure to particulate air pollution: epidemiological evidence of general pathophysiological pathways of disease. *Circulation* **109**, 71-7.

Pope, C. A., 3rd, and Dockery, D. W. (2006). Health effects of fine particulate air pollution: lines that connect. *Journal of the Air & Waste Management Association (1995)* **56**, 709-42.

Pope, C. A., 3rd, Renlund, D. G., Kfoury, A. G., May, H. T., and Horne, B. D. (2008). Relation of heart failure hospitalization to exposure to fine particulate air pollution. *The American journal of cardiology* **102**, 1230-4.

Pope, C. A., 3rd, Verrier, R. L., Lovett, E. G., Larson, A. C., Raizenne, M. E., Kanner, R. E., Schwartz, J., Villegas, G. M., Gold, D. R., and Dockery, D. W. (1999). Heart rate variability associated with particulate air pollution. *American heart journal* **138**, 890-9.

Rengasamy, A., Barger, M. W., Kane, E., Ma, J. K., Castranova, V., and Ma, J. Y. (2003). Diesel exhaust particle-induced alterations of pulmonary phase I and phase II enzymes of rats. *Journal of toxicology and environmental health* **66**, 153-67.

Riedl, M., and Diaz-Sanchez, D. (2005). Biology of diesel exhaust effects on respiratory function. *The Journal of allergy and clinical immunology* **115**, 221-8; quiz 229.

Risom, L., Moller, P., and Loft, S. (2005). Oxidative stress-induced DNA damage by particulate air pollution. *Mutation research* **592**, 119-37.

Rudell, B., Blomberg, A., Helleday, R., Ledin, M. C., Lundback, B., Stjernberg, N., Horstedt, P., and Sandstrom, T. (1999). Bronchoalveolar inflammation after exposure to diesel exhaust: comparison between unfiltered and particle trap filtered exhaust. *Occupational and environmental medicine* **56**, 527-34.

Rudell, B., Ledin, M. C., Hammarstrom, U., Stjernberg, N., Lundback, B., and Sandstrom, T. (1996). Effects on symptoms and lung function in humans experimentally exposed to diesel exhaust. *Occupational and environmental medicine* **53**, 658-62.

Rusznak, C., Mills, P. R., Devalia, J. L., Sapsford, R. J., Davies, R. J., and Lozewicz, S. (2000). Effect of cigarette smoke on the permeability and IL-1beta and sICAM-1 release from cultured human bronchial epithelial cells of never-smokers, smokers, and patients with chronic obstructive pulmonary disease. *American journal of respiratory cell and molecular biology* **23**, 530-6.

Sagai, M., Saito, H., Ichinose, T., Kodama, M., and Mori, Y. (1993). Biological effects of diesel exhaust particles. I. In vitro production of superoxide and in vivo toxicity in mouse. *Free radical biology & medicine* **14**, 37-47.

Salvi, S., Blomberg, A., Rudell, B., Kelly, F., Sandstrom, T., Holgate, S. T., and Frew, A. (1999). Acute inflammatory responses in the airways and peripheral blood after short-term exposure to diesel exhaust in healthy human volunteers. *American journal of respiratory and critical care medicine* **159**, 702-9.

Samet, J. M., Dominici, F., Curriero, F. C., Coursac, I., and Zeger, S. L. (2000). Fine particulate air pollution and mortality in 20 U.S. cities, 1987-1994. *The New England journal of medicine* **343**, 1742-9.

Schmelz, M., and Franke, W. W. (1993). Complexus adhaerentes, a new group of desmoplakin-containing junctions in endothelial cells: the syndesmos connecting retothelial cells of lymph nodes. *European journal of cell biology* **61**, 274-89.

Senger, D. R., Connolly, D. T., Van de Water, L., Feder, J., and Dvorak, H. F. (1990). Purification and NH2-terminal amino acid sequence of guinea pig tumor-secreted vascular permeability factor. *Cancer research* **50**, 1774-8.

Senger, D. R., Galli, S. J., Dvorak, A. M., Perruzzi, C. A., Harvey, V. S., and Dvorak, H. F. (1983). Tumor cells secrete a vascular permeability factor that promotes accumulation of ascites fluid. *Science (New York, N.Y* **219**, 983-5.

Silva, G., Cunha, A., Gregoire, I. P., Seldon, M. P., and Soares, M. P. (2006). The antiapoptotic effect of heme oxygenase-1 in endothelial cells involves the degradation of p38 alpha MAPK isoform. *J Immunol* **177**, 1894-903.

Simionescu, M., and Simionescu, N. (1991). Endothelial transport of macromolecules: transcytosis and endocytosis. A look from cell biology. *Cell Biol Rev* **25**, 5-78.

Siner, J. M., Jiang, G., Cohen, Z. I., Shan, P., Zhang, X., Lee, C. G., Elias, J. A., and Lee, P. J. (2007). VEGF-induced heme oxygenase-1 confers cytoprotection from lethal hyperoxia in vivo. *Faseb J* **21**, 1422-32.

Singh, P., DeMarini, D. M., Dick, C. A., Tabor, D. G., Ryan, J. V., Linak, W. P., Kobayashi, T., and Gilmour, M. I. (2004). Sample characterization of automobile and forklift diesel exhaust particles and comparative pulmonary toxicity in mice. *Environmental health perspectives* **112**, 820-5.

Skurk, C., Maatz, H., Rocnik, E., Bialik, A., Force, T., and Walsh, K. (2005). Glycogen-Synthase Kinase3beta/beta-catenin axis promotes angiogenesis through activation of vascular endothelial growth factor signaling in endothelial cells. *Circulation research* **96**, 308-18.

Somanath, P. R., Razorenova, O. V., Chen, J., and Byzova, T. V. (2006). Akt1 in endothelial cell and angiogenesis. *Cell cycle (Georgetown, Tex* **5**, 512-8.

Steerenberg, P. A., Zonnenberg, J. A., Dormans, J. A., Joon, P. N., Wouters, I. M., van Bree, L., Scheepers, P. T., and Van Loveren, H. (1998). Diesel exhaust particles induced release of interleukin 6 and 8 by (primed) human bronchial epithelial cells (BEAS 2B) in vitro. *Experimental lung research* **24**, 85-100.

Stevenson, B. R., and Keon, B. H. (1998). The tight junction: morphology to molecules. *Annual review of cell and developmental biology* **14**, 89-109.

Stone, P. H., and Godleski, J. J. (1999). First steps toward understanding the pathophysiologic link between air pollution and cardiac mortality. *American heart journal* **138**, 804-7.

Strugar, J., Rothbart, D., Harrington, W., and Criscuolo, G. R. (1994). Vascular permeability factor in brain metastases: correlation with vasogenic brain edema and tumor angiogenesis. *Journal of neurosurgery* **81**, 560-6.

Sugimoto, R., Kumagai, Y., Nakai, Y., and Ishii, T. (2005). 9,10-Phenanthraquinone in diesel exhaust particles downregulates Cu,Zn-SOD and HO-1 in human pulmonary

epithelial cells: intracellular iron scavenger 1,10-phenanthroline affords protection against apoptosis. *Free radical biology & medicine* **38**, 388-95.

Sumanasekera, W. K., Ivanova, M. M., Johnston, B. J., Dougherty, S. M., Sumanasekera, G. U., Myers, S. R., Ali, Y., Kizu, R., and Klinge, C. M. (2007). Rapid effects of diesel exhaust particulate extracts on intracellular signaling in human endothelial cells. *Toxicology letters* **174**, 61-73.

Suwa, T., Hogg, J. C., Quinlan, K. B., Ohgami, A., Vincent, R., and van Eeden, S. F. (2002). Particulate air pollution induces progression of atherosclerosis. *Journal of the American College of Cardiology* **39**, 935-42.

Sydbom, A., Blomberg, A., Parnia, S., Stenfors, N., Sandstrom, T., and Dahlen, S. E. (2001). Health effects of diesel exhaust emissions. *Eur Respir J* **17**, 733-46.

Taddei, A., Giampietro, C., Conti, A., Orsenigo, F., Breviario, F., Pirazzoli, V., Potente, M., Daly, C., Dimmeler, S., and Dejana, E. (2008). Endothelial adherens junctions control tight junctions by VE-cadherin-mediated upregulation of claudin-5. *Nature cell biology* **10**, 923-34.

Takizawa, H., Abe, S., Okazaki, H., Kohyama, T., Sugawara, I., Saito, Y., Ohtoshi, T., Kawasaki, S., Desaki, M., Nakahara, K., Yamamoto, K., Matsushima, K., Tanaka, M., Sagai, M., and Kudoh, S. (2003). Diesel exhaust particles upregulate eotaxin gene expression in human bronchial epithelial cells via nuclear factor-kappa B-dependent pathway. *American journal of physiology* **284**, L1055-62.

Takizawa, H., Ohtoshi, T., Kawasaki, S., Abe, S., Sugawara, I., Nakahara, K., Matsushima, K., and Kudoh, S. (2000). Diesel exhaust particles activate human bronchial epithelial cells to express inflammatory mediators in the airways: a review. *Respirology (Carlton, Vic* **5**, 197-203.

Taneda, S., Mori, Y., Kamata, K., Hayashi, H., Furuta, C., Li, C., Seki, K., Sakushima, A., Yoshino, S., Yamaki, K., Watanabe, G., Taya, K., and Suzuki, A. K. (2004). Estrogenic and anti-androgenic activity of nitrophenols in diesel exhaust particles (DEP). *Biological & pharmaceutical bulletin* **27**, 835-7.

Terada, N., Hamano, N., Maesako, K. I., Hiruma, K., Hohki, G., Suzuki, K., Ishikawa, K., and Konno, A. (1999). Diesel exhaust particulates upregulate histamine receptor mRNA and increase histamine-induced IL-8 and GM-CSF production in nasal epithelial cells and endothelial cells. *Clin Exp Allergy* **29**, 52-9.

Terry, C. M., Clikeman, J. A., Hoidal, J. R., and Callahan, K. S. (1998). Effect of tumor necrosis factor-alpha and interleukin-1 alpha on heme oxygenase-1 expression in human endothelial cells. *The American journal of physiology* **274**, H883-91.

Terry, C. M., Clikeman, J. A., Hoidal, J. R., and Callahan, K. S. (1999). TNF-alpha and IL-1alpha induce heme oxygenase-1 via protein kinase C, Ca2+, and phospholipase A2 in endothelial cells. *The American journal of physiology* **276**, H1493-501.

Tornqvist, H., Mills, N. L., Gonzalez, M., Miller, M. R., Robinson, S. D., Megson, I. L., Macnee, W., Donaldson, K., Soderberg, S., Newby, D. E., Sandstrom, T., and Blomberg, A. (2007). Persistent endothelial dysfunction in humans after diesel exhaust inhalation. *American journal of respiratory and critical care medicine* **176**, 395-400.

Ulrich, M. M., Alink, G. M., Kumarathasan, P., Vincent, R., Boere, A. J., and Cassee, F. R. (2002). Health effects and time course of particulate matter on the cardiopulmonary system in rats with lung inflammation. *Journal of toxicology and environmental health* **65**, 1571-95.

Unemori, E. N., Ferrara, N., Bauer, E. A., and Amento, E. P. (1992). Vascular endothelial growth factor induces interstitial collagenase expression in human endothelial cells. *Journal of cellular physiology* **153**, 557-62.

Venkiteswaran, K., Xiao, K., Summers, S., Calkins, C. C., Vincent, P. A., Pumiglia, K., and Kowalczyk, A. P. (2002). Regulation of endothelial barrier function and growth by VE-cadherin, plakoglobin, and beta-catenin. *Am J Physiol Cell Physiol* **283**, C811-21.

Veranth, J. M., Cutler, N. S., Kaser, E. G., Reilly, C. A., and Yost, G. S. (2008). Effects of cell type and culture media on Interleukin-6 secretion in response to environmental particles. *Toxicol In Vitro* **22**, 498-509.

Vincent, M. A., Clerk, L. H., Lindner, J. R., Klibanov, A. L., Clark, M. G., Rattigan, S., and Barrett, E. J. (2004). Microvascular recruitment is an early insulin effect that regulates skeletal muscle glucose uptake in vivo. *Diabetes* **53**, 1418-23.

Vittet, D., Buchou, T., Schweitzer, A., Dejana, E., and Huber, P. (1997). Targeted null-mutation in the vascular endothelial-cadherin gene impairs the organization of vascular-like structures in embryoid bodies. *Proceedings of the National Academy of Sciences of the United States of America* **94**, 6273-8.

Vousden, K. H., and Prives, C. (2009). Blinded by the Light: The Growing Complexity of p53. *Cell* **137**, 413-31.

Wagner, E. M., and Foster, W. M. (1996). Importance of airway blood flow on particle clearance from the lung. *J Appl Physiol* **81**, 1878-83.

Wallez, Y., Vilgrain, I., and Huber, P. (2006). Angiogenesis: the VE-cadherin switch. *Trends in cardiovascular medicine* **16**, 55-9.

Wang, Z., Armando, I., Asico, L. D., Escano, C., Wang, X., Lu, Q., Felder, R. A., Schnackenberg, C. G., Sibley, D. R., Eisner, G. M., and Jose, P. A. (2007). The elevated

blood pressure of human GRK4gamma A142V transgenic mice is not associated with increased ROS production. *Am J Physiol Heart Circ Physiol* **292**, H2083-92.

Watanabe, N. (2005). Decreased number of sperms and Sertoli cells in mature rats exposed to diesel exhaust as fetuses. *Toxicology letters* **155**, 51-8.

Wichmann, H. E. (2007). Diesel exhaust particles. *Inhalation toxicology* **19 Suppl 1**, 241-4.

Wold, L. E., Simkhovich, B. Z., Kleinman, M. T., Nordlie, M. A., Dow, J. S., Sioutas, C., and Kloner, R. A. (2006). In vivo and in vitro models to test the hypothesis of particle-induced effects on cardiac function and arrhythmias. *Cardiovascular toxicology* **6**, 69-78.

Xiao, K., Allison, D. F., Buckley, K. M., Kottke, M. D., Vincent, P. A., Faundez, V., and Kowalczyk, A. P. (2003a). Cellular levels of p120 catenin function as a set point for cadherin expression levels in microvascular endothelial cells. *The Journal of cell biology* **163**, 535-45.

Xiao, K., Allison, D. F., Kottke, M. D., Summers, S., Sorescu, G. P., Faundez, V., and Kowalczyk, A. P. (2003b). Mechanisms of VE-cadherin processing and degradation in microvascular endothelial cells. *The Journal of biological chemistry* **278**, 19199-208.

Yang, H. M., Ma, J. Y., Castranova, V., and Ma, J. K. (1997). Effects of diesel exhaust particles on the release of interleukin-1 and tumor necrosis factor-alpha from rat alveolar macrophages. *Experimental lung research* **23**, 269-84.

Yue, W., Li, X., Liu, J., Li, Y., Yu, X., Deng, B., Wan, T., Zhang, G., Huang, Y., He, W., Hua, W., Shao, L., Li, W., and Yang, S. (2006). Characterization of PM(2.5) in the ambient air of Shanghai City by analyzing individual particles. *The Science of the total environment* **368**, 916-25.

Yun, Y. P., Lee, J. Y., Ahn, E. K., Lee, K. H., Yoon, H. K., and Lim, Y. (2009). Diesel exhaust particles induce apoptosis via p53 and Mdm2 in J774A.1 macrophage cell line. *Toxicol In Vitro* **23**, 21-8.

Zanobetti, A., Canner, M. J., Stone, P. H., Schwartz, J., Sher, D., Eagan-Bengston, E., Gates, K. A., Hartley, L. H., Suh, H., and Gold, D. R. (2004). Ambient pollution and blood pressure in cardiac rehabilitation patients. *Circulation* **110**, 2184-9.

Zhou, X., Stuart, A., Dettin, L. E., Rodriguez, G., Hoel, B., and Gallicano, G. I. (2004). Desmoplakin is required for microvascular tube formation in culture. *Journal of cell science* **117**, 3129-40.

Zimrin, A. B., Villeponteau, B., and Maciag, T. (1995). Models of in vitro angiogenesis: endothelial cell differentiation on fibrin but not matrigel is transcriptionally dependent. *Biochemical and biophysical research communications* **213**, 630-8.

Curriculum Vitae

Ming-Wei Chao

EDUCATION HISTORY

10/2009, PhD Degree
Rutgers, State University of New Jersey, New Brunswick/Piscataway, New Jersey
08854-8020, USA
Joint Graduate Program in Toxicology, Environmental and Occupational Health Sciences
Institute, (2004~2009)

06/2002, B.S. Degree
National Taiwan University, Taipei, Taiwan 106
Department of Agriculture Chemistry[1], College of Agriculture[2], (1999~2002)

RESEARCH EXPERIENCE

10/2009, Graduate Assistance
Joint Graduate Program in Toxicology, Environmental and Occupational Health Sciences
Institute, Rutgers, State University of New Jersey, Lab of Dr. Marion K. Gordon
(10/05~10/2009)

08/2005, Student Assistance
Department of Physiology and Biophysics, Robert Wood Johnson Medical School,
University Medical and Dentistry of New Jersey, Laboratory of Dr. Macro Brotto
(07/05~08/05)

06/2004, Research Assistance
Graduate Institute of Clinical Density, School of Density, National Taiwan University,
Taipei, Taiwan, Pharmacology and Toxicology Laboratory of Professor Dr. Jiiang-Huei
Jeng (01/04~06/04)

12/2003, Research Assistance
Graduate Institute of Biomedical Material, Taipei Medical University, Taipei, Taiwan, Lab
of Professor Dr. Win-Ping Deng (06/02~12/03)

TEACHING EXPERIENCE

06/2006, Teaching Assistance
Department of Biochemistry and Microbiology, Cook College of Rutgers, State University of New Jersey, Lab of Advanced Biochemistry (01/06~06/06)

PUBLICATION

- Lin CP, Chen YJ, Lee YL, Wang JS, Chang MC, Lan WH, Chang HH, **Chao MW**, Tai TF, Lee MY, Lin BR, Jeng JH. Effects of Root-End Filling Materials and Eugenol on Mitochondrial Dehydrogenase Activity and Cytotoxicity to Human Periodontal Ligament Fibroblasts. *J Biomed Mater Res*. 2004 Nov 15;71B(2):429-440.

- Deng WP, **Chao MW**, Lai WF, Sun C, Chung CY, Wu CC, Lin IH, Hwang JJ, Wu CH, Chiu WT, Chen CY. Correction of malignant behavior of tumor cells by traditional Chinese herb medicine through a restoration of p53. *Cancer Letters*. 2006 Feb 28; 233(2):315-327.

- **Chao, MW**, Pettit, A., Song, R., Gerecke, D.R., Laumbach, R., and Gordon, M.K. The Effect of Diesel Particles On Capillary Endothelial Tubes Grown In Vitro. *The Toxicologist* A2111, p. 436, 2007.

- **Chao, MW**, Pettit, A., Gerecke, D.R., Laumbach, R., and Gordon, M.K. Treatment of Endothelial Cells in vitro with Varying Concentrations of Diesel Particles and Carbon Black. 2007 Experimental Biology meeting abstracts *FASEB J.* 21:73.5, 2007.

- **Chao, MW**, Po, IP, Koslosky, J, Gerecke, D.R., Laumbach, R., and Gordon, M.K. Changes in Endothelial Tube Cell-Cell Borders in Response to Diesel Exhaust Particles. *The Toxicologist* A742, p. 152, 2008.

- **Chao, MW**, Po, IP., Koslosky, J., Gerecke, D.R., Laumbach, R., Svoboda, K.K.H. and Gordon, M. K. Capillary Endothelial Tubes Lose Cell Junctional Integrity And Apoptose In Response To Diesel Exhaust Particles. *FASEB J*. 22:524.8, 2008.

- **Chao MW**, Koslosky J, Po IP, Gerecke DR, Svoboda KK, Laumbach R, and Gordon MK. Diesel Exhaust Particles Increase Permeability Induce Reactive Oxygen Species And Are Cytotoxic To In Vitro Capillary Endothelial Tubes. *The Toxicologist* A207, p. 47, 2009.

- **Chao MW**, Koslosky J, Po IP, Gerecke DR, Svoboda KK, Laumbach R, and Gordon MK. In Vitro Capillary Endothelial Tubes as A Model System To Study Cytotoxicity of Diesel Particles. *FASEB J.* 23:639.1, 2009

- **Chao MW**, Kozlosky J, Po IP, Svoboda KKH, Laumbach R, Gordon MK. Capillary Endothelial Tubes as an *in vitro* culture model to Study the Effects of Diesel Exhaust Particles. *Toxicology* (*In Revision*).

- **Chao MW**, Po IP, Laumbach R, Kozlosky J, Cooper K, Gordon MK. ROS and Pro-inflammatory Cytokines Contribute to DEP-Induced Permeability of Capillary-like Endothelial Tubes. *Free Radical Biology and Medicine* (*Submitted*).

- **Chao MW**, Po IP, Laumbach R, Gordon MK. Diesel Exhaust Particles Induce HUVEC Tube Apoptosis by Inhibition of the Akt Pathway and activation of p53. (*In prepare*).